INFORMATION TO USERS

This manuscript has been reproduced from the microfilm master. UMI films the text directly from the original or copy submitted. Thus, some thesis and dissertation copies are in typewriter face, while others may be from any type of computer printer.

The quality of this reproduction is dependent upon the quality of the copy submitted. Broken or indistinct print, colored or poor quality illustrations and photographs, print bleedthrough, substandard margins, and improper alignment can adversely affect reproduction.

In the unlikely event that the author did not send UMI a complete manuscript and there are missing pages, these will be noted. Also, if unauthorized copyright material had to be removed, a note will indicate the deletion.

Oversize materials (e.g., maps, drawings, charts) are reproduced by sectioning the original, beginning at the upper left-hand corner and continuing from left to right in equal sections with small overlaps.

Photographs included in the original manuscript have been reproduced xerographically in this copy. Higher quality 6" x 9" black and white photographic prints are available for any photographs or illustrations appearing in this copy for an additional charge. Contact UMI directly to order.

Bell & Howell Information and Learning
300 North Zeeb Road, Ann Arbor, MI 48106-1346 USA

UMI®
800-521-0600

Laboratory studies of till deformation with implications for Des Moines Lobe motion and sediment transport

by

Thomas Scott Hooyer

A dissertation submitted to the graduate faculty

in partial fulfillment of the requirements for the degree of

DOCTOR OF PHILOSOPHY

Major: Geology

Major Professor: Neal R. Iverson

Iowa State University

Ames, Iowa

1999

Bell & Howell Information and Learning Company
300 North Zeeb Road
P.O. Box 1346
Ann Arbor, MI 48106-1346

Graduate College
Iowa State University

This is to certify that the Doctoral dissertation of

Thomas Scott Hooyer

has met the dissertation requirements of Iowa State University

Signature was redacted for privacy.

Major Professor

Signature was redacted for privacy.

For the Major Program

Signature was redacted for privacy.

For the Graduate College

TABLE OF CONTENTS

ACKNOWLEDGMENTS

I am grateful to Neal Iverson for his guidance and support throughout this research project. His imaginative ideas and clear thinking helped me understand many problems, and his editorial skills and thorough review of this thesis were invaluable. I would also like to thank Roger LeB. Hooke, Peter Hudleston and my thesis committee members including Carl Jacobson, Bill Simpkins, Bruce Kjartanson, and Lee Burras for their constructive criticism during various stages of this thesis. I wish to acknowledge Carrie Patterson, Gary Meyer, and Howard Hobbs who were always willing to answer questions regarding the geology of Minnesota. Throughout this project I was assisted at various times in the laboratory and the field by Dan Sailsbury, Nick Davis, Dan Nelsen, Jane Pedrick-Dawson, and Bob Dawson. Thanks to DeAnn Frisk who on numerous occasions helped me navigate the bureaucracy of the university system.

Many people have provided friendship, encouragement, and the occasional muscle power to lift heavy laboratory equipment. Among them were Dan Doctor, Paul Cutler, Ginny Catania, Doug Allen, Christoph Geiss, Martin Helmke, Rob Andress, and Mark Mathison. In particular, I want to thank Denis Cohen for always expressing an interest in my work. I also want to thank Jill Rosenberg for helping me with some laboratory experiments as well as solving various computer problems and document formatting. I am indebted to my friends Eric Offerdahl and Sean Lambert who were always there to provide encouragement.

Finally, I wish to express my gratitude to my parents, John and Ihla Hooyer, and the rest of my family for their support from the beginning.

ABSTRACT

Pervasive deformation of subglacial till has been suggested as the primary mechanism of motion and sediment transport for many modern glaciers and portions of Pleistocene ice sheets. Unfortunately, standard field observations of the geologic record are insufficient to determine whether basal tills have experienced the high strains required of this model.

To establish field criteria for identifying highly sheared till, a ring-shear device is used to study both clast-fabric development and mixing between lithologically-distinct till units as a function of shear strain. In some experiments, the relation between the alignment of prolate clasts and shear strain is explored. The results indicate that a strong fabric develops in the direction of shearing at low strains and remains strong with continued deformation. Thus, clast fabric can be used to distinguish otherwise featureless tills that have been sheared from those that have not. Other experiments are performed to investigate if the degree of mixing between subglacial till layers provides a means of estimating bed shear strain. Two lithologically distinct Pleistocene tills are added as discrete layers to the ring-shear device and sheared parallel to their contact. The results indicate that mixing across the contact is diffusive and proportional to the cumulative shear strain. Using diffusion theory to model this mixing allows the maximum bed shear strain to be estimated from mixing profiles measured across the contact between these two tills in the field.

These laboratory observations were used, together with other data, to help determine the primary flow mechanism of the Des Moines Lobe. Reconstructions of the lobe from

geomorphic data reveal that motion occurred at its base, and results of consolidation tests on basal till samples indicate that the lobe was near floatation. Field measurements of fabric and mixing in the basal till of the lobe indicate that bed deformation was not significant. This is supported by the results of a theoretical model of plowing and sliding that predicts, albeit with some uncertainty, that motion should have occurred at the bed surface, rather than at depth in the bed.

CHAPTER 1. GENERAL INTRODUCTION

The climatic record preserved in polar ice cores indicates that the Pleistocene Epoch was characterized by rapid and severe environmental change (Johnsen et al., 1992; Dansgaard et al, 1993; Grootes and Stuiver, 1997; Severinghaus et al., 1998). The growth and decay of large ice sheets in the Northern Hemisphere were the most significant of these changes. Although ultimately driven by orbitally forced variations in insolation (Hays et al, 1976; Imbrie et al., 1992, 1993; Koç and Jansen, 1994), these ice sheets sometimes underwent rapid advances and retreats that were apparently not climatically forced (Prest, 1970; Dreimanis and Goldthwait, 1973; Clayton et al, 1985; Heinrich, 1988; Keigwin et al., 1991; Andrews and Tedesco, 1992; Bond et al., 1992; Grosset et al., 1993; Clark, 1994). Such unstable ice sheet behavior influenced the climate system by affecting atmospheric circulation, planetary albedo, and oceanic circulation through the routing of freshwater to the North Atlantic (Manabe and Broccoli, 1985; Bond et al., 1992, 1997; Broecker, 1994). Wet-based portions of the Laurentide ice that rested on unlithified sediment were particularly unstable (Clark, 1994).

Potential mechanisms of motion of wet-based, sediment-floored glaciers include internal deformation of ice, the sliding of ice over the bed surface, plowing of clasts gripped by the ice through the bed, and pervasive shearing of the bed. The last of these mechanisms, often called the bed-deformation mechanism of glacier motion, has been the focus of recent intensive study and has been called by some a new paradigm in glaciology (Boulton, 1986;

Murray, 1997). It has been suggested this flow mechanism results in large-scale ice-sheet instability (MacAyeal, 1989, 1992; Clark, 1994).

The potential importance of subglacial sediment deformation was recognized over 20 years ago when the bed of Bredimerkerjökull, Iceland, was observed to be shearing pervasively (Boulton and Jones, 1979). Subsequent studies there established that 80-95% of the glacier's motion was due to this mechanism (Boulton and Hindmarsh, 1987). Theory developed from this work indicates that the response time of glaciers to climate forcing may be decreased by the presence of a till bed. Furthermore, Clarke et al. (1984) inferred from data collected from the bed of Trapridge Glacier, Yukon Territory, Canada, that shearing of the bed might contribute to the periodic surging of that glacier.

There was not widespread interest in the bed-deformation hypothesis until a seismic study of rapidly moving Ice Stream B (440 m a^{-1}) in West Antarctica (Blankenship et al., 1986, 1987) indicated that it was underlain by a ~6 m thick till layer of high porosity (0.4), rather than bedrock as was previously assumed. Based on these data and related theoretical considerations, some glaciologists (Alley et al., 1986, 1987; Alley, 1989) postulated that the bed was deforming pervasively and controlling the motion and stability of the ice stream. This was a major hypothesis since Ice Stream B and similar ice streams are thought to largely control the behavior of the West Antarctic Ice Sheet and its response to sea level rise (Bentley, 1997; Bindschadler, 1997). The presence of the till layer beneath part of the ice steam was verified by a series of boreholes drilled to its base in the late 1980's (Engelhardt et al, 1990). Other results from this study indicated that the water pressure at the base of the ice stream is only slightly less than that of the ice overburden. This work underscored the

importance of the basal water system and indicated that the ice stream is nearly floating on its poorly drained bed.

More recent measurements on smaller, more accessible valley glaciers that rest on sediment and subsequent measurements on Ice Stream B indicate that although bed deformation occurs, it may not be the dominant mechanism of ice motion. Bed deformation has been measured directly at Trapridge Glacier (Blake et al, 1992, 1994), Storglaciären, Sweden (Iverson et al, 1995; Hooke et al, 1997), and Columbia Glacier, Alaska (Humphrey, 1993). However, work at Trapridge Glacier and Storglaciären indicates that when water pressure in the basal hydraulic system is high, glacier motion occurs at the ice/till interface rather than at depth in the bed (Iverson et al, 1995; Fischer and Clarke, 1997; Fischer et al., 1999). Bed deformation accounted for less than 5% of the motion of Storglaciären; motion was, therefore, inferred to occur at the bed surface. Recent data collected at the base of Ice Stream B, where water pressures are continuously high, indicate similarly that more than 80% of the ice stream's motion occurs within a few centimeters of the glacier sole rather than at depth in the bed (Engelhardt and Kamb, 1998).

Despite the incomplete understanding of the motion of glaciers over unlithified sediment, bed deformation has been frequently incorporated in ice sheets models. These include analytical and numerical models of modern ice stream motion (Alley et al, 1987; MacAyeal, 1989; Kamb, 1991; Hindmarsh, 1997). Other models that incorporate the bed-deformation mechanism have been applied to Pleistocene ice sheets with the goal of better understanding their geometry and their chronology of advance and retreat (Beget, 1986; MacAyeal, 1992; Jenson et al., 1995, 1996; Clark et al., 1996; Licciardi et al, 1998).

A large number of studies have invoked bed deformation as a dominant mechanism of basal sediment transport and key process in the development of various landforms. Early studies recognized that large volumes of sediment could be efficiently transported in a deforming bed (Boulton, 1979, Boulton and Jones, 1979). Alley (1991) and Jenson et al. (1995) argued that only a glacier that deformed its bed could have transported the large volumes of sediment observed along the former southern margin of the Laurentide Ice Sheet. Other studies call upon this mechanism to explain the large sediment flux necessary to account for thick, extensive accumulations of glacigenic sediments in some nearshore marine environments (Hooke and Elverhøi, 1996; Dowdeswell and Siegert, 1999; Shipp et al., 1999). Other landforms attributed to pervasively deforming beds include drumlins (Boulton and Hindmarsh, 1987; Boulton, 1987, Menzies, 1989; Hart, 1997; Hindmarsh, 1998), tunnel valleys (Boulton and Hindmarsh, 1987; van der Wateren, 1995), rogen moraines (van der Wateren, 1995), and megaflutes (van der Wateren, 1995). Clark and Walder (1995) argued that the absence of eskers in certain regions beneath the Laurentide and Scandinavian ice sheets was due to deformable subglacial sediment in those areas, which resulted in "canal" drainage (Walder and Fowler, 1994) that impeded esker formation.

The geologic record has been studied in an attempt to develop sedimentological criteria for subglacially sheared till. Weak clast fabrics (Dowdeswell and Sharp, 1986; Hicock, 1992; Hart, 1994, Clark, 1997), microstructural rotational features (van der Meer, 1993, 1997), grain comminution (Boulton et al., 1974; Hiemstra and van der Meer, 1998), boulder pavements (Clark, 1991), and sharp stratigraphic contacts (Alley, 1991) have all been inferred to be products of subglacial till deformation. None of these features, however, provides convincing evidence that a till unit has been sheared to sufficiently large strains to

contribute significantly to glacier motion. Overall, study of the geologic record has resulted in no unequivocal criteria for testing the bed-deformation hypothesis.

A major objective of this research is to develop quantitative sedimentological criteria for distinguishing highly sheared tills in the geologic record from those that have been deformed to negligibly small strains. Experiments are conducted with a ring-shear device that shears a large, drained till specimen to high strains at glacial rates. In some experiments, the relation between the alignment of elongate clasts in the till and shear strain is examined and compared with the results of control tests using a viscous putty. The results indicate that the fabric formed by aligned clasts becomes strong at low strains and remains strong with continued deformation, contrary to inferences from the geologic record and a theoretical model based on particle rotation in a viscous fluid. In other experiments, mixing between two lithologically distinct tills is studied as they are sheared parallel to the contact between them. The results indicate that sharp stratigraphic contacts cannot persist with deformation and that mixing can be modeled as a linearly diffusive process. Consequently, mixing across stratigraphic contacts can be characterized with a single coefficient and used to help constrain the extent of glacier motion due to pervasive bed deformation.

The second objective of this research is to use these sedimentological criteria, together with other methods, to determine the principal flow mechanism of the Des Moines Lobe, a major outlet glacier of the Laurentide Ice Sheet. An important goal is to evaluate whether the Des Moines Lobe moved and transported sediment primarily by deforming its bed. This involves reconstructing the lobe using geomorphic criteria, calculating it driving stress, and estimating the effective stress at the base of the lobe from consolidation tests on basal till samples. A theoretical model of sliding and plowing is then used to estimate the strength of

the ice/bed interface. Comparing the model results with the ultimate strength of the till indicates that motion probably occurred at the bed surface and not at depth in the bed. This result is corroborated by measurements of clast orientation in the Des Moines Lobe basal till, which indicate weak fabrics inconsistent with the bed-deformation mechanism. Moreover, till samples collected across the contact between the Des Moines Lobe and Superior Lobe tills indicate mixing insufficient to support the bed-deformation hypothesis.

Dissertation organization

This thesis consists of three papers (Chapters 2, 3, and 4), organized for submission to journals, and a brief summary of conclusions (Chapter 5). I apologize for the slight redundancy between chapters that arises due to this format. A slightly condensed version of the first paper has been accepted for publication in the *Geological Society of America Bulletin*. The other two papers will be slightly revised prior to submission.

References

Alley, R.B., Blankenship, D.D., Bentley, C.R. and Rooney, S.T., 1986, Deformation of till beneath Ice Stream B, West Antarctica: Nature, v. 322, p. 57-59.

Alley, R.B., Blankenship, D.D., Bentley, C.R., and Rooney, S.T., 1987, Till beneath Ice Stream B. 3. Till deformation: evidence and implications: Journal of Geophysical Research, v. 92, no. B9, p. 8921-8929.

Alley, R.B., 1989, Water-pressure coupling of sliding and bed deformation: II. Velocity-depth profiles: Journal of Glaciology, v. 35, p. 119-129.

Alley, R.B., 1991, Deforming-bed origin for southern Laurentide till sheets?: Journal of Glaciology: v. 37, p. 67-76.

Andrews, J.T., and Tedesco, K., 1992, Detrital carbonate-rich sediments, northwestern Labrador Sea: implications for ice-sheet dynamics and iceberg rafting (Heinrich) events in the North Atlantic: Geology, v. 20, p. 1087-1090.

Beget, J.E., 1986, Modeling the influence of till rheology on the flow and profile of the Lake Michigan Lobe, Southern Laurentide Ice Sheet, v. 32, p. 235-241

Bentley, C.R., 1997, Rapid sea-level rise soon from West Antarctic Ice Sheet collapse: Science, v. 275, p. 1077-1078,

Bindschadler, R., 1997, West Antarctic Ice Sheet collapse, Science, v. 276, p. 242-246.

Blake, E.W., Clarke, G.K.C. and Gérin, M.C., 1992, Tools for examining subglacial bed deformation: Journal of Glaciology, v. 38, p. 388-396.

Blake, E.W., Fischer, U.H., and Clarke, G.K.C., 1994, Direct measurement of sliding at the glacier bed: Journal of Glaciology, v. 40, p. 595-599.

Blankenship, D.D., Bentley, C.R., Rooney, S.T. and Alley, R.B., 1986, Seismic measurements reveal a saturated porous layer beneath an active Antarctic ice stream: Nature, v. 322, p 54-57.

Blankenship, D.D., Bentley, C.R., Rooney, S.T., and Alley, R.B., 1987, Till beneath ice Stream B. 1. Properties derived from seismic travel times: Journal of Geophysical Research, v. 92 (B9), p. 8903-8911.

Bond, G., Heinrich, H., Broecker, W., Labeyrie, L., McManus, J., et al., 1992, Evidence for massive discharges of icebergs into the North Atlantic ocean during the last glacial period: Nature, v. 360, p. 245-249.

Bond, G., Showers, W., Cheseby, M., Lotti, R., Almasi, P., et al., 1997, A pervasive millennial-scale cycle in North Atlantic Holocene and glacial climates: Science, v. 278, p. 1257-66.

Boulton, G.S., 1979, Processes of glacier erosion on different substrates: Journal of Glaciology, v. 23, p. 15-38.

Boulton, G.S., 1986, A paradigm shift in Glaciology?: Nature, v. 322, p.18.

Boulton, G.S., 1987, A theory of drumlin formation by subglacial sediment deformation: In Drumlin Symposium, eds. Menzies, J., and Rose, J., A.A. Balkema, Rotterdam, p. 25-80.

Boulton, G.S., Dent, D.L., and Morris, E.M., 1974, Subglacial shearing and crushing and the role of water pressures in tills from south-east Iceland: Geografiska Annaler, v. 56A, n. 3-4, p. 135-145.

Boulton, G.S., and Jones, A.S., 1979, Stability of temperate ice caps and ice sheets resting on beds of deformable sediment: Journal of Glaciology: v. 24, p. 29-43.

Boulton G.S., and Hindmarsh, R.C.A., 1987, Sediment deformation beneath glaciers: rheology and geological consequences. Journal of Geophysical Research, v. 92 n. B9, p. 9059-9082.

Broecker, W.S., 1994, Massive iceberg discharges as triggers for global climate change: Nature, v. 372, p. 421-424.

Clark, P.U., 1991, Striated clast pavements: Products of deforming subglacial sediment?: Geology, v. 19, p. 530-533.

Clark, P.U., 1994, Unstable behavior of the Laurentide Ice Sheet over deforming sediment and its implications for climate change: Quaternary Research, v. 41, p. 19-25.

Clark, P.U., 1997, Sediment deformation beneath the Laurentide Ice Sheet, *in* Martini, I.P., ed., Late glacial and postglacial environmental changes, Quaternary, Carboniferous-Permian and Proterozoic: Oxford University Press, New York, p. 81-97.

Clark, P.U., and Walder, J.S., 1995, Subglacial drainage, eskers, and deforming beds beneath the Laurentide and Eurasian ice sheets: Geological Society of America Bulletin, v. 106, p. 304-314.

Clark, P.U., Licciardi, J.M., MacAyeal, D.R., and Jenson, J.W., 1996, Numerical reconstruction of a soft-bedded Laurentide Ice sheet during the last glacial maximum: Geology, v. 24, n. 8, p. 679-682.

Clarke, G.K.C., Collin, S.G., and Thompson, D.E., 1984, Flow, thermal structure, and subglacial conditions of a surge-type glacier: Canadian Journal of Earth Science, v. 21, p. 232-240.

Clayton, L., Teller, J.T., and Attig, J.W., 1985 Surging of the southwestern part of the Laurentide Ice Sheet: Boreas, v. 14, p. 235-242.

Dansgaard, W., Johnsen, S.J., Clausen, D., et al., 1993, Evidence for general instability of past climate from a 250-kyr ice-core record: Nature, v. 364, p. 218-220

Dowdeswell, J.A., and Sharp, M.J. 1986, Characterization of pebble fabrics in modern terrestrial glacigenic sediments: Sedimentology, v. 33, p. 699-710.

Dowdeswell, J.A., and Siegert, M.J., 1999, Ice-sheet numerical modeling and marine geophysical measurements of glacier-derived sedimentation on the Eurasian Arctic continental margins: Geological Society of America Bulletin, v. 111, p. 1080-1097.

Dreimanis, A., and Goldthwait, R.P., 1973, Wisconsin glaciation in the Huron, Erie, and Ontario lobes. *In* the Wisconsinan Stage. Edited by Black R.F., Goldthwait, R.P., and Willman, H.B., Ohio State University Press, Columbus, Ohio, p. 71-106.

Engelhardt, H., Humphrey, N., Kamb, B., and Fahnestock, M., 1990 Physical conditions at the base of a fast moving Antarctic ice stream: Science, v. 248, p. 57-59.

Engelhardt, H. and Kamb, B. 1998, Basal sliding of Ice Stream B, West Antarctica: Journal of Glaciology, v. 44, p. 233-230.

Fischer, U.H., Clarke, G.K.C., 1997, Stick-slip sliding behaviour at the base of a glacier: v. 40, p. 97-106.

Fischer, U.H., Clarke, G.K.C. and Blatter, H., 1999, Evidence for temporally varying "sticky spots" at the base of Trapridge Glacier, Yukon Territory, Canada: Journal of Glaciology, V. 45, p. 352-360.

Grootes, P.M., Stuiver, M. 1997, Oxygen 18/16 variability in Greenland snow and ice with 10^{-3} to 10^{-5}-year time resolution: Journal of Geophysical Research, v. 102, p. 26455-26470.

Grousset, F.E., Labeyrie, L., Sinko, J.A., Cremer, M., Bond, G., et al., 1993, Patterns of ice-rafted detritus in the glacial North Atlantic (40-55° N): Paleoceanography, v. 8, p. 175-192.

Hart, J.K., 1994, Till fabric associated with deformable beds: Earth Surface Processes and Landforms, v. 19, p. 15-32.

Hart, J.K., 1997, The relationship between drumlins and other forms of subglacial glaciotectonic deformation: Quaternary Science Reviews, v. 16, p. 93-107.

Hays, H.D., Imbrie, J., and Shackleton, N.J., 1976, Variations in the earth's orbit: pacemaker of the ice ages: Science, v. 194, p. 1121-1134.

Heinrich, H., 1988, Origin and consequences of cyclic ice rafting in the northeast Atlantic Ocean during the past 130,000 years: Quaternary Research, v. 29, p. 143-152.

Hicock, S.R., 1992, Lobal interactions and rheologic superposition in subglacial till near Bradtville, Ontario, Canada: Boreas, v. 21, p. 73-88.

Hiemstra, J.F., and van der Meer, J.J.M., 1998, Pore-water controlled grain fracturing as an indicator for subglacial shearing in tills: Journal of Glaciology, v. 43, p. 446-454.

Hindmarsh, R., 1997, Deforming beds: viscous and plastic scales of deformation: Quaternary Science Reviews, v. 16, p. 1039-1056.

Hindmarsh, R., 1998, Ice-stream surface texture, sticky spots, waves and breather: the coupled flow of ice, till and water: Journal of Glaciology, v. 44, p. 589-614.

Hooke, R. LeB., and Elverhøi, A., 1996, Sediment flux from a fjord during glacial periods, Isfjorden, Spitsbergen: Global and Planetary Change, v. 12, p. 237-249.

Hooke, R. LeB., Hanson, B., Iverson, N.R., Jansson, P. and Fischer, U.H., 1997, rheology of till beneath Storglaciären, Sweden: Journal of Glaciology: v. 43, p. 172-179.

Humphrey, N., 1993, Characteristics of the bed of the lower Columbia Glacier, Alaska: Journal of Geophysical research, v. 98, n. B1, pg. 837-846.

Imbrie, J., Boyle, E.A., Clemens, S.C., Duffy, A., Howard, W.R., et al. 1992, On the structure and origin of major glaciation cycles 1. Linear responses to Milankovitch forcing; Paleoceanography, v. 7, p. 701-738.

Imbrie, J., Berger, A., Boyle, E.A., Clemens, S.C., Duffy, A., et al. 1993, On the structure and origin of major glaciation cycles: 2. The 100,000-year cycle, Paleoceanography, v. 8, p. 699-735.

Iverson, N.R., Hanson, B., Hooke, R. LeB., and Jansson, P., 1995, Flow mechanism of glaciers on soft beds: Science, v. 267, no. 5194, p. 80-81.

Jenson, J.W., Clark, P.U., MacAyeal, D.R., Ho, C., and Vela, J.C., 1995, Numerical modeling of advective transport of saturated deforming sediment beneath the Lake Michigan Lobe, Laurentide Ice Sheet: Geomorphology, v. 14, p. 157-166.

Jenson, J.W., MacAyeal, D.R., Clark, P.U., Ho, C.L. and Vela, J.C., 1996, Numerical modeling of subglacial sediment deformation: implications for the behavior of the Lake Michigan Lobe, Laurentide Ice Sheet: Journal of Geophysical Research, v. 101, B4, p. 8717-8728.

Johnsen, S.J., Clausen, H.B., Dansgaard, W., et al., 1992, Irregular glacial interstadials recorded in a new Green land ice core: Nature, v. 359, p. 311-313.

Kamb, B., 1991, Rheological nonlinearity and flow instability in the deforming bed mechanism of ice stream motion. Journal of Geophysical Research, v. 96, n. B10, p. 16,585-16,595.

Keigwin, L.D., Jones, G.A., Lehman, S.J., and Boyle, E., 1991, Deglacial meltwater discharge, North Atlantic deep circulation, and abrupt climate change: Journal of Geophysical Research, v. 96, p. 16811-16826.

Koç, N., and Jansen, E., 1994, Response of the high-latitude northern hemisphere to orbital climate forcing: Evidence from the Nordic seas. Geology, v. 22, p. 523-526.

Licciardi, J.M., Clark, P.U., Jenson, J.W., and MacAyeal, D.R., 1998, Deglaciation of a soft-bedded Laurentide Ice Sheet: Quaternary Science Reviews, v. 17, p. 427-448.

Lorius, C., Jouzel J., Raynaud, D., Hansen J., Le Treut, H., 1990, The ice-core record: climate sensitivity and future greenhouse warming: Nature, v. 347, p. 139-145.

MacAyeal, D.R., 1989, Large-scale ice flow over a viscous basal sediment: theory and application to Ice Stream B, Antarctica: Journal of Geophysical Research, v. 94, n. B4, p. 4071-4087.

MacAyeal, D.R., 1992, Irregular oscillations of the West Antarctic ice sheet: Nature, v. 359, p. 29-32.

Manabe, S., and Broccoli, A.J., 1985, The contributions of continental ice, atmospheric CO_2, and land albedo to the climate of the last glacial maximum: Climate Dynamics, v. 1, p. 87-99.

Menzies, J., 1989, Drumlins – products of controlled or uncontrolled glaciodynamic response?: Quaternary Science Reviews, v. 8, p. 151-158.

Murry, T., 1997, Assessing the Paradigm shift: deformable glacier beds: Quaternary Science Reviews, v. 16, p. 995-1016.

Prest, V.K., 1970, Quaternary geology of Canada. *In* Geology and Economic Minerals of Canada, Ed., Douglas, R.J.W., Geological Survey of Canada, Economic Geology Report 1, 5th ed., Ottawa, p. 676-764.

Severinghaus, J.P, Sowers, T., Brook, E.J., Alley, R.B., Bender, M.L., 1998, Timing of abrupt climate change at the end of the Younger Dryas interval from thermally fractionated gases in polar ice: Nature, v. 391, p. 141-146.

Shipp, S., Anderson, J., and Domack, E., 1999, Late Pleistocene-Holocene retreat of the West Antarctic Ice Sheet system in the Ross Sea: Part 1-Geophysical results: Geological Society of America Bulletin, v. 111, p. 1486-1516.

Van der Wateren, F.M., 1995, Processes of Glaciotectonism: In Modern glacial environments: Processes, Dynamics and Sediments, ed. Menzies, J., p. 309-335, Butterworth-Heinemann, Oxford.

Van der Meer, J.J.M., 1993, Microscopic evidence of subglacial deformation: Quaternary Science Reviews, v. 12, p. 553-587.

Van der Meer, J.J.M., 1997, Particle and aggregrate mobility in till: microscopic evidence of subglacial processes: Quaternary Science Reviews, v. 16, p. 827-831.

Walder, J.S., and Fowler, A., 1994, Channelized subglacial drainage over a deformable bed, Journal of Glaciology, v. 40, p. 3-15.

CHAPTER 2. CLAST-FABRIC DEVELOPMENT IN A SHEARING GRANULAR MATERIAL: IMPLICATIONS FOR SUBGLACIAL TILL AND FAULT GOUGE

A paper accepted by the Geological Society of America Bulletin

Thomas S. Hooyer and Neal R. Iverson
Department of Geological and Atmospheric Sciences
Iowa State University, Ames, IA 50011

ABSTRACT

Elongate clasts in subglacial till and in fault gouge align during shearing, but the relation between clast-fabric strength and cumulative shear strain for such materials is effectively unknown. This relation was explored in experiments with a large ring-shear device in which a till and a viscous putty that contained isolated clasts were sheared to high strains. As expected, rotation of clasts in the putty is closely approximated by the theory of Jeffery (1922), who derived the orbits of rigid ellipsoids in a slowly shearing fluid. Clast rotation in the till, however, is strikingly different. Rather than orbiting through the shear plane as predicted by Jeffery, most clasts rotate into the shear plane and remain there, resulting in strong fabrics regardless of the aspect ratios and initial orientations of clasts. This divergent behavior is likely due to slip of the till matrix along the surfaces of clasts, which is a natural expectation in a granular material but violates the no-slip condition of Jeffery's model. These results do not support the widespread belief that subglacial till deformation results in weak clast fabrics. Thus, many tills with weak fabrics thought to have been sheared subglacially to high strains, like many basal tills of the Laurentide Ice Sheet, may have been sheared only slightly with little effect on either ice-sheet dynamics or sediment transport. Also, these results indicate that in simple shear the rotation of clasts in

till and in fault gouge is best analyzed with the model of March (1932), who treated inclusions as passive markers.

INTRODUCTION

The fabrics defined by aligned particles in tills of modern and past glaciers have been used for many years to infer depositional processes and environments (e.g., Holmes, 1941; Glen et al., 1957; Harrison, 1957; Boulton, 1971, Lawson, 1979a). Recently, fabric strength has been studied in efforts to identify till layers that have been sheared pervasively to high strains as weak, water-saturated layers beneath ice sheets. Identifying and constraining such till deformation is important because it may have controlled the motion and geometry of Pleistocene ice sheets (MacAyeal, 1992; Clark, 1994; Jenson et al., 1996; Clark et al., 1996; Licciardi et al., 1998). In addition, it may have been a primary mechanism of sediment transport (e.g., Alley, 1991, Jenson et al., 1995; Boulton, 1996; Hooke and Elverhøi, 1996), and thus may have contributed to the formation of various landforms, including drumlins, eskers, and moraines (e.g., Menzies, 1989; Clark and Walder, 1995; Hart, 1997).

Efforts to use clast fabric as an indicator of till deformation rely on the widely held belief that subglacial shearing of till results in a weak fabric parallel to the direction of glacier flow (Dowdeswell and Sharp, 1986; Hicock, 1992; Hicock and Dreimanis, 1992; Hart, 1994; 1997; Clark, 1997). In contrast, stronger fabrics are usually interpreted to be the result of lodgment, a poorly understood process in which debris in sliding basal ice is released from ice and plastered onto the bed. Limited data indicate that particles in basal ice are often aligned (Lawson, 1979b; Ham and Mickelson, 1994), and a reasonable conjecture, therefore, is that these strong fabrics should be preserved, to some extent, in lodgment tills.

However, the assertion that subsequent subglacial shearing of such tills should weaken their fabrics is more uncertain. It is based on weak fabrics that have been measured in tills where field observations provide independent support for till deformation. Some of these observations, which include microstructural rotational features and shear bands (van der Meer, 1993; 1997), are convincing. However, these observations provide little information about strain magnitude. A shear strain of 1.0, for example, cannot be distinguished from a shear strain of 10, 100 or 1000. This is a critical limitation of such observations, since the deforming-bed mechanism of glacier motion and sediment transport (e.g., Alley et al., 1986) requires very high shear strains. For example, a glacier that moves at its base at a modest rate of 50 m yr^{-1} and shears uniformly the uppermost 5 m of its bed for only 100 yr would cause a bed shear strain of 1000.

Unfortunately, clast fabric has never been measured in sediment samples collected from beneath modern glaciers where the bed is independently and unequivocally known to have experienced such high strains. Nor have there been laboratory studies of clast fabric development in sheared till. The result is that the critical relation between fabric strength and shear strain is effectively unknown.

Similar to studies of subglacial till, fabric-forming elements in gouge have been used to characterize the kinematics of deformation in fault zones. In particular, field studies (e.g., Engelder, 1974; Rutter et al., 1986; Chester and Logan, 1987) have shown that gouge fabric can be useful in determining the sense of shearing and shear-strain distribution, and laboratory studies (Byerlee et al., 1978; Moore et al., 1989; Logan et al. 1992) have linked fabric development to cumulative shear strain.

These gouge studies, however, have concentrated mainly on the orientation and

development of microfractures and on the orientation of clay-sized particles, not on the orientations of larger isolated grains that are sometimes observed in gouge (Engelder, 1974; Chester and Logan, 1987; Cladouhos, 1999). These grains, sometimes termed survivor clasts, have escaped intense comminution and are usually found isolated in a fine-grained matrix. Cladouhos (1999) has recognized the potential importance of these clasts in better understanding fault-gouge deformation. Interestingly, he found that unlike the weak fabrics hypothesized for sheared till, the fabric strengths displayed by survivor clasts are generally strong, either in the direction of shearing or at a relatively low angle to the shear plane. However, like clast-fabric development in subglacial till, the relation between fabric strength and cumulative shear strain is poorly known.

Various models that attempt to predict the motion of either rigid clasts or passive markers in slowly deforming fluids have been applied to clast-fabric development. These models treat rigid-clast rotation in simple shear (Jeffery, 1922), rigid-clast rotation in combined simple and pure shear (Ghosh and Ramberg, 1976), and passive-marker rotation in general shear (March, 1932). In subglacial till and in fault gouge, in which clasts are rigid and simple shear may be dominant, Jeffery's theory is expected to be the most appropriate. Indeed, Jeffery's model, which predicts discernable but weak fabrics at high strains, has been embraced by glacial geologists (e.g., Hart; 1994; Clark, 1997) and considered in studies of gouge fabric (Cladouhos, 1999), but unknown cumulative shear strain in field settings precludes an unequivocal test of the model. Various laboratory studies that support Jeffery's theory have been conducted with rigid inclusions in shearing fluids (Trevelyan and Mason, 1951; Ghosh and Ramberg, 1976; Fernandez et al., 1983; Ildefonse et al., 1992). However, it is well known that shearing granular materials do not generally behave as fluids (Jaeger and

Nagel, 1992). For example, the common fluid mechanical assumption that there is no slip between a fluid and its substrate often does not hold for granular materials, as indicated by laboratory studies of the slow deformation of clay (e.g., Tika-Vassilikos, 1991) and fault gouge (e.g., Dieterich, 1981; Biegel et al., 1989) adjacent to rigid substrates.

In this study, the evolution of clast fabric with shear strain is investigated using a ring-shear device to slowly shear a large till specimen to high strains. The results are compared with those of experiments with a viscous fluid (putty) that contained elongate rigid clasts. The experiments indicate that, although the Jeffery model adequately describes clast rotation in a fluid, it fails to predict clast rotation and fabric development in till and, by extension, in similar granular materials like gouge. These results imply that the clast-fabric criterion used by glacial geologists to help identify highly deformed till layers should be rejected and that clasts in till and gouge subjected to simple shear are best modeled as passive markers.

THEORY

The theory of Jeffery (1922) describes the rotation of rigid ellipsoidal clasts in a uniformly shearing fluid. The theory assumes that clasts are neutrally buoyant and do not interact, that the flow is non-inertial, and that there is no slip between clasts and the fluid. If shearing is assumed to occur in a vertical plane (x-z) (Fig. 1A), then the angle, ϕ, measured in this plane between the long axis of the clast and the vertical coordinate (z), is given by:

$$\tan \phi = \frac{a}{b} \tan\left[\frac{ab\gamma}{(a^2 + b^2)} + \tan^{-1}\left(\frac{b}{a} \tan \phi_i \right) \right] , \qquad (1)$$

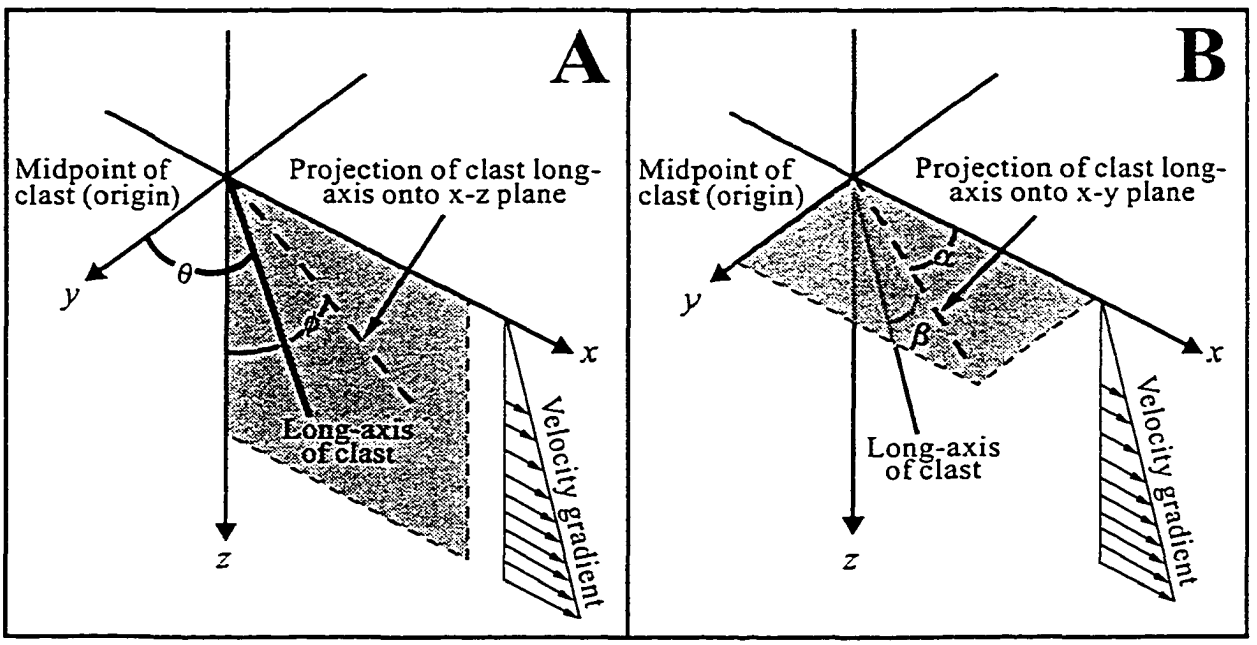

Figure 1. Coordinate system for describing clast rotation. (A) Angles ϕ and θ and (B) angles α (trend) and β (plunge).

where a and b are the longest and shortest axes of the clast, respectively, ϕ_i is the initial value of ϕ, and γ is shear strain. The angle, θ, between the long axis of the clast and the transverse coordinate (y) is then given as a function of its initial value, θ_i, ϕ, and ϕ_i, such that

$$\tan^2\theta = \left(\frac{1}{a^2\cos^2\phi + b^2\sin^2\phi} \right) (\tan^2\theta_i)(a^2\cos^2\phi_i + b^2\sin^2\phi_i) \qquad (2)$$

(Reed and Tryggvason, 1974). From Equations (1) and (2), the angles ϕ□ and θ can be transformed into a trend, α, and plunge, β (Fig. 1B), using the relations:

$$\tan\alpha = \frac{1}{\tan\theta\sin\phi} \text{ , and} \qquad (3)$$

$$\tan\beta = \frac{\cos\alpha}{\tan\phi} \text{ .} \qquad (4)$$

The paths taken by a clast with three different initial plunges and an aspect ratio of 2.0 are shown on a lower hemisphere, equal-area stereonet in Figure 2, in which points are plotted at equal increments of shear strain. The clast will rotate in a set orbit and, for this aspect ratio, make one complete rotation at a shear strain of 15.8. The angular velocities of the clasts are not constant but have minimum and maximum values when parallel and normal to the shear plane, respectively. Consequently, clasts will spend more of their time at orientations in or near the shear plane than away from it. Thus, if a fluid containing randomly oriented clasts is sheared, a weak but discernable flow-parallel fabric is expected to develop.

In addition to formally describing clast rotation, Jeffery suggested that at very high shear strains, clasts would tend to become oriented such that they dissipate the least energy during rotation. This orientation is with the long-axis transverse to the direction of shearing,

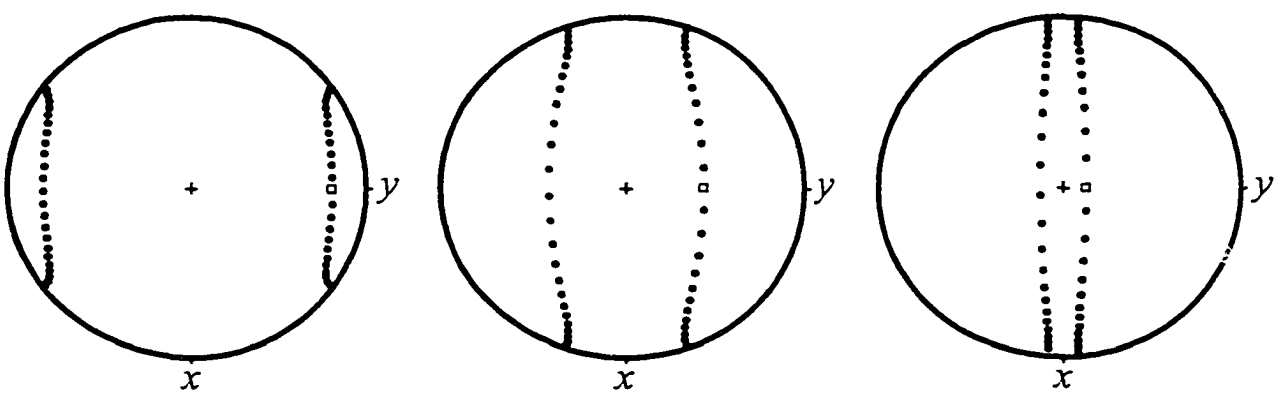

Figure 2. Stereograms of predicted clast rotation for three clasts with an initial trend of 90° and initial plunges of 20°, 55°, and 80°. Points are plotted at increments of equal shear strain and represent the orientations of the long axis of a clast as it traces a path on a lower-hemisphere, equal-area stereonet.

so that clasts roll in the shear zone about that axis. This effect would obviously weaken the flow-parallel fabric. This aspect of Jeffery's paper, although only a postulate, has been emphasized by those who associate weak fabrics with sheared glacier beds (Hart, 1994; Clark, 1997).

APPARATUS

The ring-shear device used in this study (Fig. 3A) shears an 11 liter sediment specimen at a constant shearing rate under a steady stress normal to the shearing direction (Iverson et al., 1996, 1997, 1998, 1999). The sample chamber is sufficiently large to accommodate gravel-size clasts. Transparent outer walls made of hard-coated acrylic allow continuous observation of the outer edge of the specimen during shearing.

The specimen is bounded on the top and bottom by aluminum platens and on its sides by confining walls. The sample chamber has an outside diameter of 0.6 m, a width of 0.115 m, and a height of 0.085 m (Fig. 3B). The sediment is sheared by rotating the lower platen beneath the upper platen with a variable-speed motor and gear boxes. Both the lower and upper platens contain teeth that grip the specimen. The platens contain hundreds of small holes that connect to an internal water reservoir that is open to the atmosphere. The walls bounding the lower half of the specimen move with the lower platen, while those bounding the upper half remain fixed. A uniform normal stress is applied to the sediment by dead weights suspended on a lever arm that presses down on a thick aluminum plate. This plate, termed the normal-load plate, is fixed to the upper platen and is able to move vertically as the sample thickness changes during the early stages of shearing.

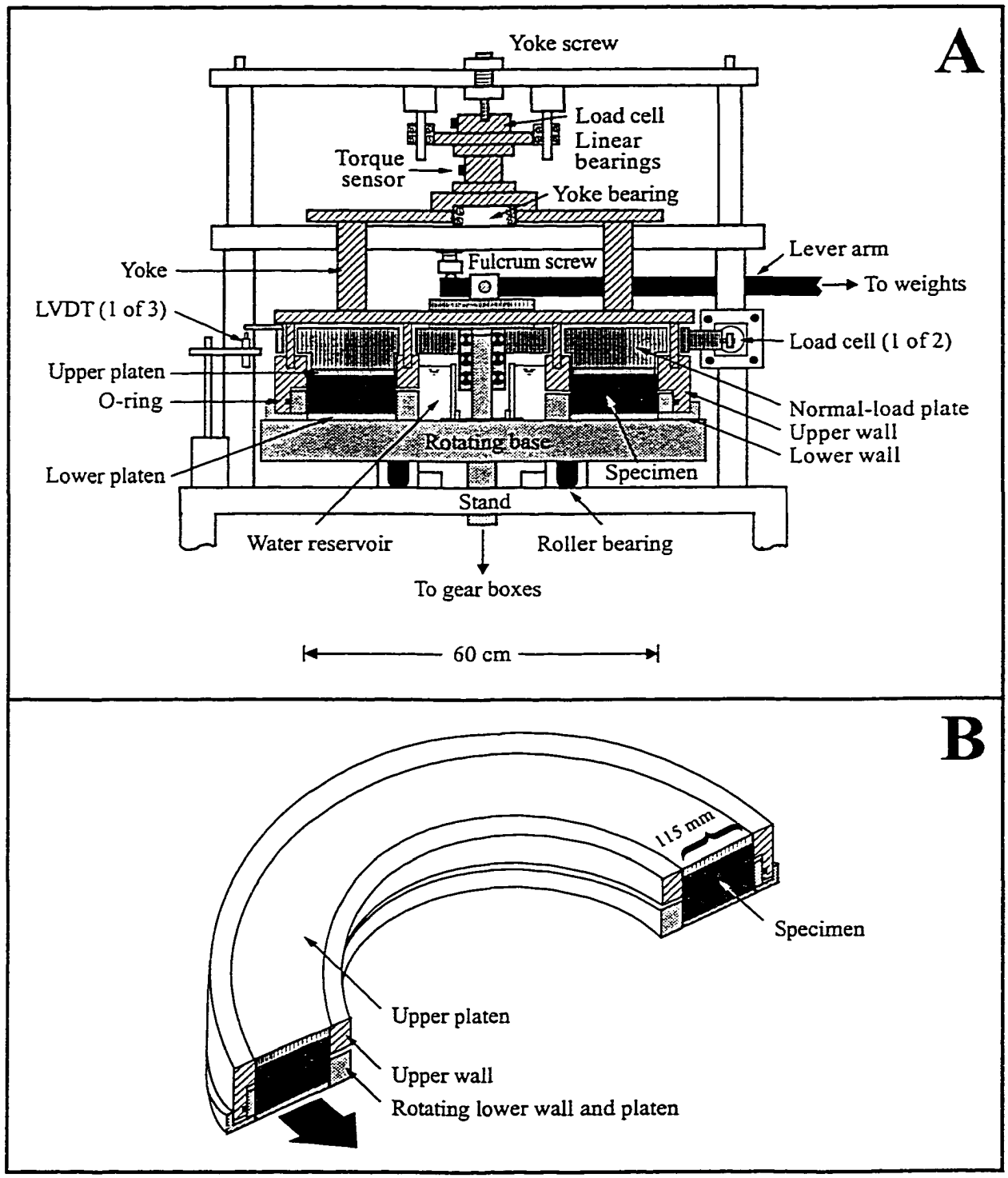

Figure 3. (A) Cross-section of the ring-shear device and (B) schematic of the sample chamber. Lightly-shaded components rotate.

METHODOLOGY

Experiments were performed with two different materials: a transparent linear-viscous putty manufactured by Rhone Poulenc Inc. (RG-20) and a till (4% clay, 21% silt, and 75% sand and gravel) collected from beneath Storgläciaren, a valley glacier in northern Sweden. The till grain-size distribution has a fractal dimension of 2.92 (Hooke and Iverson, 1995), similar to that of some fault gouges (An and Sammis, 1994). Experiments with the putty provided a test of Jeffery's theory for the case of an idealized fluid. The Storgläciaren till was chosen because previous experiments had indicated that a thicker shear zone developed in it than in tills containing more clay (Iverson et al., 1997). In the experiments with till, clasts larger than 6 mm, one-tenth of the smallest specimen dimension, were removed in accordance with suggested geotechnical testing procedures (Head, 1989, p. 83). These clasts, on average, represented 8% of the till by volume. All tests were conducted at a steady shearing rate of 770 m yr^{-1}, comparable to the velocities of some fast-moving glaciers and slow enough to insure the absence of inertial effects.

In experiments with putty, three sets of wooden ellipsoidal clasts with different aspect ratios and sizes (Table 1) were placed vertically in the putty (normal to the shear plane) along the centerline of the specimen annulus. To make clasts neutrally buoyant, they were weighted with copper wire inserted in holes drilled along their long axes. Each clast was marked for identification and separated from its nearest neighbor by at least three times the length of its longest axis. In addition to the clasts, five columns of displacement markers, consisting of small-segmented aluminum rods 3-4 mm in diameter, were placed in the putty at evenly spaced intervals across the width of the specimen to assess the distribution of strain. A small normal stress (5 kPa) was then applied to insure complete coupling between the putty and the

Table 1. Characteristics of clasts in putty experiments.

Shape	Long-axis length (mm)	Intermediate/ short-axis length (mm)	Aspect ratio
ellipsoidal	10.0	8.0	1.25
ellipsoidal	10.0	5.0	2.0
ellipsoidal	14.0	5.0	2.8

normal stress (5 kPa) was then applied to insure complete coupling between the putty and the upper and lower platens, and the putty was sheared. The location of the displacement markers and the angle ϕ for each clast were measured every 15 minutes through the transparent walls. A protractor was used to measure ϕ. Repeated measurements indicated an error of $\pm 2°$.

Two sets of experiments were performed with the till. In the first set, tests were conducted in which wooden clasts (Table 1) were initially oriented vertically. Unlike the tests with the transparent putty, clasts could not be observed continuously during shearing. Therefore, to determine the relation between clast rotation and shear strain, a series of 11 tests was carried out to various displacements, corresponding to shear strains ranging from 1.4 to 372.0. Clasts were marked on one end to help constrain the extent of their rotation at the end of a test. In a second set of experiments, tests were carried out to shear strains greater than 200 with clasts initially oriented randomly in the till. Both natural and idealized clasts of various sizes and aspect ratios (Table 2) were used to help assess the possible effects of clast size and shape on fabric development. As in the experiments with putty, clasts were separated from their nearest neighbors by, at least, three times the length of their longest axis. Vertical columns of displacement markers, spherical wooden beads 4 mm in diameter, were inserted across the width of the specimen to assess the distribution of shear strain. The device was then assembled and the till sheared to a predetermined displacement under a normal stress of 85 kPa, comparable to effective stresses measured beneath some ice sheets (e.g., Engelhardt et al., 1990). The sample was then unloaded, drained, and carefully dissected to measure the orientation of each clast and the location of the displacement markers. A point gauge was used to measure the coordinates of the ends of each clast from

Table 2. Characteristics of clasts in till experiments.

Shape and composition	Long-axis length (mm)	Intermediate/ short-axis length (mm)	Aspect ratio
glass cylinders	6.0	2.0	3.0
wooden ellipsoids	10.0	5.0	2.0
natural clasts (limestone)	7.0-16.0	3.0 - 9.0	>2.0

which orientations were derived.

Clast fabric was evaluated using the eigenvalue method of Mark (1973), which has been used extensively to evaluate the three-dimensional fabric of glacigenic sediments (e.g., Lawson, 1979a; Shaw, 1982; Dowdeswell and Sharp, 1986). To use this method, the long axis of each clast is represented as a unit vector. Each unit vector expressed in Cartesian coordinates is multiplied by its transpose, and the products are summed for all observations to obtain the 3 x 3 matrix, A:

$$A = \sum_{i=1}^{n} X_i X_i^t \ , \tag{5}$$

where X_i is the unit vector that corresponds to the i^{th} observation, X_i^t is the transpose of X_i, and n is the number of observations. This matrix is used to calculate the eigenvectors V_1, V_2, and V_3, and the corresponding normalized eigenvalues S_1, S_2, and S_3. The eigenvalues represent the strength of the fabric, or the degree of clustering around each of the axes defined by the eigenvectors. S_1 values of 1.0 and 0.33 indicate perfectly aligned and randomly oriented clasts, respectively, neglecting the unlikely possibility that clast orientations are both bimodal and orthogonal (Mark, 1973). In practice, if the number of clasts considered is not extremely large, randomly oriented clasts may yield S_1 values significantly larger than 0.33 (Woodcock and Naylor, 1983). For example, the random number generator used to calculate the position of 50 clasts at the beginning of some of our experiments yielded an S_1 value of 0.49.

RESULTS

Putty

The columns of segmented aluminum rods, inserted in the putty at the beginning of each experiment, indicate that near the specimen center at the site of the clasts strain was distributed uniformly over the thickness of the specimen (Fig. 4). Shear strain, therefore, could be easily calculated from the specimen thickness and shearing displacement.

The rotation of clasts in the vertical flow plane and the predictions of Jeffery's theory are presented in Figure 5. Also shown is the rotation of a passive line, consistent with the model of March (1932), who treated inclusions as passive markers. Clasts in the putty rotate in a set orbit that closely matches the Jeffery theory with a slight deviation for clasts with aspect ratios of 2.8. Clasts with smaller aspect ratios rotate more quickly, and thus, spend less time in or near the shear plane than more elongate clasts. For example, clasts with aspect ratios of 1.25 and 2.8 make one complete rotation at shear strains of 12.5 and 20, respectively (Fig. 5A and 5C). No interactions between clasts occurred.

Till

At the centerline of the specimen, shear strain within the till occurred in a 40-50 mm thick zone, as indicated by the final location of displacement markers (Fig. 6). Strain in this zone was distributed roughly uniformly, and thus, using the thickness of this zone, shear strain could be determined from the shearing displacement. The shear-zone thickness decreased laterally away from the centerline toward the walls, forming a lens-shaped region in transverse cross-section (Fig. 7). The post-shearing position of clasts usually fell well within the center of this zone. Clasts that did not were disregarded in fabric analyses. The

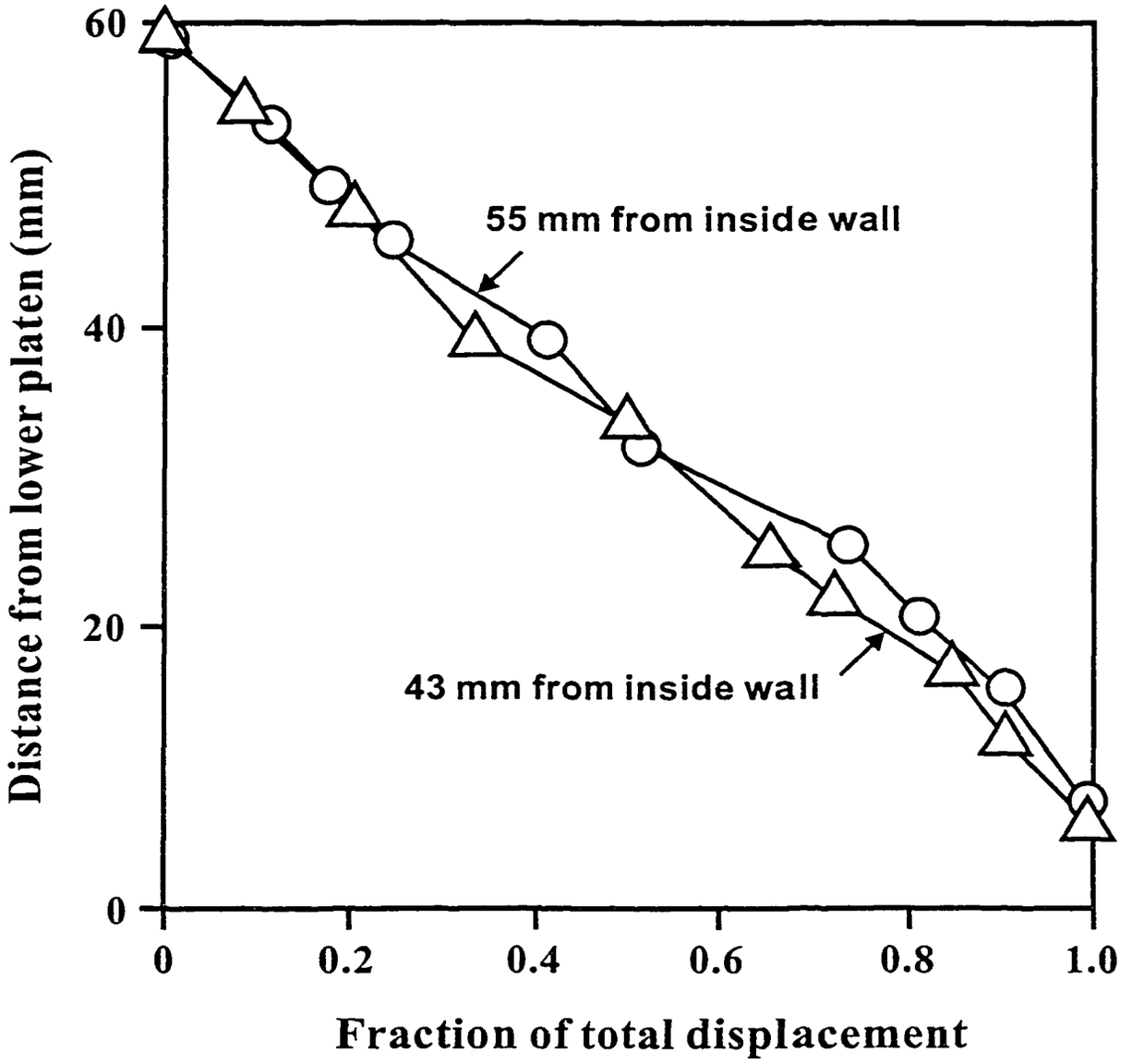

Figure 4. Profiles of longitudinal displacement in the putty. Profiles are 43 mm and 55 mm from the inside wall (specimen center is at 57.5 mm). See also Iverson et al. (1997).

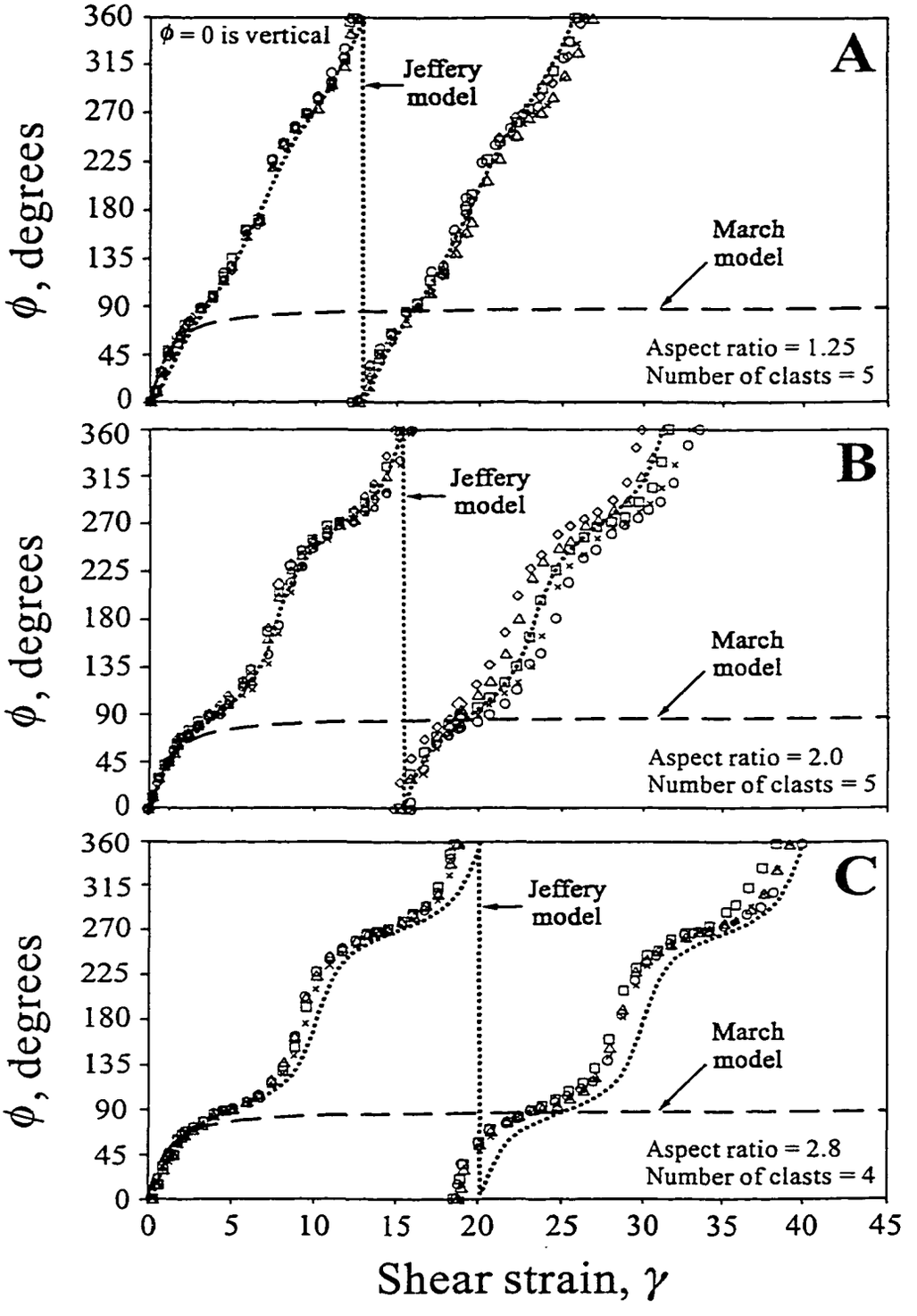

Figure 5. Rigid clast rotation in the putty of (A) 5 clasts with an aspect ratio of 1.25, (B) 5 clasts with an aspect ratio of 2.0, and (C) 4 clasts with an aspect ratio of 2.8. Various symbols represent the orientations of individual clasts. Model predictions of Jeffery (1922) and March (1932) are also shown.

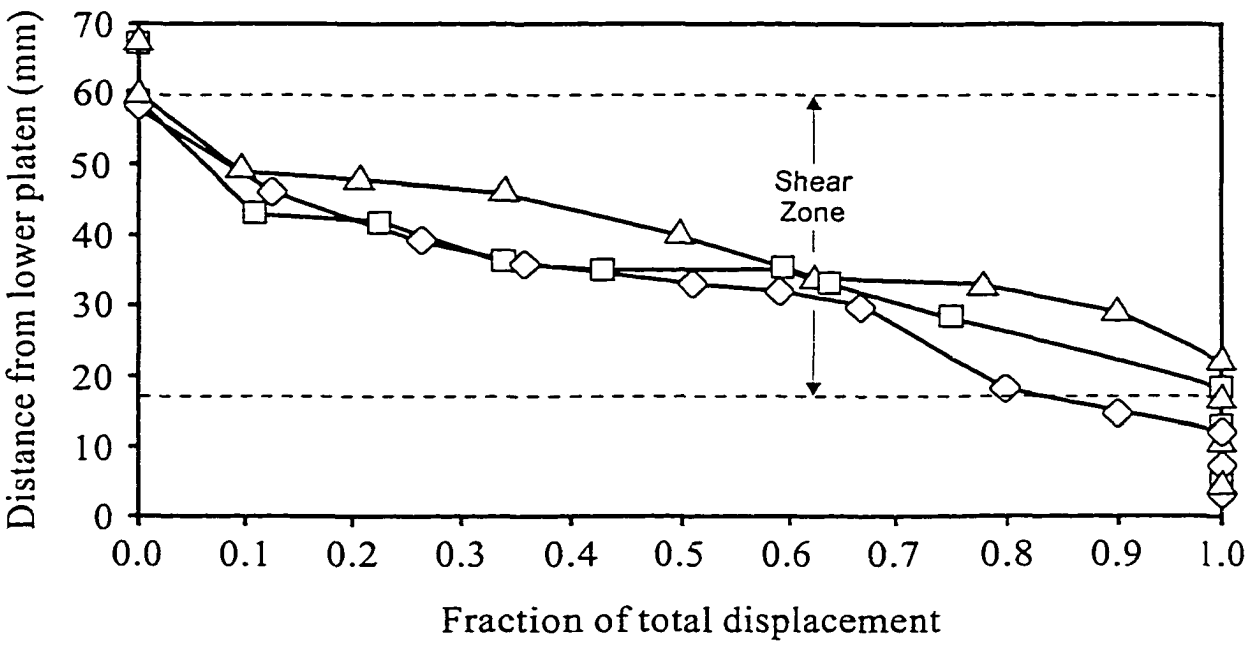

Figure 6. Profiles of longitudinal displacement in the till. Profiles are 38,57, and 78 mm from inner wall.

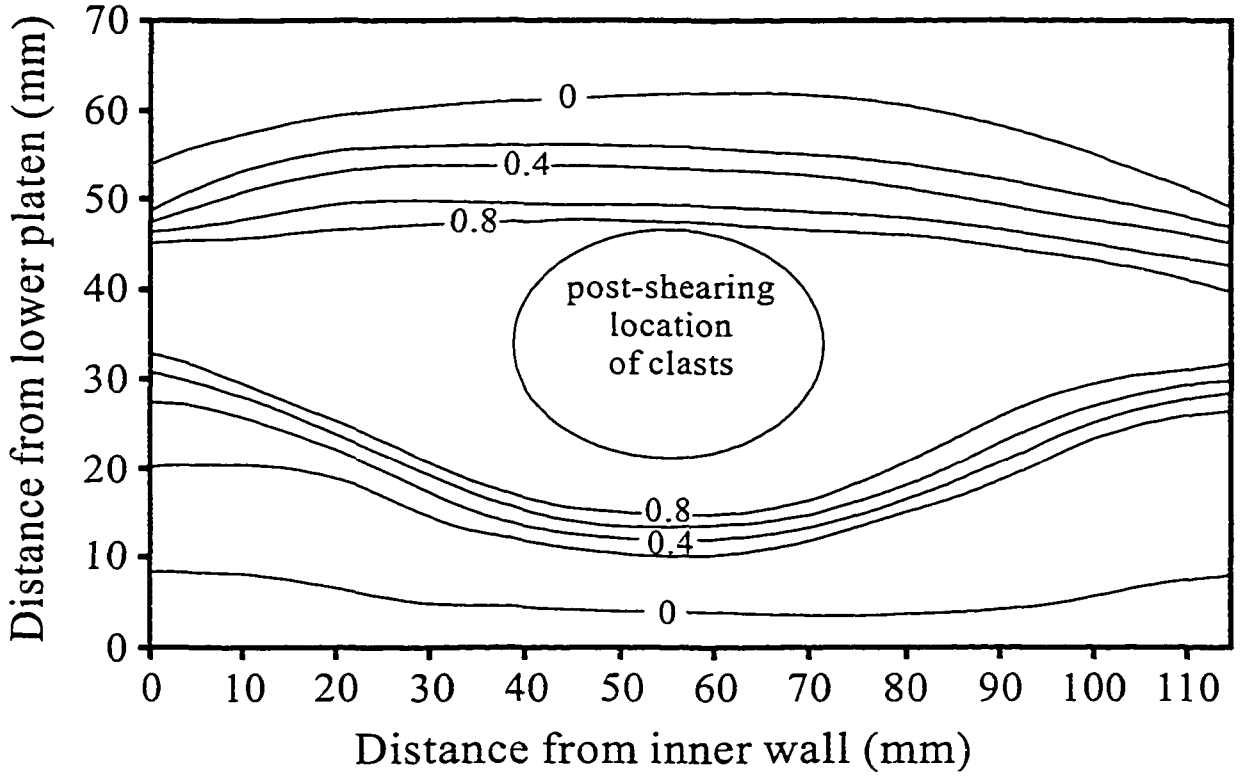

Figure 7. Distribution of shear strain in the till in a transverse cross-section. Shear strain has been normalized to the total cumulative strain at each position across the specimen width. The centers of those clasts used to compute fabrics were within the ellipse at the ends of experiments. Confining walls are at 0 and 115 mm.

thinning of the shear zone toward the edge of the specimen implies that the till underwent some shear strain transverse to the flow direction that varied with position. Analysis of displacement markers across the specimen width indicates that transverse shear strain across any single clast was never more than 2% of the longitudinal strain.

Rotation of clasts in the till experiments was markedly different from that of the putty experiments. Contrary to Jeffery's theory, most clasts rotated into the plane of shearing and remained there with continued deformation, similar to the behavior of a passive marker and consistent with the model of March. This was demonstrated in the tests carried out to various shear strains in which the long axes of approximately 10 to 50 clasts were initially oriented vertically (Fig. 8). The average rotation of the clasts quickly increased to near ϕ=90°, the orientation of the shear plane, and thereafter, increased very slowly with strain as a result of a few clasts sporadically rotating out of the shear plane. Plotting fabric strength as a function of shear strain for these tests reveals that the initial fabric weakened slightly in experiments carried out to relatively small shear strains (γ<25), but then remained strong (S_1~0.80) at larger strains, up to values greater than 300 (Fig. 9). Stereograms for all of the tests are presented in Figure 10.

Fabric results from four tests using clasts in initially random orientations (S_1=0.49) and run to shear strains greater than 200 are presented in Figure 11. The data show that a strong fabric parallel to the shearing direction developed in all tests with a mean S_1 eigenvalue of 0.83. This was true, regardless of the different shapes and sizes of the clasts used in these tests (Table 2). Statistics from the four fabrics (Table 3) indicate that the eigenvectors of the long axes of clasts (V_1) dip slightly (4-8°) in the direction of the rotating base or "upglacier".

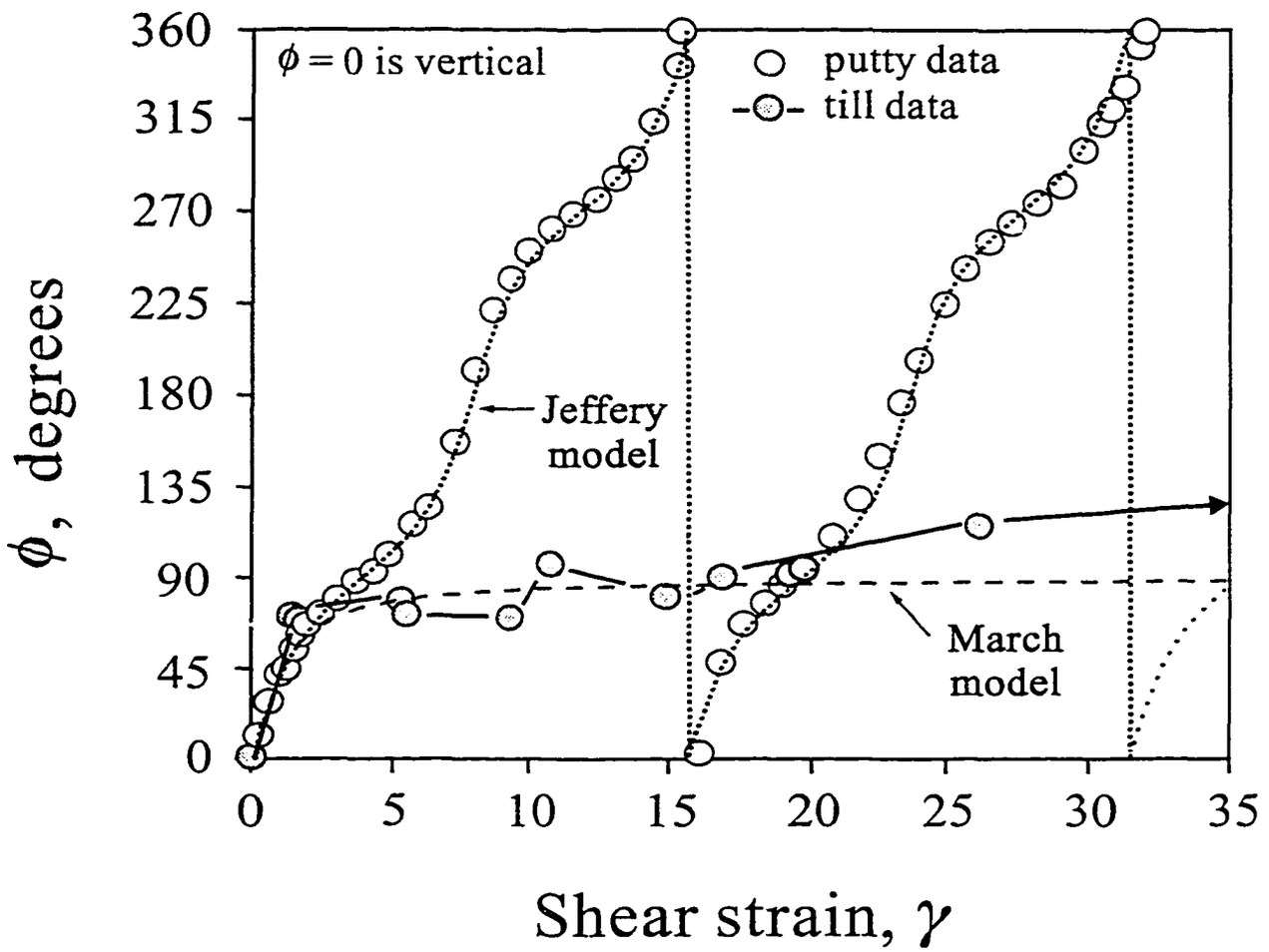

Figure 8. Rotation of clast long axes as predicted by Jeffery (1922) and March (1932), as observed in the putty (open circles), and as observed in the till (solid circles). Orientations of clasts in the putty are based on the average orientation of 5 clasts presented in Figure 5B (aspect ratio = 2.0). Orientations of clasts in till are based on the average orientation of approximately 50 clasts (aspect ratio = 2.0) in experiments terminated at the indicated strains.

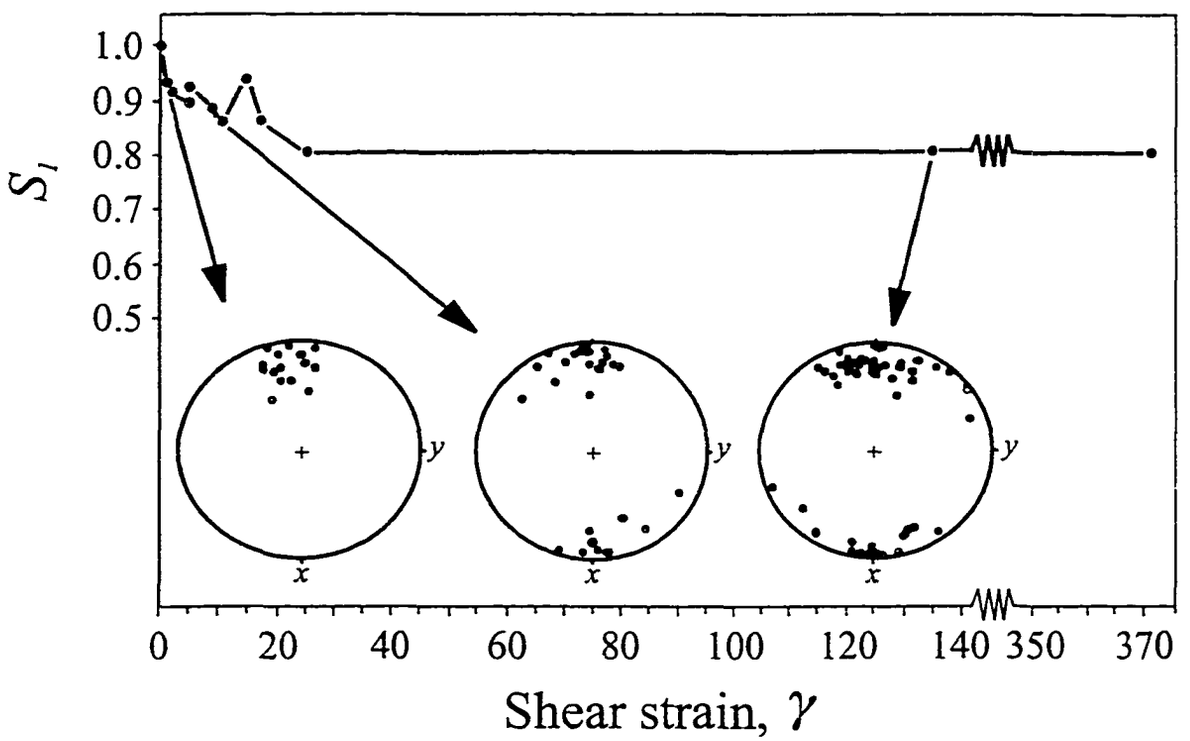

Figure 9. Fabric strength (S_1 eigenvalue) as a function of shear strain in till experiments with initially vertical clasts. The sense of shearing in the stereograms is bottom north\top south.

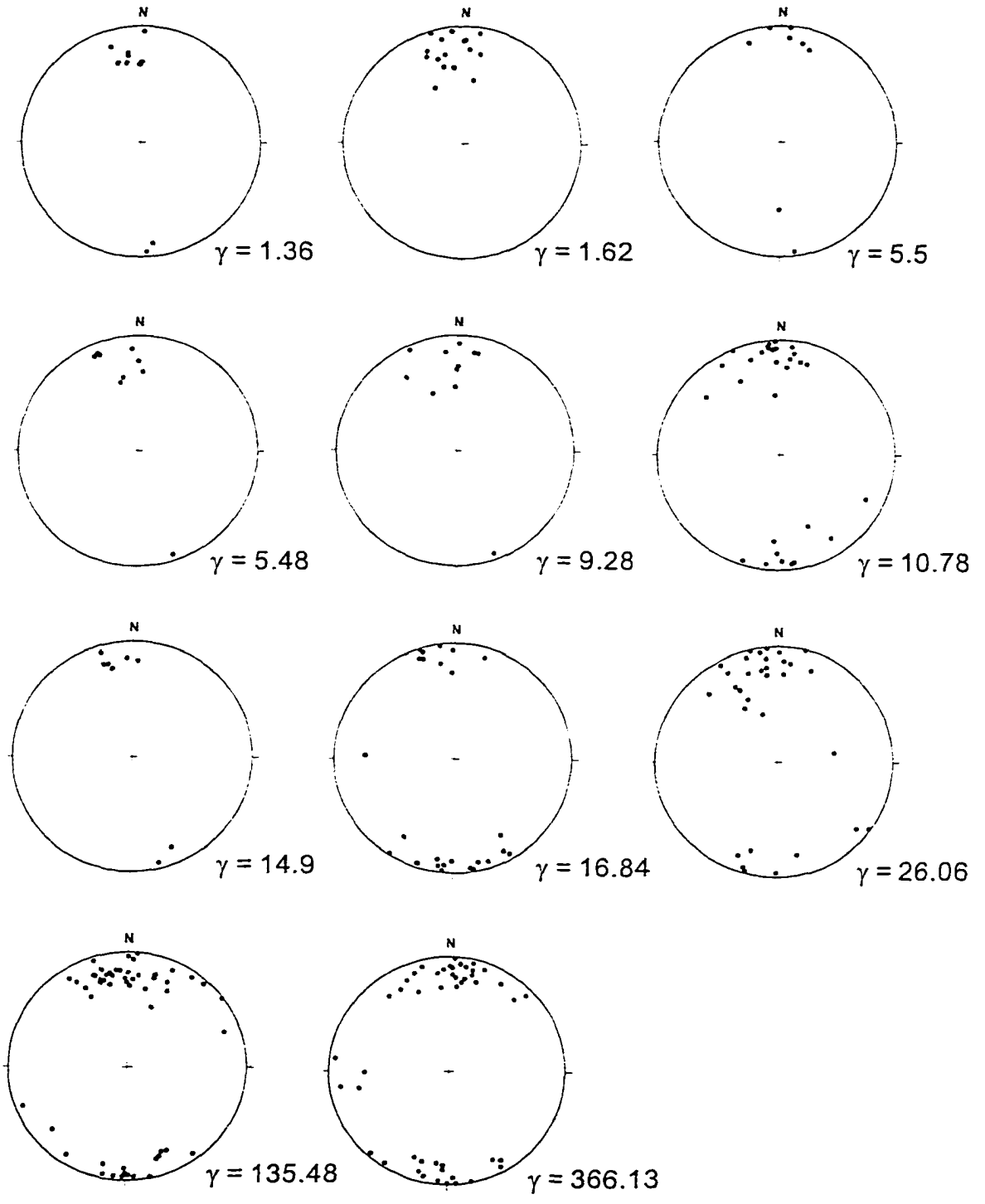

Figure 10 Stereograms for 11 till experiments with initially vertical clasts at various shear strains. The points represent the orientations of the long axes of clasts on a lower-hemisphere, equal-area stereonet.

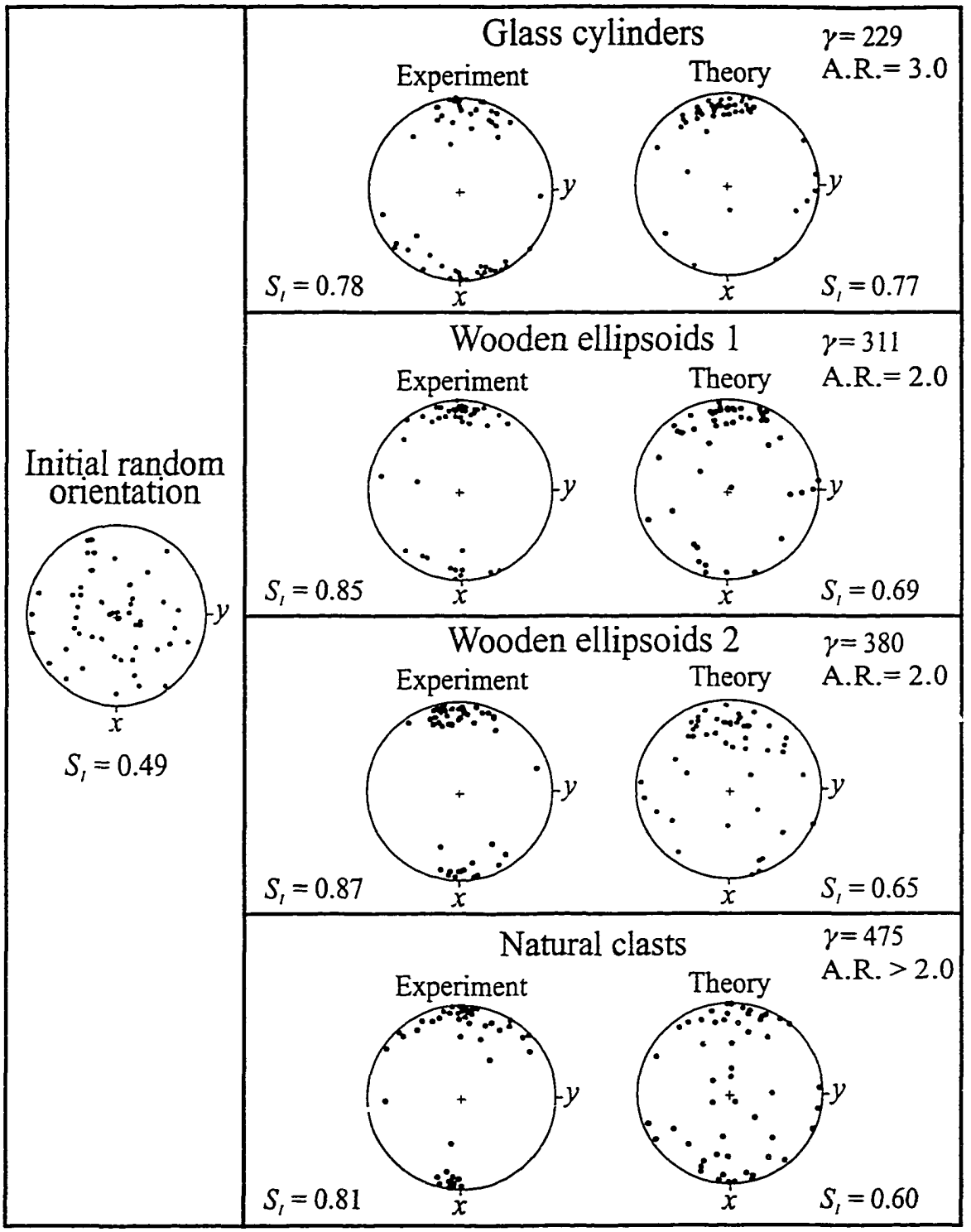

Figure 11. Experimental fabrics and those predicted by the theory of Jeffery (1922) in tests carried out to high strains (>229). Idealized and natural clasts of various aspect ratios (A.R.) were used with the same initially random fabric. Complete fabric statistics are included in Table 3. The sense of shearing is bottom north\top south.

Table 3. Fabric results for clasts originally oriented randomly in till.

		Experiments					Theory				
Shape and composition	Aspect ratio	No. of clasts	S_1	S_3	Trend	Plunge	No. of clasts	S_1	S_3	Trend	Plunge
glass cylinders	3.0	51	0.78	0.06	2°	4°	51	0.77	0.05	355°	15°
wooden ellipsoids 1	2.0	46	0.85	0.04	359°	8°	51	0.69	0.09	2°	12°
wooden ellipsoids 2	2.0	47	0.87	0.05	356°	7°	51	0.65	0.12	357°	23°
natural clasts (limestone)	>2.0	47	0.81	0.06	3°	6°	51	0.60	0.09	4°	21°

In contrast, given the same set of initially random clasts, Jeffery's theory predicts significantly weaker fabrics overall with a mean S_1 eigenvalue of 0.68. The only exception was the S_1 value indicated by Jeffery's theory in the experiment with glass cylinders, 0.77, which was close to the experimental value of 0.78. This probably reflects the large aspect ratio of the glass cylinders (3.0). The Jeffery model is expected to be a better approximation in this case because it predicts that clasts with high aspect ratios should spend more time oriented in or near the shear plane than less elongate clasts.

DISCUSSION

Laboratory results

These experiments demonstrate that clasts in shearing till rotate into the shear plane and tend to remain there, contrary to Jeffery's theory. Although clasts occasionally rotate out of the shear zone and thereby flip 180°, presumably due to sporadic interactions with other large particles, the rotation of a passive marker (March, 1932) provides a better estimate of clast rotation (Fig. 8). The overall result is that strong fabrics develop parallel to the shearing direction with no obvious sensitivity to the shapes and sizes of clasts. This behavior is likely to be due to slip between the till matrix and clasts as clasts align in the direction of shearing. Such slip, or alternatively the focusing of strain in the matrix immediately adjacent to clasts, deviates from Jeffery's theoretical assumption of a no-slip boundary. It is a reasonable conjecture given that till is a frictional-plastic granular material (Iverson et al., 1998; Tulaczyk, 1999), rather than a fluid like that considered by Jeffery. Such slip commonly occurs between rigid substrates and slowly deforming clays and gouges (Tika-Vassilikos, 1991; Dieterich, 1981; Biegel et al., 1989). Furthermore, strain in the rheologically plastic

matrix is expected to be focused immediately adjacent to clasts where gradients in deviatoric stress are larger than elsewhere.

Analogue experiments, indeed, demonstrate that slip of the matrix along the surfaces of clasts results in stronger fabrics than if there is no slip. In the experiments of Ildefonse and Mancktelow (1993), paraffin wax of different melting points was used to simulate differing degrees of slip between rigid clasts and the wax matrix. Although these experiments were carried out to only small shear strains (γ<4), clasts rotated toward the shear plane and tended to remain parallel to it, resulting in a significantly stronger preferred orientation than in identical tests with no slip. Consequently, Ildefonse and Mancktelow concluded that slip results in clast behavior similar to that of passive markers.

As in any experimental study, we must consider whether the results, in this case the deviation between Jeffery's theoretical prediction and the results of the till experiments, somehow reflect the peculiarities of the experimental technique. The results of the putty experiments (Fig. 5) not only validate Jeffery's theory for the case of a viscous fluid, as has been done in other studies (e.g., Trevelyan and Mason, 1951; Ghosh and Ramberg, 1976; Fernandez et al., 1983; Ildefonse et al., 1992), but also indicate that the experimental approach is sound. The failure of Jeffery's theory to predict the rotation of clasts in till, therefore, must reflect a violated assumption, such as the no-slip boundary condition as suggested here, or some other uncertainty associated with the granular nature of till.

One such source of uncertainty was the non-uniform distribution of shear strain within the till. In about a 40 mm thick zone at the specimen center, however, shear strain was distributed relatively uniformly (Fig. 6). The thickness of this zone was 4 to 7 times the length of the long axes of clasts. If clasts were too large relative to the thickness of this zone,

the behavior of clasts should have varied systematically with their size. No such variation occurred.

Another source of uncertainty in the till experiments is the potential interaction of clasts within the shear zone. This is important because experiments by Ildefonse and Fernandez (1988) and Arberet et al. (1996) have shown that interacting clasts maintain a metastable orientation close to the direction of shearing longer than isolated clasts, resulting in a stronger fabric. Unlike the putty experiments during which clasts could be continuously observed, clasts in the till were only visible at the end of a given test. However, dissection of the specimen at the ends of tests indicated that approximately 75 % of clasts had no nearest neighbor closer than 25 mm, as might be expected from the large initial clast spacing. Therefore, clast interaction was apparently minimal.

A final potential source of uncertainty is the transverse shear strain that occurred due to the thinning of the shear zone toward the walls of the sample chamber (Fig. 7). Such flow is not expected subglacially or along fault zones and was not considered by Jeffery. Transverse shear strain should cause clasts to rotate toward the vertical flow plane (x-z plane), potentially strengthening the fabric. For clasts located at the specimen center, the transverse shear strains caused by the symmetric thinning of the shear zone toward the inner and outer walls are equal, resulting in no rotation. However, some clasts located initially at the specimen center moved up to 15 mm from the centerline during shearing. Despite this effect, however, calculations using the measured displacement field indicate, as noted earlier, that none of the clasts experienced a transverse shear strain that was greater than 2% of the longitudinal strain. Furthermore, clasts at the centerline were not oriented differently than those displaced laterally. Therefore, transverse shear strain likely had a negligible influence

on the fabric results. This conclusion is supported by the results of the putty experiments, in which there were also small transverse strains but good agreement with Jeffery's theory (Fig. 5 and 8).

Implications for field studies

As noted earlier, glacial geologists have often inferred from field observations that subglacial deformation of till produces a weaker clast fabric than the lodgment process (e.g., Dowdeswell and Sharp, 1986; Hicock, 1992; Hart, 1994; Clark, 1997). Eigenvalues from such studies are shown in Figure 12, along with our laboratory results. Figure 12 illustrates that if the inferred lodgment tills are really a result of the lodgment process, then deformation should strengthen, rather than weaken, the fabric of such tills. Indeed, the strengths of fabrics generated in our experiments, as represented by S_1 eigenvalues, are greater than those of either the deformation or lodgment tills inferred from these field studies (Fig. 12).

A possible source of uncertainty in this comparison of laboratory and field results is that the experimental clasts were smaller than those often used in field studies. If clasts are surrounded by predominately smaller particles, however, the behavior of clasts during shearing should be independent of their size. About 75% of the till mass consisted of particles that were more than an order of magnitude smaller than the experimental clasts. Furthermore, the self-similar particle-size distributions of some basal tills (Hooke and Iverson, 1995) indicate that clasts, regardless of their sizes, should be surrounded by smaller particles.

The results in Figure 12 indicate that there is good reason to be skeptical of the field criteria used to independently identify so-called "deformation tills." In fact, the state of the

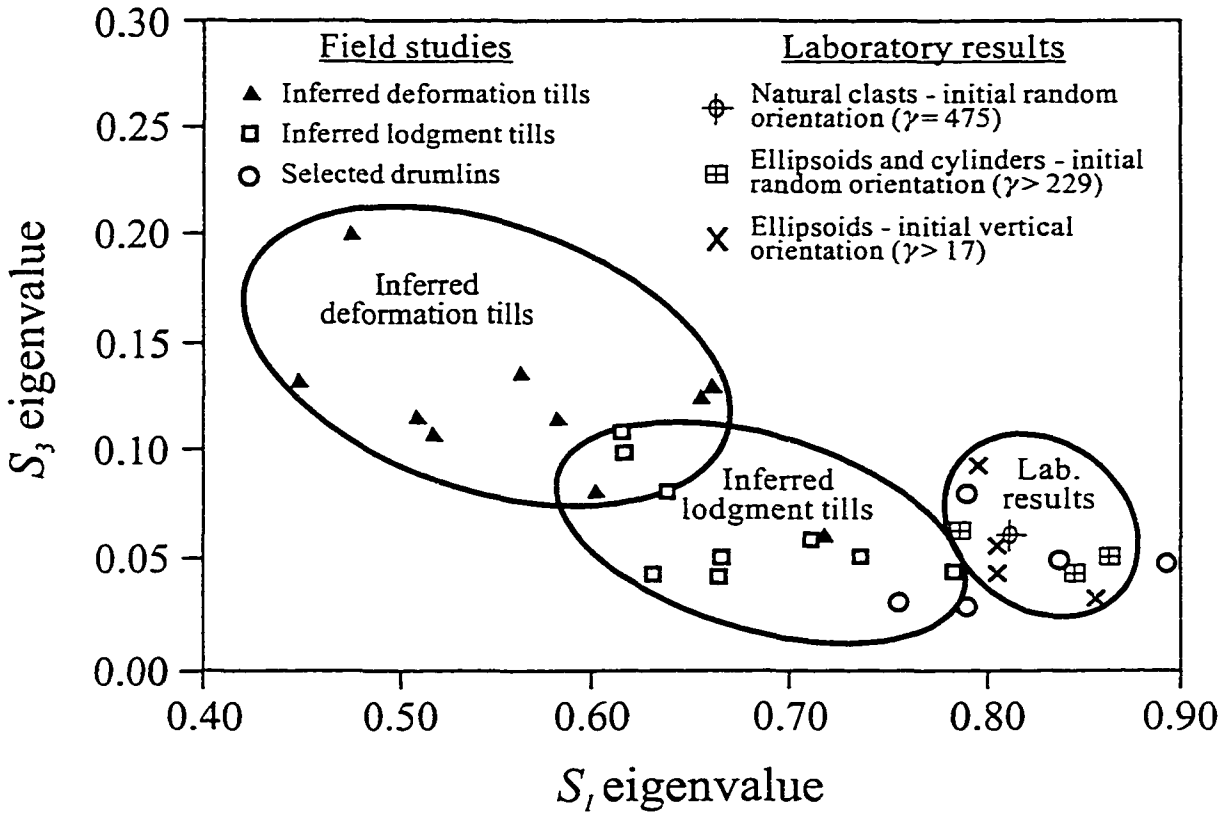

Figure 12. Eigenvalues from these experiments, those from data collected from selected drumlins (Evenson, 1971, Krüger and Thomsen, 1984; Stanford and Mickelson, 1985), those for inferred lodgment tills, and those thought to have been deformed (Dowdeswell and Sharp, 1986). The last of these are labeled as "deformation tills," although Dowdeswell and Sharp used the terminology, "deformed lodgment till."

art is such that two scientists working on the same till exposures may reach markedly different conclusions. For example, Allen et al. (1991) measured fabrics in two till units in East Anglia, U.K. The lower unit, which they thought had been sheared subglacially, has strong fabrics with S_1 eigenvalues of 0.77 to 0.86 (as calculated by Hart, 1994), similar to those of these experiments. The upper unit, which Allen et al. (1991) interpreted to be a lodgment till, has a weaker fabric. In contrast, Hart (1994), after studying the same stratigraphy, reached the opposite conclusion: that the upper unit had been highly deformed and that the lower unit had been sheared significantly less. Similarly, certain characteristics of basal tills of the Laurentide Ice Sheet, such as sharp till contacts and overconsolidation, have been interpreted as indicators of both relatively rigid (e.g., Clayton et al., 1989) and highly deformed (Alley, 1991) beds. This level of disagreement demonstrates the difficulty of confidently identifying highly sheared tills in the field and casts doubt on whether fabric fields based on only field interpretations, like those for deformation and lodgment till in Figure 12, are meaningful.

Our laboratory results indicate that basal tills with weak fabrics probably have not undergone the high strains required of the deforming-bed mechanism of glacier motion. Thus, basal tills with weak fabrics currently interpreted as "deformed lodgment tills" or "deformation tills" (e.g., Dowdeswell and Sharp; 1986; Hicock and Dreimanis, 1992; Hicock, 1992; Hart, 1994; Clark, 1997) either have been deformed only slightly or may well be the result of other processes associated with lodgment, melting out of debris from stagnate ice, or inertial post-depositional debris flows. For example, Clark (1997) has noted that basal tills of the Laurentide Ice Sheet often have weak fabrics. Our fabric results, therefore, indicate that these extensive till sheets have not been pervasively sheared to high strains. This

is contrary to assumptions made in some models (Jenson et al., 1996; Clark et al., 1996; Licciardi et al., 1998) but supported by interpretations of measurements beneath some modern glaciers (Iverson et al., 1995) and ice sheets (Engelhardt and Kamb, 1998), which indicate that motion is focused at the glacier sole rather than at depth in the bed.

Interestingly, strong fabrics quantitatively consistent with our results are sometimes observed in drumlinized moraine, where a convincing independent case can sometimes be made for a mobile bed that experienced significant deformation, at least locally. Particle orientations in some drumlins (Evenson, 1971; Krüger and Thomsen, 1984; Stanford and Mickelson, 1985) yield eigenvalues similar to those of this study (Fig. 12). In addition, at least some basal tills not associated with drumlins have fabrics that are similarly strong (Johnson and Hansel, 1990; Allen et al., 1991). Our fabric results, therefore, fall within the range of some field observations and agree with the belief that some drumlins are associated with bed deformation (Smalley and Unwin, 1968; Menzies, 1989; Boulton, 1987).

Clasts that have survived comminution in fault gouge are commonly aligned (e.g., Chester and Logan, 1987; Cladouhos, 1999). An important question is whether our fabric results can be extended to gouge, which is texturally and genetically similar to basal till but may deform at different effective confining pressures and scales. Studies of other fabric forming elements in gouge, however, demonstrate that fabric development is generally insensitive to such factors. For example, styles of microfracture development in simple shear do not vary significantly in laboratory tests conducted over a wide range of confining pressures, and field studies of natural fault zones have documented these same relatively invariant fracture styles in gouge layers that vary widely in thickness (see Logan et al., 1992, for a review).

Therefore, there is reason to believe that these experimental results can be applied to gouge deformation. They indicate that any gouge with a weak survivor-grain fabric either has undergone only minor shear strain or has been subject to a contemporaneous or subsequent process that disrupted clast alignment.

As end-members of the general model of Ghosh and Ramberg (1976), Cladouhos (1999) considered the models of both Jeffery (1922) and March (1932) in his study of fabrics formed by sub-millimeter survivor grains in gouge. The March model predicts that inclusions rotate toward but not through the shear plane with strain. Despite the observed tendency for clasts to occasionally rotate out of the shear plane, our results indicate that this model is the better of the two idealizations for describing fabric development in a granular material undergoing simple shear. This conclusion, although consistent with analogue experiments in which there was slip between clasts and a shearing matrix (Ildefonse and Mancktelow, 1993), should not necessarily be extended to other materials that may behave as fluids and adhere to inclusions. For example, porphyroblasts in rocks that have undergone solid-state deformation (e.g., Simpson and Schmid, 1983; Bell, 1985; Johnson, 1990) may exhibit a range of slip behavior and thus may have behaved quite differently from clasts in our tests.

CONCLUSIONS

Isolated elongate clasts in shearing till, regardless of their shapes, sizes, and initial orientations, rotate into the plane of shearing, and generally remain there to high strains, contrary to the widely applied model of Jeffery (1922). Consistent with results of other experiments with inclusions (Ildefonse and Mancktelow, 1993), we hypothesize that this

behavior is due to either slip or strain localization at or near the surfaces of clasts, a reasonable expectation in a granular material. Resulting fabrics are essentially parallel to the flow direction and strong, with an average S_1 eigenvalue of 0.83 for initially random clasts in till sheared to strains of 229-475. This degree of clast alignment is considerably greater than that measured in many basal tills interpreted to be the result of bed deformation but is similar to that measured in some drumlins.

Basal tills or fault gouges with weak clast fabrics, therefore, either have undergone little or no shear strain or have been subjected to some other process that may have disrupted clast alignment. The widely applied criterion that attributes weak clast fabrics in basal till to bed deformation should be rejected. This implies that many basal tills of the Laurentide Ice Sheet, which have weak fabrics and are thought by some to have been sheared to high strains, may have undergone little or no deformation.

In studies of clast rotation in shearing geological materials, either the Jeffery or March model is often considered. In granular materials like till and gouge, the March model better approximates the kinematics of clast rotation and fabric development during simple shear.

ACKNOWLEDGMENTS

These experiments were initiated when both authors were at the University of Minnesota. We thank the Department of Geology and Geophysics there for enabling us to transfer our equipment to Iowa State University. We also thank J. Marchetti, foreman of the electrical engineering machine shop at the University of Minnesota, for his skillful assistance in constructing the ring-shear device, and R. Baker for assisting with some of the experiments. This work was supported by the NSF, OPP-9530814.

REFERENCES

Allen, P., Cheshire, D.A., and Whiteman, C.A., 1991, The tills of southern East Anglia, *in* Ehlers, J., Gibbard, P.L., and Rose, J. eds., Glacial deposits in Great Britain and Ireland: Balkema, Rotterdam, p. 255-278.

Alley, R.B., Blankenship, D.D., Bentley, C.R. and Rooney, S.T., 1986, Deformation of till beneath ice stream B, West Antarctica: Nature, v. 322, p. 57-59.

Alley, R.B., 1991, Deforming-bed origin for southern Laurentide till sheets?: Journal of Glaciology, v. 37, p. 67-76.

An, L.J., and Sammis, C.G., 1994, Particle size distribution of cataclastic fault materials from southern California: a 3-D study: Pure and Applied Geophysics, v. 143, p. 203-227.

Arberet, L., Diot, H., and Bouchez, J.L., 1996, Shape fabrics of particles in low concentration suspensions: analogue experiments and application to tiling in magma: Journal of Structural Geology, v. 18, p. 941-950.

Bell, T.H., 1985, Deformation partitioning and porphyroblast rotation in metamorphic rocks: a radical reinterpretation: Journal of Metamorphic Geology, v. 3, p 109-118.

Biegel, R.L., Sammis, C.G., and Dieterich, J.H., 1989, The frictional properties of a simulated gouge having a fractal particle distribution: Journal of Structural Geology, v. 11, p. 827-846.

Boulton, G.S., 1971, Till genesis and fabric in Svalbard, Spitsbergen, *in* Goldthwait, R.P., ed., Till, a symposium: Columbus, Ohio State University Press, p. 41-72.

Boulton, G.S., 1987, A theory of drumlin formation by subglacial sediment deformation, in Menzies, J., and Rose, J., eds., Drumlin Symposium: A.A. Balkema, Rotterdam, p. 25-80.

Boulton, G.S., 1996, The theory of glacial erosion, transport and deposition as consequence of subglacial sediment deformation: Journal of Glaciology, v. 42, p. 43-62.

Byerlee, J.D., Mjachkin, V., Summers, R., and Voevoda, O., 1978, Structures developed in fault gouge during stable sliding and stick-slip: Tectonophyiscs, v. 44, p. 161-171.

Chester, F.M. and Logan, J.M., 1987, Composite planar fabric of gouge from the Punchbowl Fault, California: Journal of Structural Geology, v. 9, p. 621-634.

Cladouhos, T.T., 1999, Shape preferred orientations of survivor grains in fault gouge: Journal of Structural Geology, v. 21, p.419-436.

Clark, P.U., 1994, Unstable behavior of the Laurentide Ice Sheet over deforming sediment and its implications for climate change: Quaternary Research, v. 41, p. 19-25.

Clark, P.U., and Walder, J.S., 1995, Subglacial drainage, eskers, and deforming beds beneath the Laurentide and Eurasian ice sheets: Geological Society of America Bulletin, v. 106, p. 304-314.

Clark, P.U., Licciardi, J.M., MacAyeal, D.R., and Jenson, J.W., 1996, Numerical reconstruction of a soft-bedded Laurentide Ice sheet during the last glacial maximum: Geology, v. 24, p. 679-682.

Clark, P.U., 1997, Sediment deformation beneath the Laurentide Ice Sheet, *in* Martini, I.P., ed., Late glacial and postglacial environmental changes, Quaternary, Carboniferous-Permian and Proterozoic: Oxford University Press, New York, p. 81-97.

Clayton, L., Teller, J.T., Attig, J.W., and Mickelson, D.M. 1989, Evidence against pervasively deformed bed material beneath rapidly moving lobes of the southern Laurentide ice sheet: Sedimentary Geology, v. 62, p. 203-208.

Dieterich, J.H., 1981, Constitutive properties of faults with simulated gouge, *in* Carter, N.L., Friedman, M., Logan, J.M., and Sterns, D.W., eds., American Geophysical Union Monograph 24: p. 103-120.

Dowdeswell, J.A., and Sharp, M.J. 1986, Characterization of pebble fabrics in modern terrestrial glacigenic sediments: Sedimentology, v. 33, p. 699-710.

Evenson, E.B., 1971, The relationship of macro- and microfabric of till and the genesis of glacial landforms in Jefferson County, Wisconsin, *in* Goldthwait, R.P., ed., Till: a symposium: Columbus, OH, Ohio State University Press, p. 345-64.

Engelder, J.T., 1974, Cataclasis and the generation of fault gouge: Geological Society of America Bulletin, v. 85, p. 1515-1522.

Engelhardt, H.G., Humphrey, N., Kamb, B., and Fahnstock, M., 1990, Physical conditions at the base of a fast moving Antarctic ice stream: Science, v. 248, p. 57-59.

Engelhardt, H., and Kamb, B., 1998, Basal sliding of Ice Stream B: Journal of Glaciology, v. 44 (in press).

Fernandez, A., Feybesse, J.L. and Mezure, J.F., 1983, Theoretical and experimental study of fabric developed by different shaped markers in two-dimensional simple shear: Geological Society of France Bulletin, v. 25, p. 319-326.

Glen, J.W., Donner, J.J. and West, R.G., 1957, On the mechanism by which stones in till become oriented: American Journal of Science, v. 255, p. 194-205.

Ghosh, S.K., and Ramberg, H., 1976, Reorientation of inclusions by combinations of pure and simple shear: Tectonophysics, v. 34, p. 1-70.

Ham, N.R., and Mickelson, D.M., 1994, Basal till fabric and deposition at Burroughs Glacier, Glacier Bay, Alaska: Geological Society of America Bulletin, v. 106, p. 1552-1559.

Harrison, P.W., 1957, A clay-till fabric: its character and origin: Journal of Geology: v. 65, p. 275-308.

Hart, J.K., 1994, Till fabric associated with deformable beds: Earth Surface Processes and Landforms: v. 19, p. 15-32.

Hart, J.K., 1997, The relationship between drumlins and other forms of subglacial glaciotectonic deformation: Quaternary Science Reviews, v. 16, p. 93-107.

Head, K.H., 1989, Soil Technician's Handbook: John Wiley and Sons, New York. p. 83.

Hicock, S.R., 1992, Lobal interactions and rheologic superimposition in subglacial till near Bradtville, Ontario, Canada: Boreas, v. 21, p. 73-88.

Hicock, S.R. and Dreimanis, A., 1992, Deformation till in the Great Lakes regions: implications for rapid flow along the south-central margin of the Laurentide Ice Sheet: Canadian Journal of Earth Science, v. 29, p. 1565-1579.

Holmes, C.D., 1941, Till fabric: Geological Society of America Bulletin, v. 52, p. 1299-1354.

Hooke, R. LeB., and Iverson, N.R., 1995, Grain-size distribution in deforming subglacial till: role of grain fracture: Geology, v. 23, p. 57-60.

Hooke, R. LeB., and Elverhøi, A., 1996, Sediment flux from a fjord during glacial periods, Isfjorden, Spitsbergen: Global and Planetary Change, v. 12, p. 237-249.

Ildefonse, B. and Fernandez, A., 1988, Influence of the concentration of rigid markers in a viscous medium on the production of preferred orientations. An experimental contribution, 1. Non-coaxial strain: Bulletin of the Geological Institutions University, Uppsala, v. 14, p. 55-60.

Ildefonse, B., Sokoutis, D. and Mancktelow, N.S., 1992, Mechanical interactions between rigid particles in a deforming ductile matrix. Analogue experiments in simple shear flow: Journal of Structural Geology, v. 14, p. 1253-1256.

Ildefonse, B. and Mancktelow, N.S., 1993, Deformation around rigid particles: the influence of slip at the particle/matrix interface: Tectonophysics, v. 221, p. 345-359.

Iverson, N.R., Hanson, B., Hooke, R. LeB., and Jansson, P., 1995, Flow mechanism of glaciers on soft beds: Science, v. 267, p. 80-81.

Iverson, N.R., Hooyer, T. and Hooke, R. LeB., 1996, A laboratory study of sediment deformation: Stress heterogeneity and grain-size evolution: Annals of Glaciology, v. 22, p. 167-175.

Iverson, N.R., Baker, R., and Hooyer, T., 1997, A ring-shear device for the study of till deformation: tests on a clay-rich and a clay-poor till: Quaternary Science Reviews, v. 16, p. 1057-1066.

Iverson, N.R., Hooyer, T.S., and Baker, R., 1998, Ring-shear studies of till deformation: Coulomb-plastic behavior and distributed strain in glacier beds: Journal of Glaciology, v. 44, p. 634-641.

Iverson, N.R., Baker, R.W., Hooke, R. LeB., Hanson, B., and Jansson, P., 1999, Coupling between a glacier and a soft bed: I. A relation between effective pressure and local shear stress determined from till elasticity: Journal of Glaciology, v. 45, p. 31-40.

Jaeger, H.M., and Nagel, S.R., 1992, Physics of the granular state: Science, v. 255, p. 1523-1531.

Jenson, J.W., Clark, P.U., MacAyeal, D.R., Ho, C., and Vela, J.C., 1995, Numerical modeling of advective transport of saturated deforming sediment beneath the Lake Michigan Lobe, Laurentide Ice Sheet: Geomorphology, v. 14, p. 157-166.

Jenson, J.W., MacAyeal, D.R., Clark, P.U., Ho, C.L. and Vela, J.C., 1996, Numerical modeling of subglacial sediment deformation: implications for the behavior of the Lake Michigan Lobe, Laurentide Ice Sheet: Journal of Geophysical Research, v. 101, p. 8717-8728.

Jeffery, G.B., 1922, The motion of ellipsoidal particles immersed in a viscous fluid: Proceedings of the Royal Society of London, Ser. A, v. 102, p. 169-179.

Johnson, W.H., and Hansel, A.K., 1990, Multiple Wisconsinan glacigenic sequences at Wedron, Illinois: Journal of Sedimentary Petrology, v. 60, p. 26-41.

Johnson, S.E., 1990, Lack of porphyroblast rotation in the Otago Schists, South Island, New Zealand, implications for crenulation cleavage development, folding and deformation partitioning: Journal of Metamorphic Geology, v. 8, p. 13-30.

Krüger, J., and Thomsen, H.H., 1984, Morphology, stratigraphy, and genesis of small drumlins in front of the glacier Myrdalsjokull, south Iceland: Journal of Glaciology, v. 30, p. 94-105.

Lawson, D.E., 1979a, A comparison of the pebble orientation in ice and deposits of the Matanuska Glacier, Alaska: Journal of Geology, v. 87, p. 629-645.

Lawson, D.E., 1979b, Sedimentological analysis of the western terminus region of the Matanuska Glacier, Alaska: U.S. Army Cold Regions Research and Engineering Lab Report 79-9, 112 p.

Licciardi, J.M., Clark, P.U., Jenson, J.W., and MacAyeal, D.R., 1998, Deglaciation of a soft-bedded Laurentide Ice Sheet: Quaternary Science Reviews, v. 17, p. 427-448.

Logan, J.M., Dengo, C.A., Higgs, N.G. and Wang, Z.Z., 1992, Fabrics of experimental fault zones; their development and relationship to mechanical behavior, *in* Evans, B., and Wong, T.F., eds., Fault mechanics and transport properties of rocks: London, Academic Press, p. 33-67.

MacAyeal, D.R., 1992, Irregular oscillations of the West Antarctic ice sheet: Nature, v. 359, p. 29-32.

March, A., 1932, Mathematische theorie der regelung nach der korngestalt bei affiner deformation: Zeitschr. F. Kristallogr., v. 81, p. 285-297.

Mark, D.M., 1973, Analysis of axial orientation data, including till fabrics: Geological Society of America Bulletin, v. 84, p. 1369-1374.

Menzies, J., 1989, Drumlins – products of controlled or uncontrolled glaciodynamic response?: Quaternary Science Reviews, v. 8, p. 151-158.

Moore, D.E., Summers, R., and Byerlee, J.D., 1989, Sliding behavior and deformation textures of heated illite gouge: Journal of Structural Geology, v. 11, p. 329-342.

Reed, L.J., and Tryggvason, E., 1974, Preferred orientations of rigid particles in a viscous matrix deformed by pure shear and simple shear: Tectonophysics, v. 24, p. 85-98.

Rutter, E.H., Maddock, R.H., Hall, S.H., and White, S.H., 1986, Comparative microstructures of natural and experimentally produced clay bearing fault gouges: Pure and Applied Geophysics: v. 124, p. 3-39.

Shaw, J., 1982, Melt-out till in the Edmonton area, Alberta, Canada: Canadian Journal of Earth Science, v. 19, p. 1548-1569.

Simpson, C., and Schmid, S.M., 1983, An evaluation of criteria to deduce the sense of movement in sheared rocks: Geological Society of America Bulletin, v. 94, p. 1281-1288.

Smalley, I.J., and Unwin, D.J., 1968, The formation and shape of drumlins and their distribution and orientation in the drumlin fields: Journal of Glaciology, v. 7, p. 377-90.

Stanford, S.D., and Mickelson, D.M., 1985, Till fabric and deformational structures in drumlins near Waukesha, Wisconsin, U.S.A.: Journal of Glaciology, v. 31, p. 220-228.

Tika-Vassilikos, T.E., 1991, Clay-on-steel ring shear tests and their implications for displacement piles: Journal of Geotechnical Testing, v. 14, p. 457-463.

Trevelyan, B.J., and Mason, S.G., 1951, Particle motions in sheared suspensions. I. Rotations: Journal of Colloid Science, v. 6, p. 354-367.

Tulaczyk, S., 1999, Basal Mechanics and Geologic Record of Ice Streaming, West Antarctica [Ph.D. Thesis]: Pasadena, California, California Institute of Technology, 320 p.

Van der Meer, J.J.M., 1993, Microscopic evidence of subglacial deformation: Quaternary Science Reviews, v. 12, p. 553-587.

Van der Meer, J.J.M., 1997, Particle and aggregrate mobility in till: microscopic evidence of subglacial processes: Quaternary Science Reviews, v. 16, p. 827-831.

Woodcock, N.H., and M.A. Naylor, 1983, Randomness testing in three-dimensional orientation data: Journal of Structural Geology, v. 5, p. 539-548.

CHAPTER 3. LABORATORY STUDIES OF MIXING BETWEEN TWO TILL LAYERS: A NEW METHOD FOR ASSESSING BED DEFORMATION BENEATH ICE SHEETS

A paper to be submitted to the Journal of Glaciology

Thomas S. Hooyer and Neal R. Iverson
Department of Geological and Atmospheric Sciences
Iowa State University, Ames, IA 50011

INTRODUCTION

Pervasive deformation of water-saturated subglacial till has been suggested as the primary mechanism of glacier motion and sediment transport (Alley, 1991; Clark, 1994; Jenson et al., 1995, 1996; Boulton, 1996; Clark et al., 1996; Hooke and Elverhøi, 1996; Licciardi et al., 1998; Dowdeswell and Siegert, 1999). This process may have occurred beneath the southern margin of the Laurentide Ice Sheet, where laterally extensive sheets of generally fine-grained till overlie bedrock (Clark and Walder, 1995; Clark, 1997). Many field studies of Pleistocene tills have attempted to establish sedimentological criteria for deformation (e.g., Hicock and Dreimanis, 1992; Menzies and Maltman, 1992; Hart, 1994, 1997; Hart and Roberts, 1994). Convincing observations from some of these studies include microstructural rotational features and shear bands (Menzies et al., 1997; van der Meer, 1993, 1997), folds and boudinage (Hart and Boulton, 1991; Hart and Roberts, 1994), grain fracturing (Hiemstra and van der Meer, 1997), and slightly deformed pods of sorted sediment incorporated within basal tills (Hart, 1995; Piotrowski and Kraus, 1997). None of these observations, however, provides a quantitative means of characterizing the very high shear strains required of the bed-deformation hypothesis.

Efforts have recently been made in laboratory experiments to determine if the alignment of gravel-size clasts in shearing till can be used to estimate strain magnitude (Hooyer and Iverson, in press). The results of these experiments indicate that strong fabrics develop in the direction of shearing at relatively small shear strains (1-2) and remain strong at progressively higher strains up to 475. Although useful in determining whether an otherwise featureless till has been deformed, this method cannot be used to distinguish tills that have been deformed sufficiently to account for significant glacier motion from those that have been sheared to detectable but negligible strains.

Visually sharp stratigraphic contacts that commonly occur between basal till layers have been used as evidence both for and against deformation. Kemmis (1981) and Clayton et al. (1989) argued that pervasive deformation would result in mixing between tills thereby resulting in gradational contacts. In contrast, Alley (1991) suggested that sharp contacts are the result of deformation. Although he restricted his discussion to deformation within one till, Alley argued that, owing to the expected downward increase in effective pressure (the difference between the ice overburden and pore-water pressure), there should be a general tendency for tills to strengthen and consolidate with depth. This, he speculated, might result in a sharp contact between till that had been deformed and underlying undeformed till. It is also conceivable that a similar velocity discontinuity might occur at the contact between two tills that have different geotechnical properties, which might inhibit mixing and thereby enable a sharp contact to persist with deformation.

This study focuses on mixing between lithologically distinct tills and other more ideal granular materials undergoing slow, steady, bed-parallel shearing. Our approach is to use a rotary device that shears granular materials to various strains under conditions similar to

those beneath modern glaciers. The results indicate that mixing between granular layers, including tills, is proportional to the cumulative strain and can be modeled using diffusion theory. Consequently, the extent of mixing across a stratigraphic contact provides a useful constraint on the extent of glacier motion due to pervasive bed deformation.

THEORY

The mixing of two shearing granular layers is considered to be a one-dimensional diffusive process in the direction normal to shearing. During shearing grains climb over adjacent grains and fall into void spaces. If these grain motions normal to the shearing direction are essentially random, then a diffusive flux of grains in that direction is expected.

Consider two layers of granular material of combined thickness h in a vertical section oriented perpendicular to the shearing direction, where z is the distance from the top of the shear zone (Fig. 1A). Define an index lithology that is significantly more abundant in one layer than the other. The dimensionless concentration of this lithology C is defined as the number of index grains divided by the total number of grains. If during shearing the vertical flux of index grains associated with mixing scales linearly with $\partial C/\partial z$, then

$$\frac{\partial C}{\partial \gamma} = D\frac{\partial^2 C}{\partial z^2}, \tag{1}$$

where D is a mixing coefficient, and γ is shear strain. This is Fick's second law written in terms of γ, rather than time. Consequently, D has the dimension m^2. If C_1 and C_2 are the initial dimensionless concentrations of the index lithology in the upper and lower layers, respectively, z_o is the position of the contact between the two layers, and there is no flux of

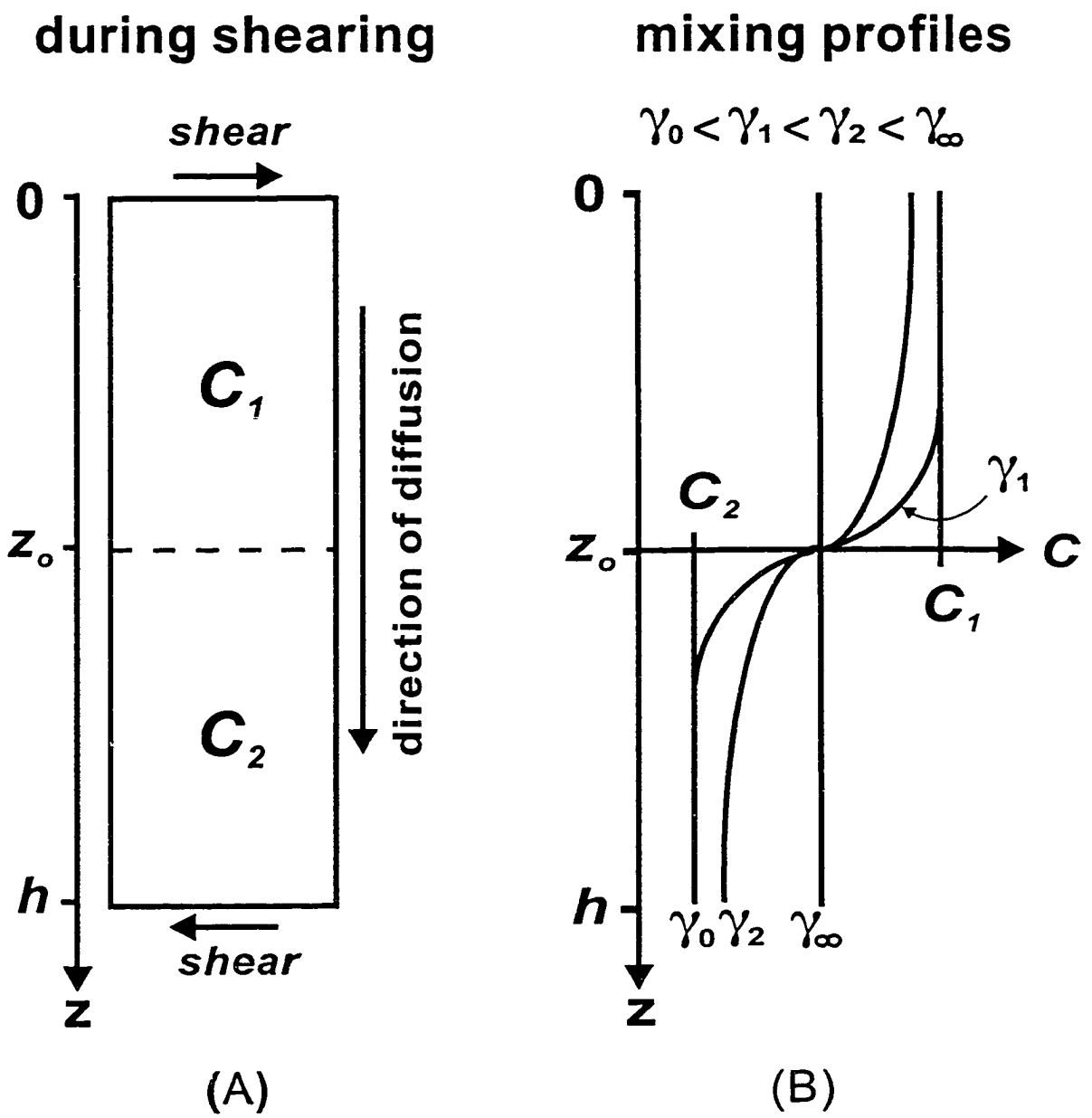

Figure 1. Mixing model schematic of (A) the model domain, and (B) concentration of an index lithology across the shear zone as a function of shear strain.

the index lithology out of the shear zone, then appropriate initial and boundary conditions are as follows:

$$C_1 = (0 < z < z_0, \gamma = 0); \qquad C_2 = (z_0 < z < h, \gamma = 0); \tag{2}$$

$$\frac{\partial C}{\partial z} = 0 \text{ at } (0, \gamma>0); \qquad \text{and} \qquad \frac{\partial C}{\partial z} = 0 \text{ at } (h, \gamma>0). \tag{3}$$

If $C_1 > C_2$, there is downward diffusion of the index lithology, and the solution to Equation 1 is

$$C(z,\gamma) = C_1 C_2 + \frac{C_1 z_o}{h} + \frac{2C_1}{\pi}\sum_{m=1}^{\infty}\frac{\exp\left(-Dm^2\pi^2\left(\gamma/h^2\right)\right)}{m}\cos\left(\frac{m\pi z}{h}\right)\sin\left(\frac{m\pi z_o}{h}\right) \tag{4}$$

(Shackelford, 1991). Figure 1B illustrates solutions for several values of γ. The approach taken in this study is to determine D by measuring mixing between two till layers in ring-shear tests in which all other variables in Equation 4 are known. Mixing profiles between till units in the field can then, in principle, be used to constrain the value of γ.

APPARATUS

Our ring-shear device (Fig. 2A) shears an annular sediment specimen at a constant rate between horizontal, parallel platens (Iverson et al., 1996, 1997, 1998a). A steady stress is applied normal to the shearing direction. The rotary design of this device allows experiments to be carried out to high shear strains, and its transparent outer walls allow continuous

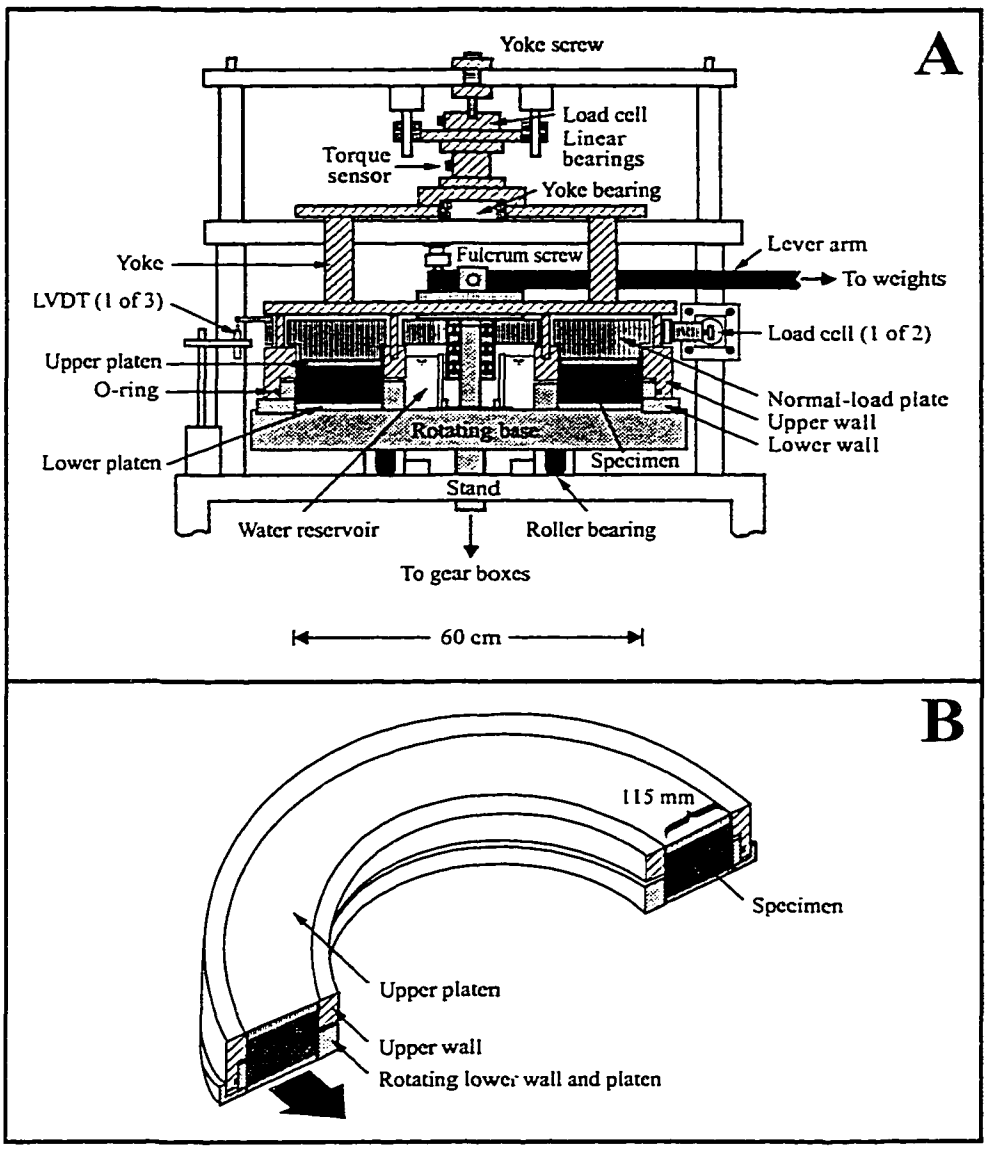

Figure 2. (A) Cross-section of the ring-shear device, and (B) schematic of the sample chamber. Lightly shaded components rotate.

observation of mixing at the outer edge of the specimen during shearing. In addition, the sample chamber is sufficiently large to accommodate till specimens with gravel-size clasts.

The sediment specimen occupies a donut-shaped chamber that has an outside diameter of 0.6 m, a width of 0.115 m and a height of 0.085 m (Fig. 2B). Both the upper and lower platens contain teeth, 6 mm high, that grip the specimen during shearing. These platens are permeable and connected to an internal water reservoir that is open to the atmosphere. The upper platen is attached to a normal-load plate that is fixed rotationally by diametrically opposed load cells secured to the frame of the device. However, the normal-load plate is allowed to move vertically if the specimen thickness changes during shearing. A downward force is applied to this plate with dead weights suspended on a hanger attached to the end of a lever arm. The lower platen is connected to a thick base plate, and the sediment is sheared by rotating this plate with a variable-speed motor and gear boxes. The specimen is confined on its sides by upper and lower walls connected to the normal-load plate and base plate, respectively. Thus, the lower walls slide beneath the upper walls during shearing.

METHODOLOGY

Mixing experiments were performed with two sets of materials: spherical glass beads of uniform size (0.8 mm in diameter) but different color, and two late Wisconsin-age tills with distinct lithologies. Initial experiments with beads provided simple tests of whether mixing can be modeled successfully as a diffusive process. Subsequent experiments were with tills from east-central Minnesota: the red Superior Lobe till and the gray Des Moines Lobe basal till. The latter directly overlies the former and was deposited by the Grantsburg Sublobe, a northeastern arm of the Des Moines Lobe. The tills have similar grain-size distributions (Fig.

3), although the Des Moines Lobe till (16% clay, 36% silt, 40% sand and 8% gravel) is somewhat finer-grained than the Superior Lobe till (12% clay, 31%silt, 51% sand and 6% gravel). The Des Moines Lobe till was deposited by ice that advanced from the northwest and is enriched in Cretaceous shale and Paleozoic carbonates. The Superior Lobe till was deposited by ice that advanced out of the Lake Superior basin to the northeast and is devoid of shale and relatively enriched in Precambrian igneous rocks and Cambrian sandstone (Chernicoff, 1983).

In each of four experiments with beads, a 35-40 mm thick layer of red beads is placed inside the sample chamber. The top of this layer is smoothed and a second layer of white beads, similar in thickness, is added forming a sharp, relatively smooth contact between the two layers (Fig. 4A). Vertical columns of displacement markers, spherical wooden beads 2-4 mm in diameter, are then placed across the width of the specimen to assess the distribution of shear strain. A normal stress of 85 kPa is then applied, and the specimen is sheared at a steady rate of 365 m yr^{-1} to a predetermined displacement. These values are similar to those of some glaciers, and this shearing rate is small enough to ensure the absence of inertial effects. The experiments were performed dry, although the behavior of granular materials, including beads, is not expected to be different under water-saturated, fully-drained conditions (Lambe and Whitman, 1969, p. 304). After shearing is completed, the device is disassembled, and the locations of the displacement markers are measured. At two locations within the chamber, bead samples are collected at approximately 1-mm intervals through the thickness of the specimen to document mixing (Fig. 4B). They are collected using a thin plate, 30 mm x 50 mm, with adhesive tape on one side. The plate is gently lowered onto the centerline of the specimen. Upon removing the plate, approximately 2000-4000 beads are

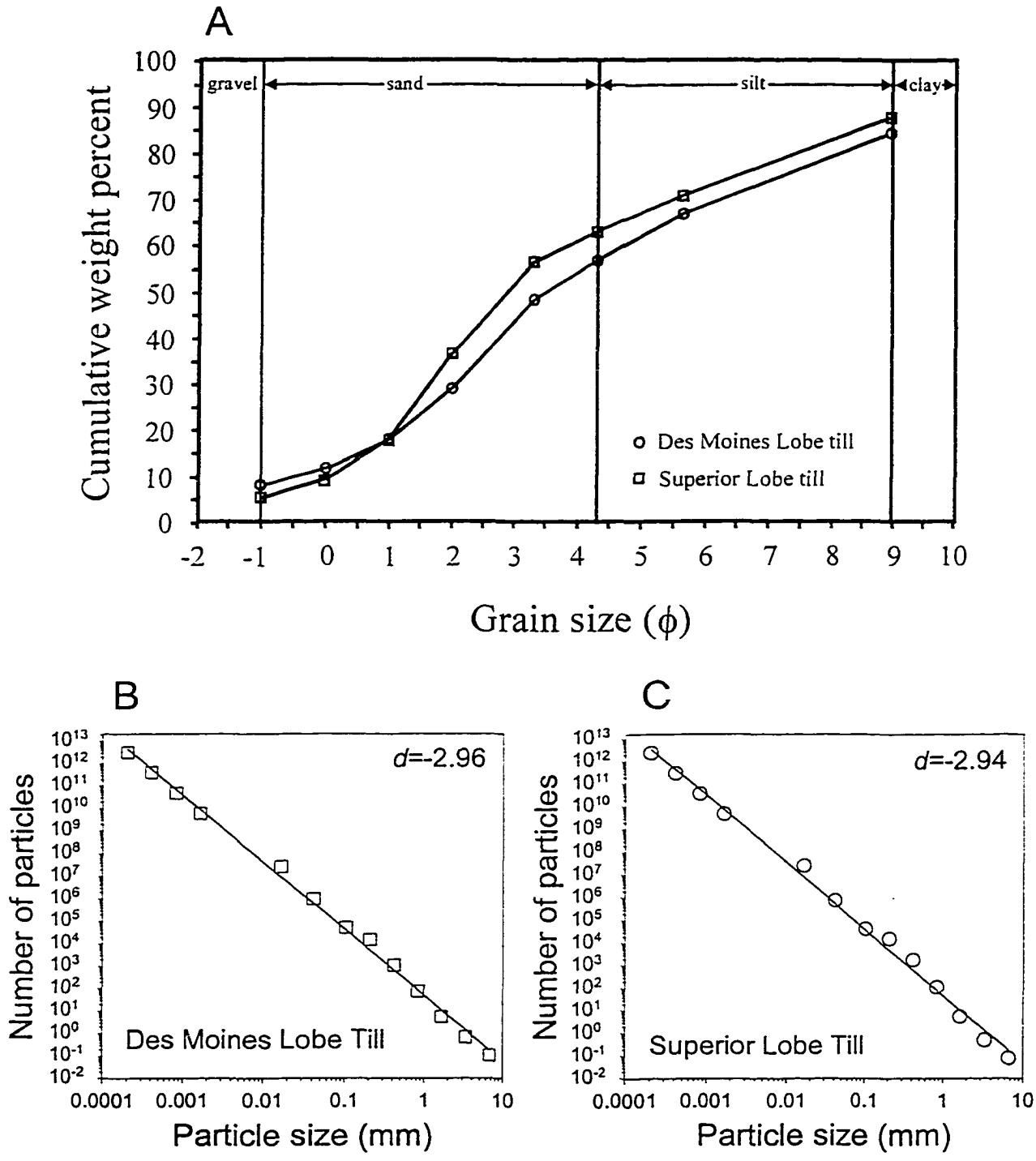

Figure 3. (A) Particle-size distribution of the Des Moines Lobe and Superior Lobe tills. (B-C) Plot of grain size vs. number of particles for both tills where the slope of the line is the fractal dimension, *d* (e.g., Sammis et al., 1987). The linear relations indicate that the grain-size distributions are self-similar.

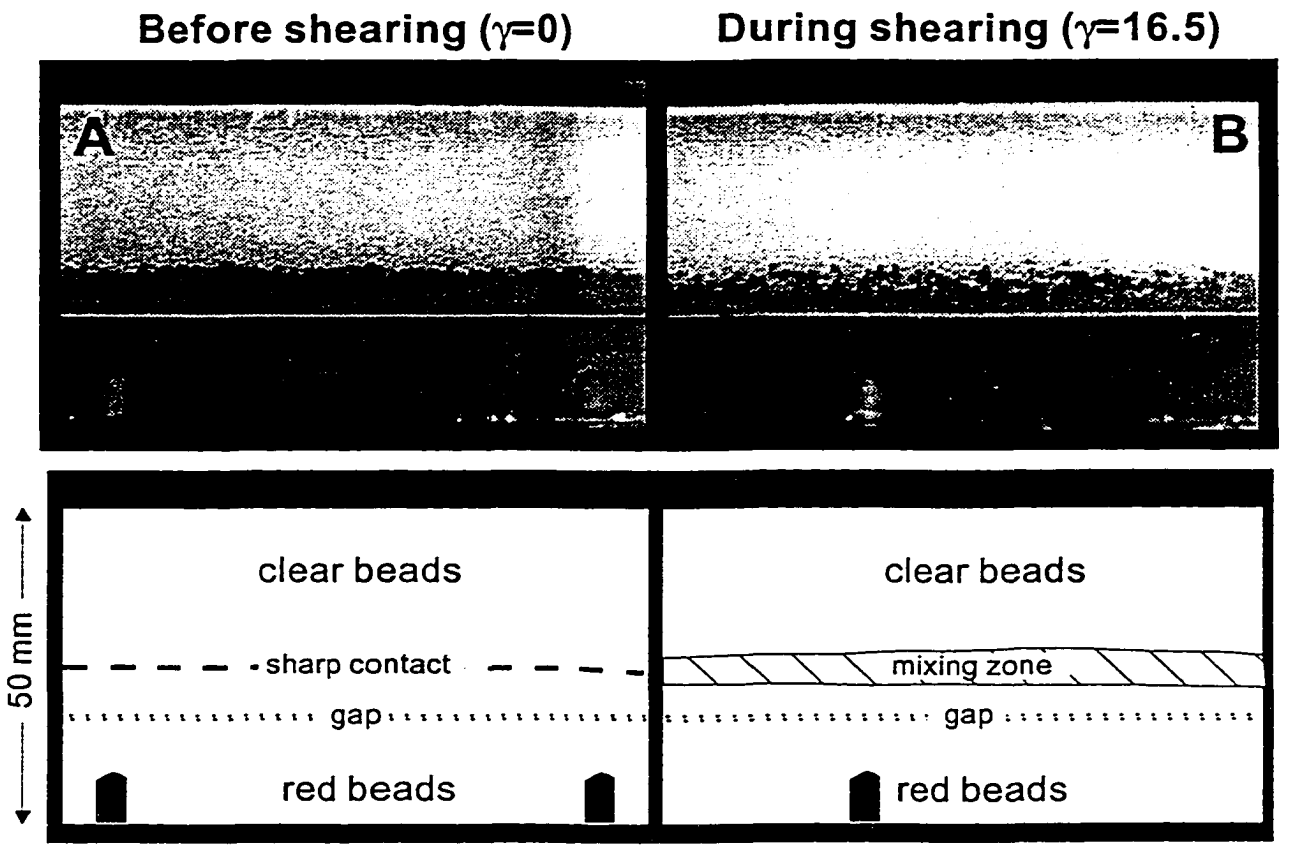

Figure 4. Photographs taken through the transparent outer wall of the ring-shear device during a bead experiment. (A) Sharp initial contact before shearing, and (B) mixing zone during shearing.

stuck to the adhesive tape. No beads within 40 mm of the walls are sampied. Each bead sample is split multiple times to obtain a representative sample of 200-500 beads that are subsequently identified by color under a binocular microscope. The relative concentrations of white beads are plotted as a function of depth. Resultant profiles are referred to, hereafter, as mixing profiles.

The procedure in the five till experiments is similar to that of the bead experiments except that the till layers are fully saturated with water upon application of the normal load, and consolidation is allowed to occur prior to shearing. In addition, all clasts larger than 8 mm are removed from both tills in accordance with geotechnical testing procedures outlined by Head (1989, pg. 83). These clasts represent approximately 2.0% and 1.2% of the Des Moines and Superior Lobe tills by volume, respectively. The Superior Lobe till is then placed in the sample chamber beneath the Des Moines Lobe till. As in the bead experiments, the contact between the two tills is initially sharp, and vertical columns of displacement markers are inserted into the till to assess the distribution of shear strain at the ends of experiments. After an experiment is complete, mixing profiles are measured at two different locations, as in the bead experiments. However, instead of collecting the samples *in-situ*, two blocks of intact till are removed from the chamber and a guided metal scraper is used to collect samples at 1-mm intervals. Each sample is then wet sieved to separate the 0.4-1.0 mm grain-size fraction. These grains are large enough to identify easily but small enough to provide a large sample (150-500) for identification.

To quantify mixing in the till experiments, a suitable index lithology must be selected. Shale is a good choice due to its abundance in the Des Moines Lobe till and its absence in the Superior Lobe till. The mean shale content of the Des Moines Lobe till in the 0.4-1.0 mm

grain-size fraction varies between 9% and 12%. A binocular microscope is used to identify and count shale grains and the total number of grains in each sample.

Equation 4 is fit to mixing profiles from both the bead and till experiments to determine the mixing coefficient, D. All other variables in Equation 4 are well constrained. The thickness of the shear zone and the total shear strain are determined from the final locations of the displacement markers. The initial concentrations of shale in the two tills (C_1 and C_2) are determined from grain counts of till samples collected prior to shearing and from undeformed portions of the specimen after shearing. The height of the initial contact, z_o, is measured prior to shearing. However, the measurement does not account for small undulations in the initial contact and changes in specimen thickness that occur during consolidation and shearing. Therefore, z_o is determined from the resulting mixing profiles as the height at which the dimensionless white bead or shale concentration equals 0.5. D is determined by minimizing the sum of the residuals between the modeled and observed concentration data. The goodness of fit of the model prediction to the observed data is evaluated using the coefficient of determination, r^2, calculated in the usual way (Steel et al., 1997). One to three D values, each corresponding to a different sampling location, are determined for each experiment. A mean value of D and a 95% confidence interval are determined from these values if there was more than one sampling location, as was the case in most experiments.

RESULTS

Strain distribution

To determine D the distribution of strain needs to be documented. The final locations of

displacement markers near the center of the specimen in each bead and till experiment are shown in Figure 5 and Figure 6, respectively. In both materials, the shear zone is always sandwiched between zones of negligible deformation where there is no detectable relative displacement between markers. The shear zones vary slightly in vertical position, and their thickness ranges from 22 to 32.5 mm in the beads and from 28 to 41 mm in the till. Shear strains are calculated using the shear-zone thickness and the total displacement of the lower platen at the specimen centerline. Strain across the shear zones is approximately linearly distributed as indicated in the two low-strain experiments (Fig. 5A and 6A). In these experiments, the total displacement of each marker in the shear zone is well known because the lower platen has rotated less than one revolution. If the lower platen has completed more than one revolution, it is not possible to unequivocally assess the number of revolutions any one marker in the shear zone has undergone (Fig. 5B-D and 6B-E).

The shear-zone thickness decreased slightly across the width of the bead and till specimens from the sample centerline to the outer walls (Fig. 7A, B). Thus, all samples used to establish the mixing profiles were collected over a 30 to 40 mm-wide area in the middle of the specimen where the shear-zone thickness was essentially uniform.

Mixing

The mixing profiles for the bead and till experiments are presented in Figures 8 and 9, respectively. The parameters for the experiments, including h, γ and the average shear strain rate, $\dot{\gamma}$, are summarized in Table 1. In the mixing profiles, z is plotted as a function of either percent white beads or shale. The different symbols on each figure represent different

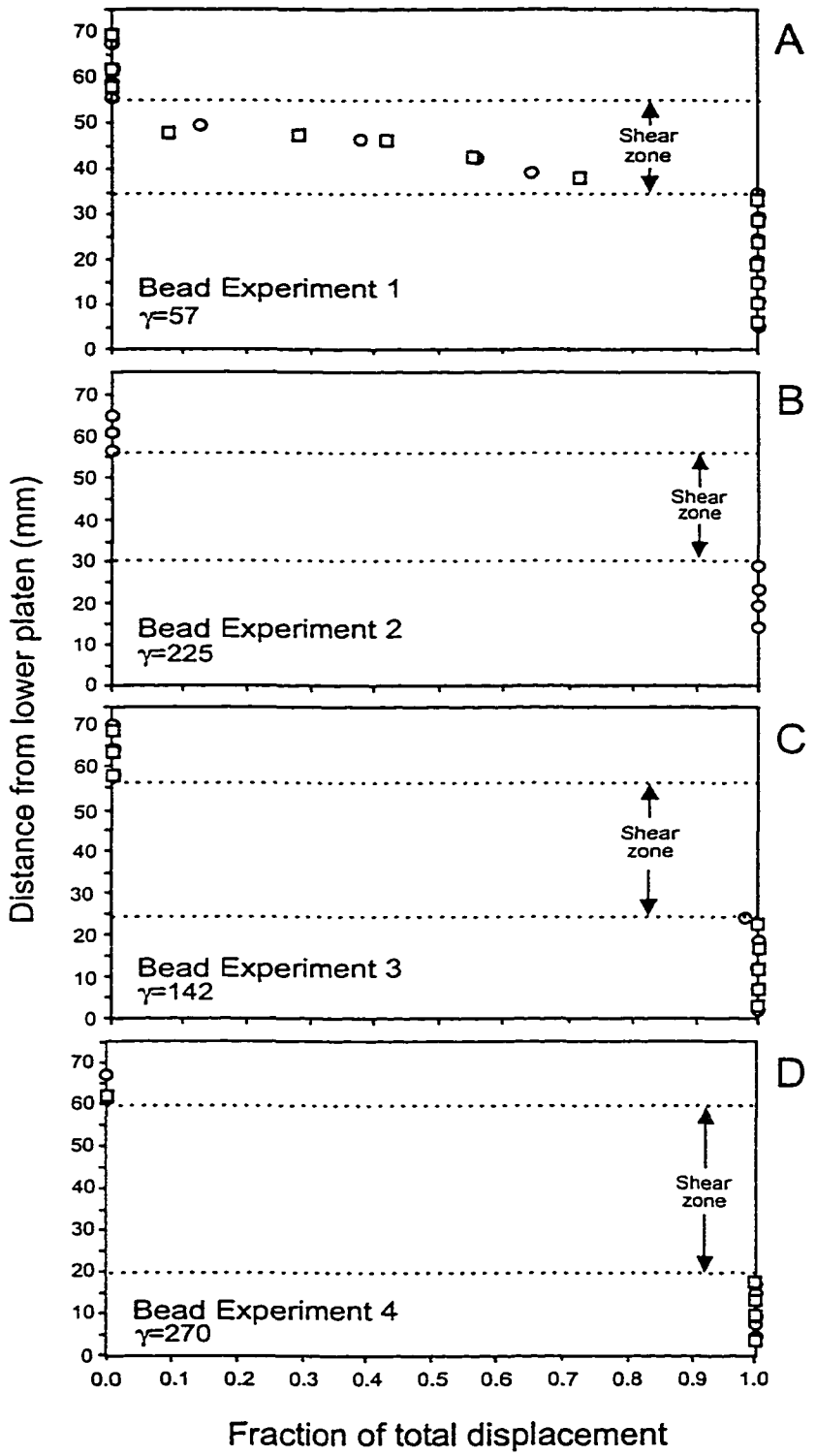

Figure 5. (A-D) Profiles of longitudinal displacement in bead experiments 1 through 4. The different symbols represent profiles measured at different locations, all near the center of specimens.

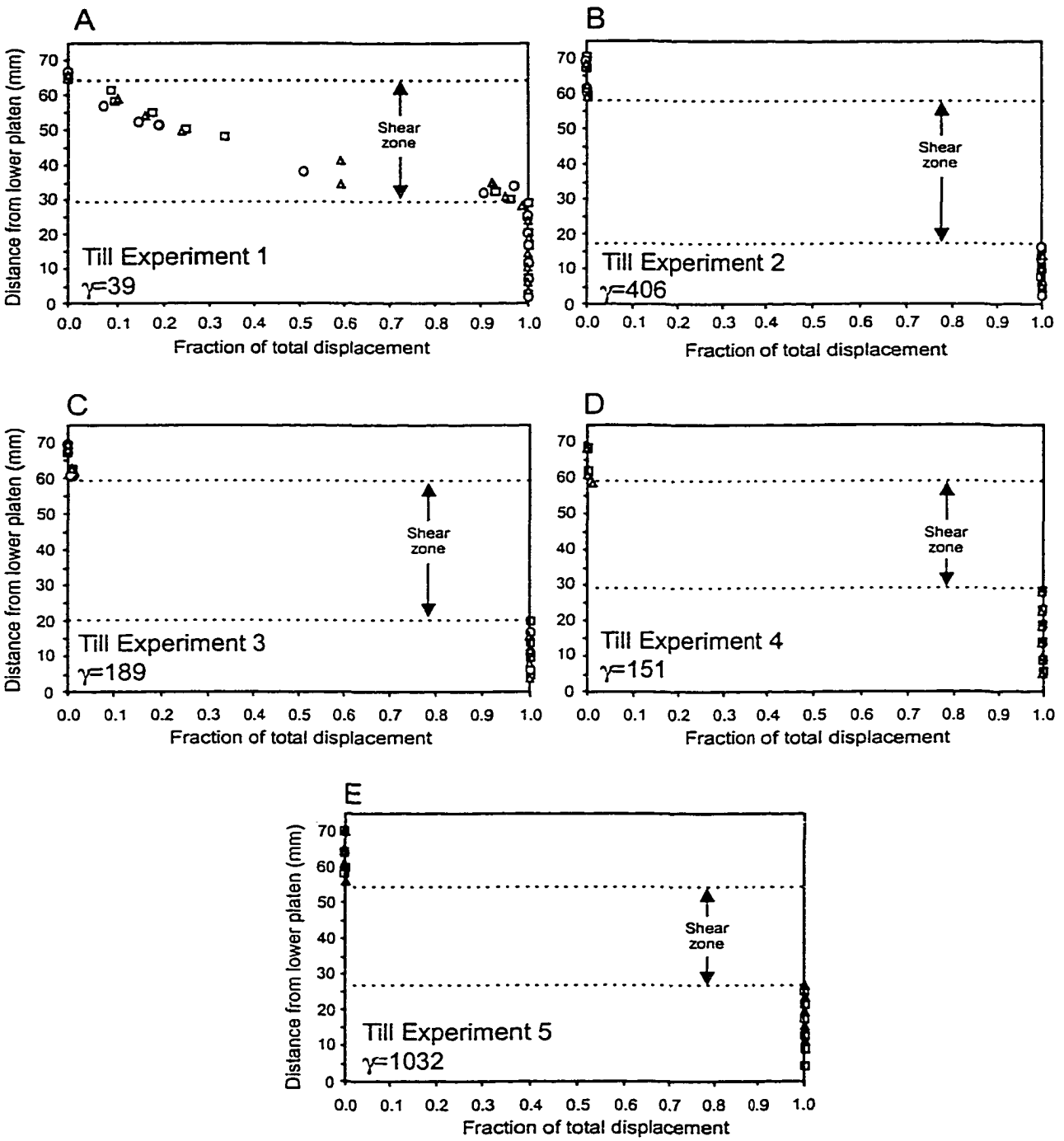

Figure 6. (A-E) Profiles of longitudinal displacement in till experiments 1 through 5. The different symbols represent profiles measured at different locations, all near the center of the specimens.

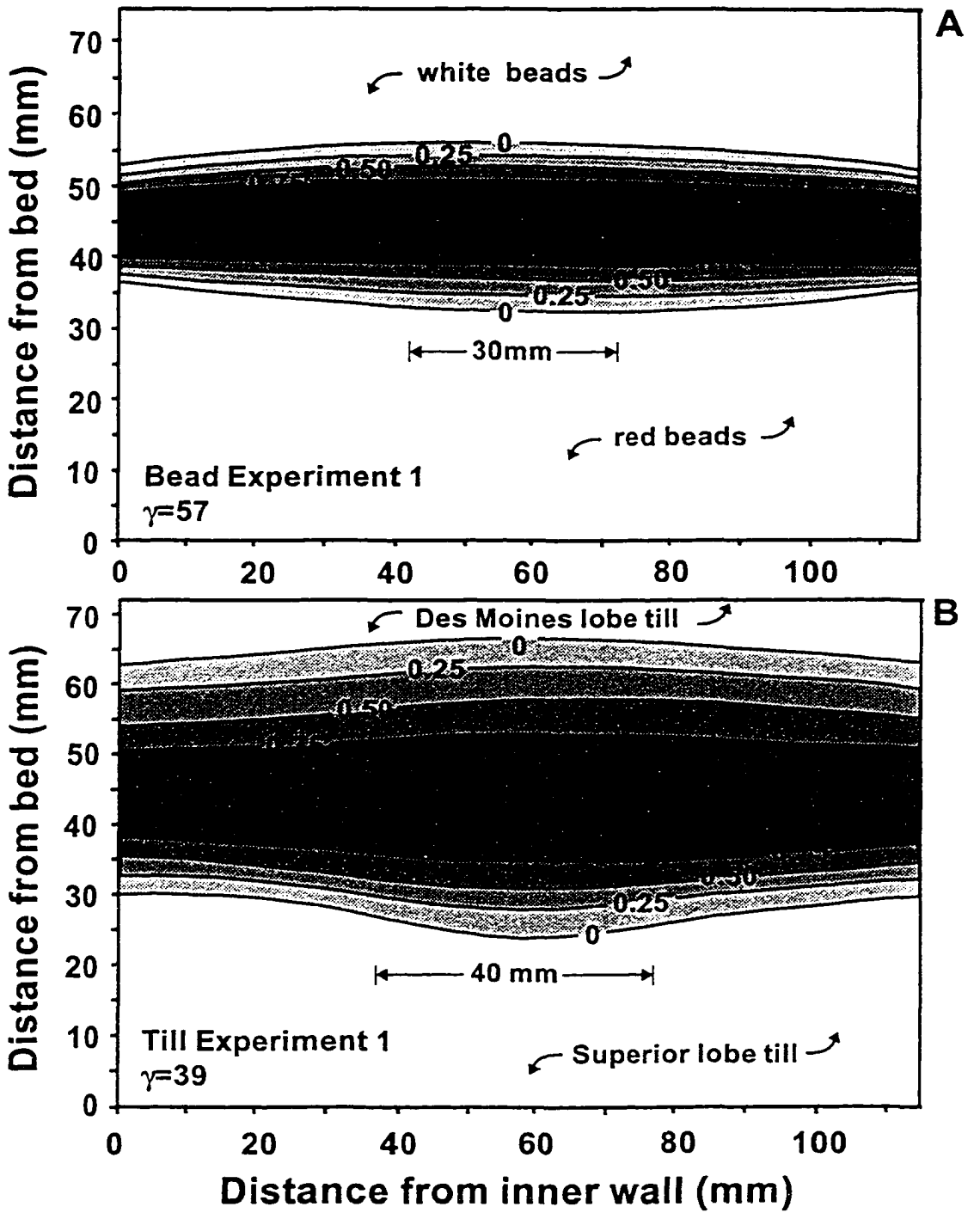

Figure 7. Distribution of shear strain in transverse cross-section in (A) a bead experiment and (B) a till experiment. Shear strain has been normalized to the total cumulative strain at each position across the specimen width. Grains were collected from the middle of the specimen over widths of 30 mm and 40 mm in the bead and till experiments, respectively.

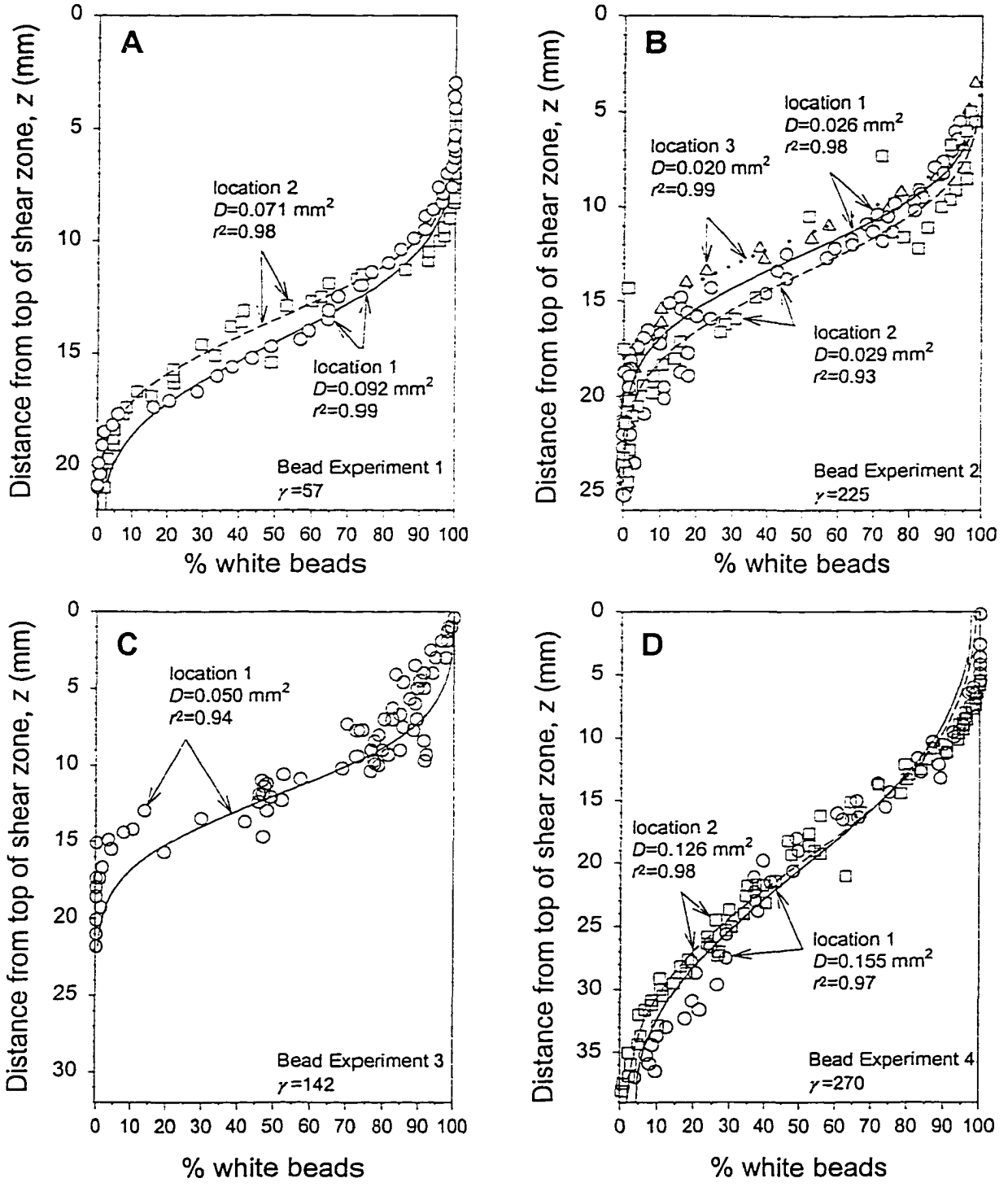

Figure 8. (A-D) Mixing profiles for bead experiments 1 through 4. In profile 3 (C), three sampling locations were combined into one profile due to difficulties with bead identification caused by the removal of the bead's colored surface coating during shearing.

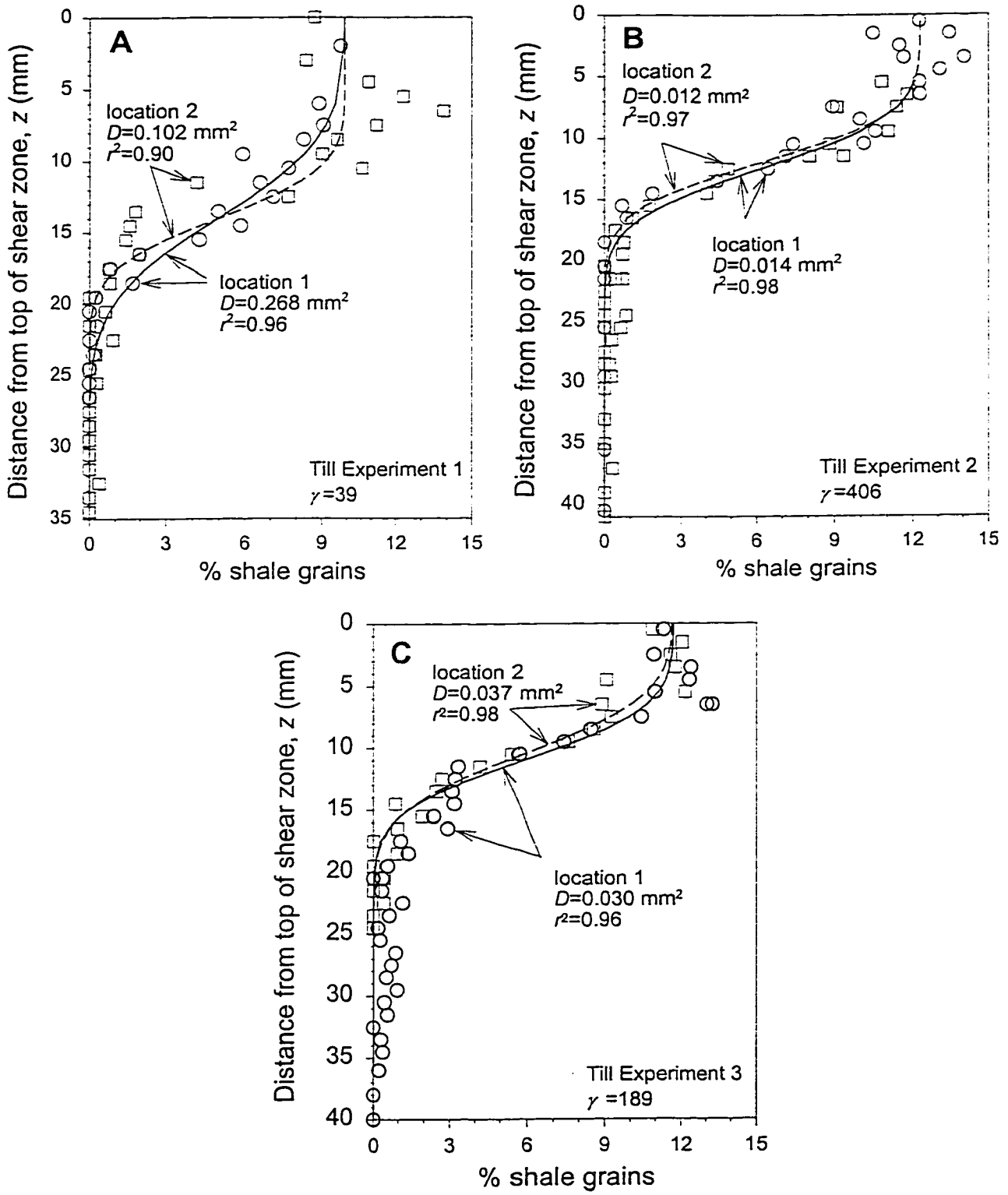

Figure 9. (A-E) Mixing profiles for till experiments 1 through 5.

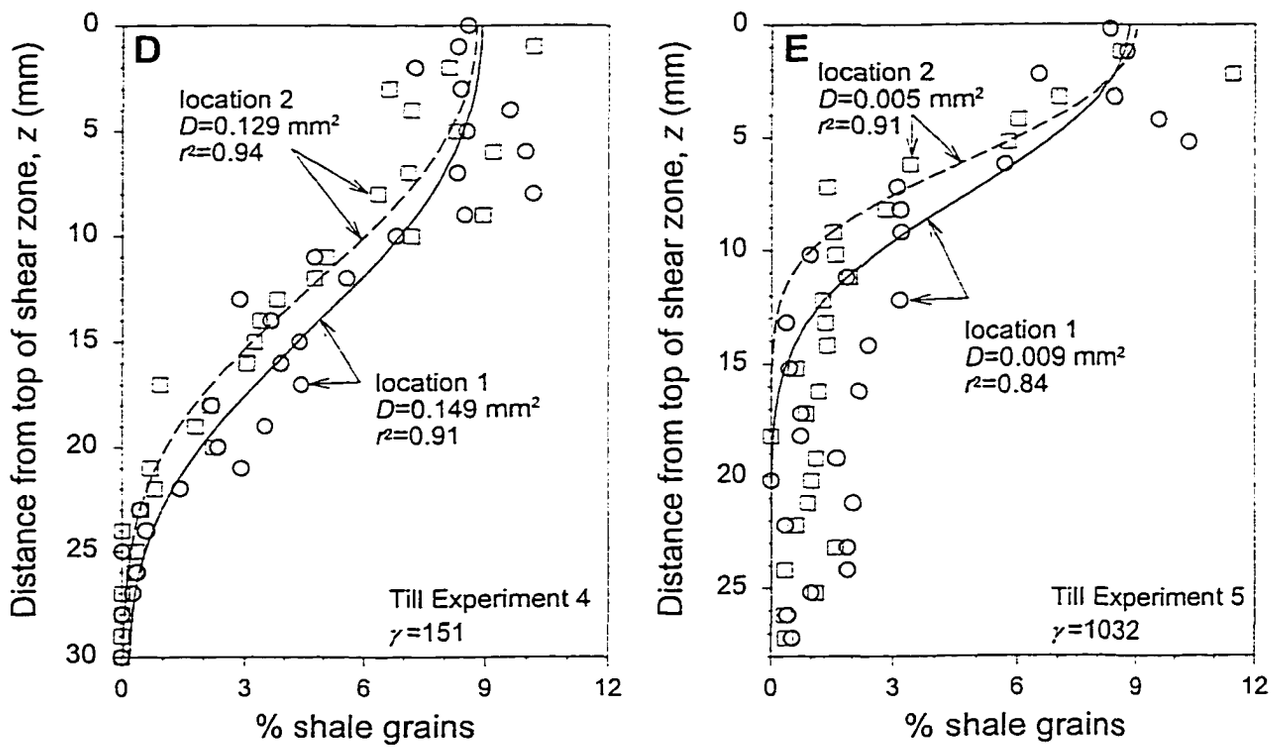

Figure 9. (continued).

Table 1. Experimental Conditions.

Experiment number	shear zone boundary* (mm)	Shear zone thickness, h (mm)	Initial shale conc. (%)	Total displacement at sample center (mm)	Shear strain, γ	Elapsed time of experiment (s)	Shearing rate (mm s^{-1})	Average shear strain rate, $\dot{\gamma}$ (s^{-1})
Bead 1	35-57	22	N/A	1245	57	88320	0.01410	6.41×10^{-4}
Bead 2	32-56	26	N/A	5846	225	456420	0.01281	5.30×10^{-4}
Bead 3	24-56	32	N/A	4550	142	359820	0.01265	3.95×10^{-4}
Bead 4	20-59	39	N/A	10518	270	716400	0.01468	4.52×10^{-4}
Till 1	29-64	35	9.9	1355	39	108120	0.01253	3.58×10^{-4}
Till 2	17-58	41	12.3	16636	406	623040	0.02670	5.93×10^{-4}
Till 3	20-60	40	11.7	7558	189	601620	0.01256	3.14×10^{-4}
Till 4	29-59	30	9.2	4522	151	346560	0.01305	4.35×10^{-4}
Till 5	26-54	28	9.6	28915	1032	2093940	0.01298 - 0.01558	4.93×10^{-4}

* Distance above bottom platen
N/A. not applicable

sampling locations. The curves are fits of the diffusion model to the data in which the only fitted variable is D. The r^2 values indicate a generally good correlation between the modeled and observed concentrations. To compare D values between the bead and till experiments, a dimensionless mixing coefficient, D^*, is determined by dividing D by the square of the particle size that was counted. For the till, this size was 0.4 to 1.0 mm and thus an average value of 0.7 mm is used. Values of D, D^*, z_o and r^2 for each experiment are summarized in Table 2.

Mean values of D^* with 95 % confidence intervals are plotted as a function of shear strain in Figure 10. Despite the different grain-size distributions of the beads and till, D^* values for the two materials are of the same order of magnitude. Mean D^* values from the four bead experiments do not vary systematically with strain and range from 0.039 to 0.219. Mean D^* values from the till experiments, however, decrease monotonically with strain from 0.378 to 0.014.

DISCUSSION

Laboratory results

These experiments demonstrate that mixing occurs between adjacent layers of granular material as they are slowly sheared. The mixing can be modeled as a one-dimensional diffusive process. As noted earlier, this implies that the vertical component of particle motion is essentially random and that the associated flux of particles is proportional to the concentration gradient of a particular index lithology.

Table 2. Experimental results.

Experiment number	Sample location	Initial contact height, z_o (mm)	D (mm^2)	D^*	r^2
Bead 1	1	14.5	0.092	0.144	0.99
	2	13.5	0.071	0.111	0.98
Bead 2	1	13.5	0.026	0.041	0.98
	2	12.5	0.029	0.045	0.93
	3	14.5	0.020	0.031	0.99
Bead 3	1	12.0	0.050	0.078	0.94
Bead 4	1	20.5	0.155	0.242	0.97
	2	20.0	0.126	0.197	0.98
Till 1	1	14.0	0.268	0.547	0.96
	2	14.0	0.102	0.210	0.90
Till 2	1	12.5	0.014	0.029	0.98
	2	12.0	0.012	0.024	0.97
Till 3	1	11.0	0.030	0.061	0.96
	2	10.5	0.037	0.076	0.98
Till 4	1	14.5	0.149	0.304	0.91
	2	12.5	0.129	0.264	0.94
Till 5	1	7.5	0.009	0.018	0.84
	2	6.0	0.004	0.010	0.91

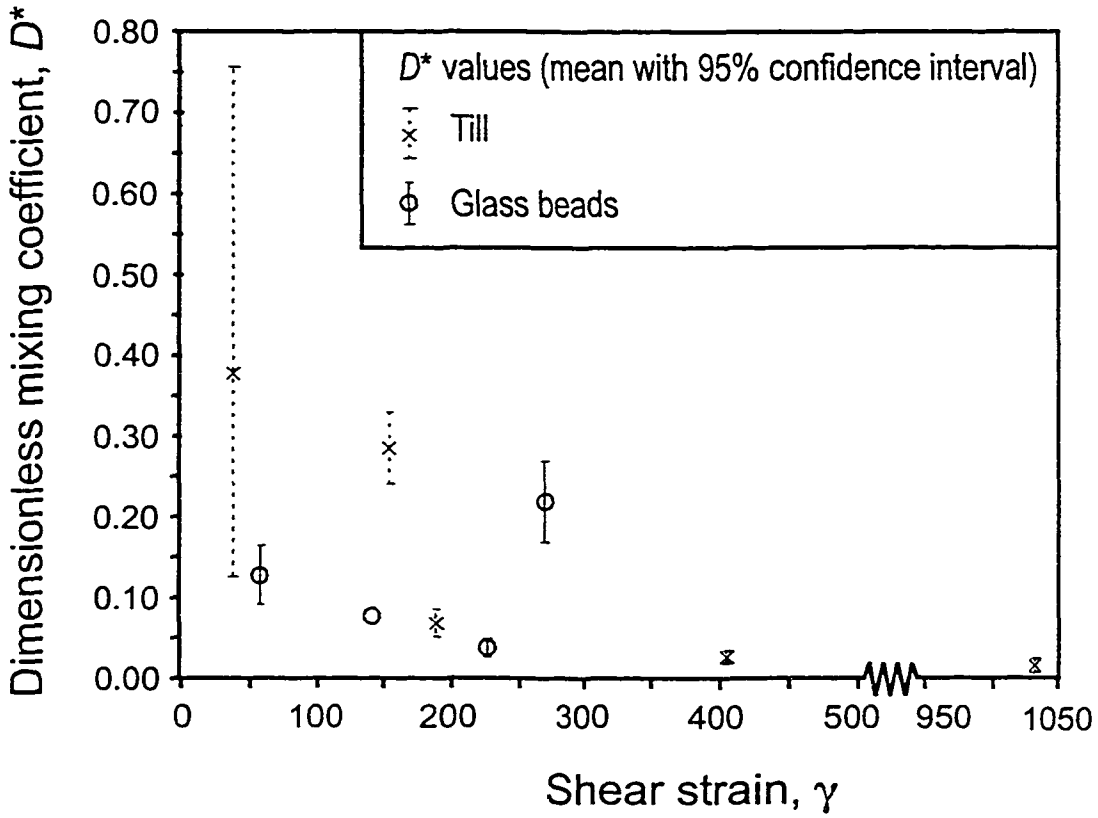

Figure 10. Dimensionless mixing coefficient D^* as a function of shear strain for the glass bead and till experiments as determined from the fit of the diffusion model to the laboratory data.

D^* values from the bead experiments vary through less than an order of magnitude and do not vary systematically with strain, but those from the till experiments vary through a factor of 27 and decrease with strain. This implies that either diffusion of particles in the till is fundamentally nonlinear or that some condition of the theory was imperfectly satisfied during the till experiments.

There are two possible explanations for why D^* values from the till experiments might decrease systemically as strain increases that do not involve nonlinear diffusion. First, the initially sharp contact between the two tills may become irregular if consolidation prior to shearing is non-uniform. An irregular contact would result in artificially large D^* values in experiments terminated at low strains. In experiments carried out to higher strains, however, the apparent mixing resulting from an irregular contact would be a smaller fraction of the total mixing, and thus D^* values calculated from such experiments would be smaller and more accurately reflect the diffusive particle flux. A second possibility is that at large strains deformation becomes focused high in the shear zone, as was observed in experiments by Mandl and others (1977) on various granular materials with a similar ring-shear device. This would lead to artificially low D^* values at high strains because till at greater depths in the shear zone where mixing occurs would be subjected to a smaller cumulative strain than that used in the determination of D^*. This possibility cannot be ruled out because the linearity of the displacement profiles can be verified only at low strains (Fig. 5 and 6).

Despite the vastly different grain-size distributions of the beads and till, D^* values for the two materials were of nearly the same order of magnitude. Apparently, the ensemble average of vertical particle motions induced by shearing was not greatly different in the two materials. In addition, the till did not undergo detectable percolation (Scott and Bridgwater,

1976; Stephens and Bridgwater, 1978; Bridgwater et al., 1985; Savage, 1987), the process by which smaller particles move down through void spaces created by a network of larger particles during shearing. This process may affect mixing profiles, leading to D^* values that are different from those due solely to random particle motion (Stephens and Bridgwater, 1978). However, percolation was not likely to be important in our experiments because over 80% of till particles were smaller than the 0.4-1.0 mm shale grains that were counted to establish the mixing profiles. These shale grains, therefore, were surrounded by predominantly smaller particles and thus, void spaces large enough to allow their percolation were probably rare. Furthermore, if percolation of shale particles did occur, till mixing profiles should have displayed systematic asymmetry. No such asymmetry was observed.

Values of D^* indicated by our experiments are similar to those determined by others (Scott and Bridgwater, 1976; Stephens and Bridgwater, 1978; Bridgwater, 1980). In the experiments of Scott and Bridgwater (1976), a simple-shear apparatus was used to study the mixing between two layers of spheres of different color undergoing shear. The same type of experiment was carried out by Stephens and Bridgwater (1978) using an annular shear device. The equivalent mean D^* values from these studies ranged from 0.022 to 0.055 and fall within the range of values determined from our bead and till experiments.

The similarity between D^* values from these studies and those from our own experiments is significant because these studies were carried out at much higher strain rates (0.161 to 3.8 s^{-1}) and lower normal stresses (1.36 to 3.42 kPa). To quantify the difference in momentum exchange and friction between these laboratory studies and our experiments, we calculated Savage numbers (see Iverson, 1997) to evaluate the ratio of inertial shear stress associated with grain collisions to the quasi-static shear stress associated with grain friction. Savage

numbers from our experiments were at least eight orders of magnitude smaller than those calculated for natural and experimental debris flows (Iverson, 1997) and from laboratory experiments (Scott and Bridgwater, 1976; Stephens and Bridgwater, 1978). The apparent insensitivity of D^* values to strain rate and effective normal stress indicates that our experimental D^* values can be applied to subglacial settings where strain rates and effective pressures may have been different from those of our experiments.

The D^* values determined from our experiments are also similar to those calculated using kinetic gas theory. Kinetic theory has been used extensively to model granular flows because of their similarities to the flow of gases and dense fluids at the molecular level (Savage and Jeffery, 1981; Jenkins and Savage, 1983; Lun et al., 1984; Savage, 1993, Hsiau and Hunt, 1993a). Particles in a granular material undergoing simple shear are in an agitated state of motion and experience frequent collisions with surrounding particles. If the velocity of individual particles after a collision is u, and the average velocity of all particles is c, then a quantity called the granular temperature, T, can be defined for uniform simple shear

$$T = \frac{C^2}{3}, \tag{5}$$

where C is the average difference between c and u (Lun et al., 1984). Knowing the diameter of the particles, σ, and the coefficient of restitution, e, that characterizes the elasticity of the particle collisions, then the diffusivity determined from kinetic theory, D_k, is

$$D_k = \frac{\sigma\sqrt{\pi T}}{8(1+e)\nu g_o}, \tag{6}$$

where g_o, the so-called radial-distribution function, represents the initial velocity distribution of particles in contact with each other (Hsiau and Hunt, 1993; Savage, 1993). An empirical approximation of g_o is given by Carnahan and Starling (1969)

$$g_o = \frac{(2-\nu)}{2(1-\nu)^3}, \tag{7}$$

where ν is the bulk solid fraction of the granular material during shearing (1-porosity). The parameters used to calculate values of D_k are presented in Table 3. A reasonable upper bound for u in our experiments is the displacement rate of the rotating lower platen; direct tracking of the velocity of individual particles in our experiments was not possible. A reasonable value for c is one-half the displacement rate of the lower platen. Experimental data and theoretical analysis by Lun and Savage (1986) suggests that e approaches 1.0 if the impact velocity between particles is small. In our experiments, impact velocities are very small, and thus, e values ranging between 0.85 and 1.0 are used in the calculation of D_k. The value of ν was determined from the bulk density. For comparison with our laboratory results, values of D_k are changed to their dimensionless equivalent D_k*, by dividing by the square of the appropriate particle size and by the shear strain rate.

The results from the kinetic gas theory and our experiments agree to within an order of magnitude (Table 3), which is perhaps surprising in light of the uncertainty in estimating u and the granular temperature. The ranges of D_k* reported result from the ranges of e and ν considered. Agreement is poorest at high strains where $D^*<D_k^*$. This may reflect the focusing of strain within the shear zone at high strains, which as described earlier, may have led to artificially small values of D^* at high strains.

Table 3. Parameters used in the kinetic gas theory calculation of D_k*.

Experiment number	c (mm s^{-1})	u (mm s^{-1})	σ (mm)	e	ν	$\dot{\gamma}$ (s^{-1})	γ	D_k* (from theory)	Mean D* (from experiments)
Bead 1	0.0141	0.0071	0.8	0.85-1.0	0.6-0.7	6.41×10^{-4}	57	0.052-0.145	0.128
Bead 2	0.0128	0.0064	0.8	0.85-1.0	0.6-0.7	5.30×10^{-4}	225	0.062-0.171	0.039
Bead 3	0.0127	0.0063	0.8	0.85-1.0	0.6-0.7	3.95×10^{-4}	142	0.076-0.211	0.078
Bead 4	0.0147	0.0073	0.8	0.85-1.0	0.6-0.7	4.52×10^{-4}	270	0.093-0.257	0.219
Till 1	0.0125	0.0063	0.7	0.85-1.0	0.6-0.7	3.58×10^{-4}	39	0.095-0.263	0.378
Till 2	0.0267	0.0134	0.7	0.85-1.0	0.6-0.7	5.93×10^{-4}	406	0.111-0.309	0.026
Till 3	0.0126	0.0063	0.7	0.85-1.0	0.6-0.7	3.14×10^{-4}	189	0.108-0.301	0.068
Till 4	0.0131	0.0065	0.7	0.85-1.0	0.6-0.7	4.35×10^{-4}	151	0.081-0.226	0.284
Till 5	0.0143	0.0071	0.7	0.85-1.0	0.6-0.7	4.93×10^{-4}	1032	0.076-0.211	0.014

Implications for field studies

If D is known from laboratory experiments then, in principle, diffusion theory can be used to test the bed-deformation hypothesis by measuring the mixing that has occurred across the contact between two till units in the geologic record. More specifically, if it is assumed a priori that the observed mixing is the result of bed deformation, then the appropriate solution to the diffusion equation can be used to obtain γ. Here we present an example of the method applied to the contact between the Des Moines Lobe and Superior Lobe tills in east-central Minnesota.

A mixing profile was measured across a typical Des Moines Lobe/Superior Lobe till contact from a gravel pit approximately 20 km north of St. Paul, Minnesota (Fig. 11). At this location, there is approximately 2-3 m of Des Moines Lobe till deposited by the Grantsburg Sublobe on top of Superior Lobe till. Samples were collected at 1-2 mm increments over a two-meter thick section centered at the visual contact between the two tills. The vertical location of each sample was measured with a point gauge anchored at the top of the section. Each sample was then wet-sieved in the laboratory to isolate the 0.4-1.0 mm size fraction. This fraction was spilt multiple times to obtain approximately 300-500 grains. Grains of shale, the selected index lithology, were then identified. These grains, as well as the total number of grains, were counted to establish a mixing profile.

The profile shows that mixing occurred between the two tills over a thickness of 40 mm, and that it was symmetric about the visual contact between the tills. A good simplification, owing to the small thickness over which mixing occurred, is that the contact was positioned in till thick enough relative to the zone of mixing to be considered infinite.

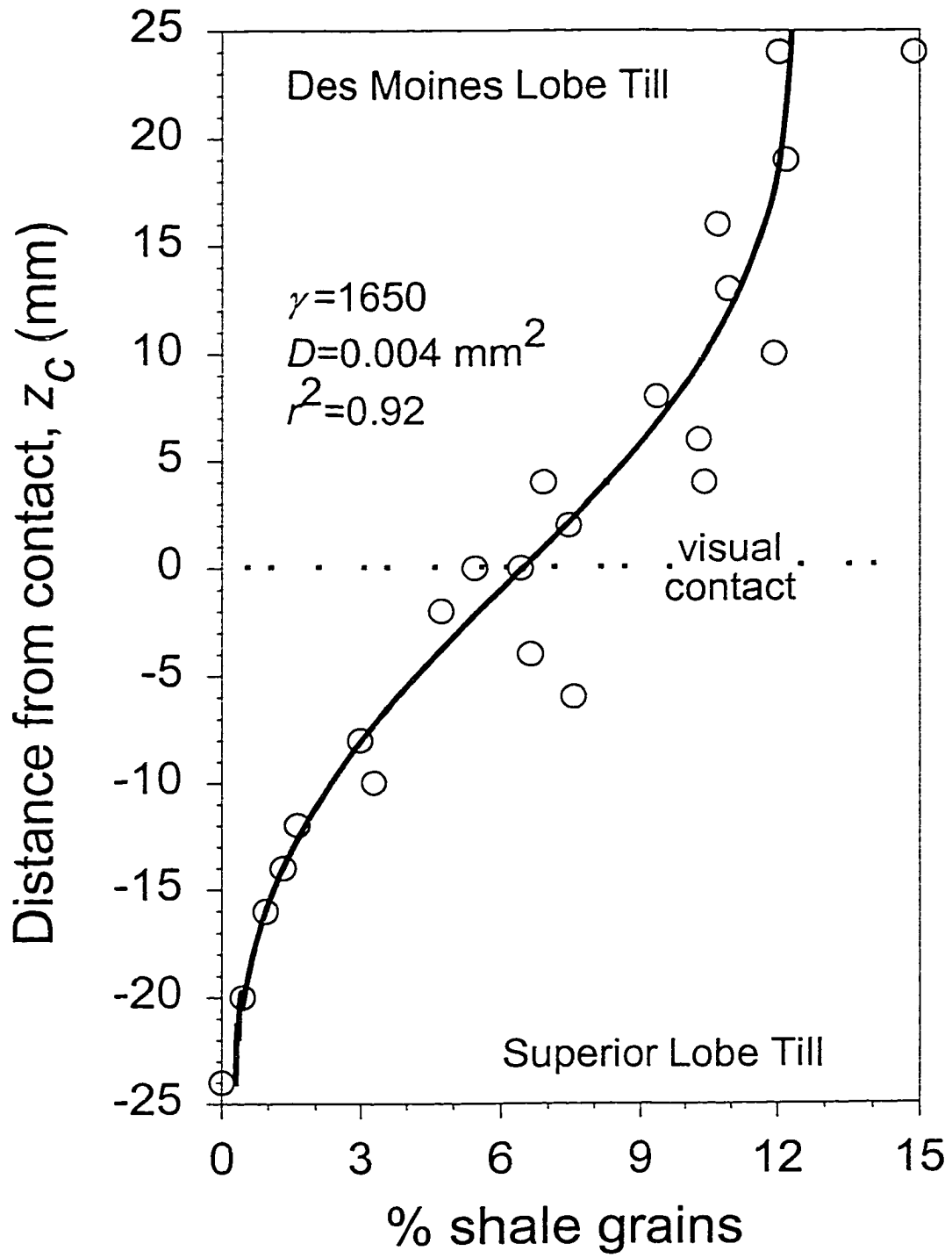

Figure 11. Mixing profile measured across the contact of the Des Moines Lobe and Superior Lobe tills at a site 20 km north of St. Paul, Minnesota. The curve represents the fit of the diffusion model to the data using a D value of 0.004 mm^2, the minimum value determined in the ring-shear experiments.

The solution to Equation 1 then reduces to

$$C(z,\gamma) = C_1 C_2 + \frac{C_1}{2} erfc\left(\frac{z_c}{2\sqrt{D\gamma}}\right) \quad (8)$$

(Crank, 1957, p. 12), where z_c is defined as the distance from the contact. Using a minimum D value of 0.004 mm^2, as determined in the laboratory experiments, the best fit of Equation 8 to the field data using the method of least squares results in $\gamma = 1650$. This is a maximum value of γ not only because a minimum value of D was used but also because an initially smooth contact between the two till units is assumed implicitly in the calculation. An initially irregular contact would result in more apparent mixing at lower strains thus reducing the calculated value of γ. The Des Moines Lobe/Superior Lobe contact is, indeed, locally irregular (Chernicoff, 1983), although it is impossible to know its original geometry.

A shear strain of 1650 may indicate that only a small portion of the Grantsburg Sublobe's displacement was due to shearing of subglacial sediment. It has been established that the sublobe most likely overrode this site for at least 2000 years (Chernicoff, 1983). If the average basal velocity of the sublobe was 400 ma^{-1} and deformation of the underlying sediment occurred over a thickness of 5 m, similar to values suggested for Ice Stream B (Alley et al., 1986), then the resultant shear strain would be 97 times greater than the maximum value inferred from the mixing profile. Put differently, bed deformation would account for only 8 of the 800 km that the lobe would have moved.

Obviously, however, there are major uncertainties in such an estimate. The speed of the Des Moines Lobe is not well known. The basal ice velocity may have been less than 400 m a^{-1}, although the radiocarbon chronology, if taken at face value, indicates advance rates on the order of 2000-3000 ma^{-1} (Clayton and Moran, 1982). Such a high rate of basal motion

would further reduce the fraction of motion accounted for by bed deformation. A second uncertainty is that strain may have focused in one of the two till units, potentially resulting in no mixing. This might occur if the shear strength of one till was much less than that of the other. Clearly, therefore, other indicators of strain such as clast fabric (Hooyer and Iverson, in press) should be used together with the approach developed here.

Several other potential sources of uncertainty are probably minor. The first of these is whether small-scale experimental D values can be applied to larger-scale shear zones in the field. The principal concern is whether the removal of large clasts from till in the experiments affects mixing. Since these clasts constitute less than only 2% of the till by volume, this is unlikely. Furthermore, the two tills have a self-similar grain-size distribution (Fig 3.), indicating that the relative sizes of adjacent particles are the same at all scales. Since relative particle size should control vertical particle motions and mixing, mixing should be independent of the scale of the shear zone. Comminution of the index lithology with shear strain may also introduce uncertainty. Comminution, however, should influence mixing profiles only if deformation, and hence comminution, is not uniform with depth. Then, for example, more of the 0.4-1.0 mm size fraction might be lost at one depth than another. However, the good fit of the diffusion model, in which uniform deformation is assumed, to the field data is evidence that deformation across the contact, if it really occurred, was relatively uniform. A final uncertainty arises from the potential influences of effective stress and shear strain rate on mixing. The similaritity of our D^* values to those of Scott and Bridgwater (1976) and Stephens and Bridgwater (1978) studies indicate that variations in these parameters are relatively unimportant.

Finally, it should be emphasized that it is quite possible that mixing resulted from a subglacial process other than pervasive deformation of the bed. Our goal here has been to attempt to place an upper limit on the extent of deformation, if, indeed it was responsible for mixing.

CONCLUSIONS

Mixing occurs between two adjacent layers of granular material undergoing simple shear. Diffusion theory provides an adequate theoretical foundation for describing this mixing, and ring-shear experiments provide the value of the only fitted parameter in the theory, the mixing coefficient, D. The value of D decreased with strain in the till experiments, either due to an irregular initial contact, or the focusing of deformation away from the contact at high strains. Kinetic gas theory provides an estimate of the dimensionless equivalent of D that is within an order of magnitude of fitted laboratory values.

The determination of D in the laboratory allows the maximum bed shear strain to be estimated from the distribution of index lithologies measured across till contacts in the field. A preliminary application of this technique at one field site, where the Des Moines Lobe/Superior Lobe till contact is exposed, indicates a shear strain of 1650, which is likely a small fraction of that required of the deforming-bed model of glacier motion. However, uncertainties are sufficiently large that the method cannot be used as the sole criterion for assessing bed deformation.

REFERENCES

Alley, R.B., Blankenship, D.D., Bentley, C.R. and Rooney, S.T., 1986, Deformation of till beneath Ice Stream B, West Antarctica: Nature, 322, p. 57-59.

Alley, R.B., 1991, Deforming-bed origin for southern Laurentide till sheets?: Journal of Glaciology, v. 37, p. 67-76.

Boulton, G.S., 1996, The theory of glacial erosion, transport and deposition as consequence of subglacial sediment deformation: Journal of Glaciology, v. 42, p. 43-62.

Bridgwater, J., 1980, Self-diffusion coefficients in deforming powders: Powder Technology: v. 25, p 129-131.

Bridgwater, J., Foo, W.S., and Stephens, K.J., 1985, Particle mixing and segregation in failure zones-theory and experiment: Powder Technology, v. 41, p. 147.

Carnahan, N.F., and Starling, K.E., 1969, Equations of state for non-attracting rigid spheres: Journal of Chemical Physics, v. 51, p. 635-636.

Crank, J., 1957, *The Mathematics of Diffusion*, Second edition, Oxford University Press, 347 p.

Chernicoff, S.E., 1983, Glacial characteristics of a Pleistocene ice lobe in east-central Minnesota: Geological Society of America Bulletin, v. 94, p. 1401-1414.

Clark, P.U., 1994, Unstable behavior of the Laurentide Ice Sheet over deforming sediment and its implications for climate change: Quaternary Research, v. 41, p. 19-25.

Clark, P.U., and Walder, J.S., 1995, Subglacial drainage, eskers, and deforming beds beneath the Laurentide and Eurasian ice sheets: Geological Society of America Bulletin, v. 106, p. 304-314.

Clark, P.U., Licciardi, J.M., MacAyeal, D.R., and Jenson, J.W., 1996, Numerical reconstruction of a soft-bedded Laurentide Ice sheet during the last glacial maximum: Geology, v. 24, n. 8, p. 679-682.

Clark, P.U., 1997, Sediment deformation beneath the Laurentide Ice Sheet, in Martini, I.P., eds., Late glacial and postglacial environmental changes, Quaternary, Carboniferous-Permian and Proterozoic: p. 81-97.

Clayton, L., and Moran, S.R., 1982, Chronology of late Wisconsinan Glaciation in middle North America: Quaternary Science Reviews, v.1, p. 55-82.

Clayton, L., Teller, J.T., Attig, J.W., and Mickelson, D.M., 1989, Evidence against pervasively deformed bed material beneath rapidly moving lobes of the southern Laurentide ice sheet: Sedimentary Geology, v. 62, p. 203-208.

Dowdeswell, J.A., and Siegert, M.J., 1999, Ice-sheet numerical modeling and marine geophysical measurements of glacier-derived sedimentation on the Eurasian Arctic continental margins: Geological Society of America Bulletin, v. 111, p. 1080-1097.

Hart, J.K., and Boulton, G.S., 1991, The interrelation of glaciotectonic and glaciodepositional processes within the glacial environment, Quaternary Science Reviews, v. 10, p. 335-350.

Hart, J.K., 1994, Till fabric associated with deformable beds: Earth Surface Processes and Landforms: v. 19, p. 15-32.

Hart, J.K. 1995, Subglacial erosion, deposition and deformation associated with deformable beds: Progress in Physical geography, v. 19,2, p. 173-191.

Hart, J.K., 1997, The relationship between drumlins and other forms of subglacial glaciotectonic deformation: Quaternary Science Reviews, v. 16, p. 93-107.

Hart, J.K., and Roberts, D.H., 1994, Criteria to distinguish between subglacial glaciotectonic and glaciomarine sedimentation. I. Deformation styles and sedimentology: Sedimentary Geology, v. 91, p. 191-213.

Head, K.H., 1989, *Soil Technician's handbook*: John Wiley and Sons, New York.

Hicock, S.R. and Dreimanis, A., 1992, Deformation till in the Great Lakes regions: implications for rapid flow along the south-central margin of the Laurentide Ice Sheet: Canadian Journal of Earth Science, v. 29, p. 1565-1579.

Hiemstra, J.F., and van der Meer J.J.M., 1997, Pore-water controlled grain fracturing as an indicator for subglacial shearing in tills, Journal of Glaciology, v. 43, p. 446-454.

Hsiau, S. S., and Hunt, 1993, Kinetic theory analysis of flow-induced particle diffusion and thermal conduction in granular material flows: Journal of Heat Transfer, v. 115, p 541-548.

Hooke, R. LeB., and Elverhøi, A., 1996, Sediment flux from a fjord during glacial periods, Isfjorden, Spitsbergen: Global and Planetary Change, v. 12, p. 237-249.

Hooyer, T.H., and Iverson, N.R., in press, Clast-fabric development in a shearing granular material: Implications for subglacial till and fault gouge: Geological Society of America Bulletin.

Iverson, N.R., Hooyer, T. and Hooke, R. LeB., 1996, A laboratory study of sediment deformation: Stress heterogeneity and grain-size evolution: Annals of Glaciology, 22, p. 167-175.

Iverson, N.R., Baker, R., and Hooyer, T., 1997, A ring-shear device for the study of till deformation: tests on a clay-rich and a clay-poor till: Quaternary Science Reviews, v. 16, p. 1057-1066.

Iverson, N.R., Hooyer, T.S., and Baker, R., 1998a, Ring-shear studies of till deformation: Coulomb-plastic behavior and distributed strain in glacier beds: Journal of Glaciology, v. 44, p. 634-642.

Iverson, N.R., Baker, R.W., Hooke, R. LeB., Hanson, B., and Jansson, P., 1998b, Coupling between a glacier and a soft bed: I. A relation between effective pressure and local shear stress determined from till elasticity: Journal of Glaciology, v. 45, p. 31-40.

Iverson, R.M., 1997, The physics of debris flows, Reviews of Geophysics, American Geophysical Union, v. 35, p 245-296.

Jenkins, J.T., and Savage, S.B., 1983, A theory for the rapid flow of identical, smooth, nearly elastic spherical particles, Journal of fluid Mechanics, v. 130, p. 187-202.

Jenson, J.W., Clark, P.U., MacAyeal, D.R., Ho, C., and Vela, J.C., 1995, Numerical modeling of advective transport of saturated deforming sediment beneath the Lake Michigan Lobe, Laurentide Ice Sheet: Geomorphology, v. 14, p. 157-166.

Jenson, J.W., MacAyeal, D.R., Clark, P.U., Ho, C.L. and Vela, J.C., 1996, Numerical modeling of subglacial sediment deformation: implications for the behavior of the Lake Michigan Lobe, Laurentide Ice Sheet: Journal of Geophysical Research, v. 101, B4, p. 8717-8728.

Kemmis, T.J., 1981, Importance of the regelation process to certain properties of basal tills deposited by the Laurentide Ice Sheet in Iowa and Illinois, U.S.A.: Annals of Glaciology, v. 2, p. 147-152.

Lambe, T.W., and Whitman, R.V., 1969, *Soil Mechanics*: John Wiley and Sons, New York, 553 p.

Licciardi, J.M., Clark, P.U., Jenson, J.W., and MacAyeal, D.R., 1998, Deglaciation of a soft-bedded Laurentide Ice Sheet: Quaternary Science Reviews, v. 17, p. 427-448.

Lun, C.K.K., Savage, S.B., Jeffrey, D.J., and Chepurniy, N., 1984, Kinetic theories for granular flow: inelastic particles in Couette flow and slightly inelastic particles in a general flowfield: Journal of Fluid Mechanics, v. 140, p. 223-256.

Lun, C.K.K., and Savage, S.B., 1986, The effects of impact velocity dependent coefficient of restitution on stresses developed by sheared granular materials: Acta Mechanica, v. 63, p. 15-44.

Mandl, G., de Jong, L.N.J., and Maltha, A., 1977, Shear zones in granular material-An experimental study of their structure and mechanical genesis: Rock Mechanics, v. 9, p. 95-144.

Menzies, J., and Maltman, A.J., 1992, Microstructures in diamictons - evidence of subglacial bed conditions: Geomorphology, v. 6, p. 27-40.

Menzies, J., Zaniewski, C., and Dreger, D., 1997, Evidence, from microstructures, of deformable bed conditions within drumlins, Chimney Bluffs, New York State: Sedimentary Geology, v. 111, p. 161-175.

Piotrowski, J.A., and Kraus, A.M., 1997, Response of sediment to ice-sheet loading in northwestern Germany: effective stresses and glacier-bed stability: Journal of Glaciology, v. 43, n. 145, p. 495-502.

Sammis, C., King, G., and Biegel, R., 1987, The kinematics of gouge deformation: Pure and Applied Geophysics, v. 125, p. 777-812.

Savage, S.B., 1987, Interparticle percolation and segregation in granular material: a review, in Selvadurai, A.P.S., ed., Developments in Engineering Mechanics, Elsevier, New York, p. 347-363.

Savage, S.B., 1993, Disorder, diffusion and structure formation in granular flows, in Bideau, D., ed., Disorder and Granular Media, Elsevier Science Publishers, Amsterdam.

Savage, S.B. and Jeffrey, D.J., 1981, The stress tensor in a granular flow at high shear rates: Journal of Fluid Mechanics, v. 110, p. 255-272.

Scott, A.M., and Bridgwater, J., 1976, Self-diffusion of spherical particles in a simple shear apparatus: Powder Technology, v. 14, p. 177-183.

Shackelford, C.D., 1991, Laboratory diffusion testing for waste disposal – A review: Journal of Contaminant Hydrology: v. 7, p. 177-217.

Steel, R.G.D., Torrie, J.H., and Dickey, D.A., 1997, *Principles and Procedures of Statistics: A Biometrical Approach*: McGraw-Hill, New York, N.Y., 666 p.

Stephens, D.J., and Bridgwater, J., 1978, The mixing and segregation of cohesionless particulate materials. Part II. Microscopic mechanisms for particles differing in size: Powder Technology, v. 21 p. 29-44.

Van der Meer, J.J.M., 1993, Microscopic evidence of subglacial deformation: Quaternary Science Reviews, v. 12, p. 553-587.

Van der Meer, J.J.M., 1997, Particle and aggregrate mobility in till: microscopic evidence of subglacial processes: Quaternary Science Reviews, v. 16, p. 827-831.

CHAPTER 4. FLOW MECHANISM OF THE DES MOINES LOBE

A paper to be submitted to the Geological Society of America Bulletin

Thomas S. Hooyer and Neal R. Iverson
Department of Geological and Atmospheric Science
Iowa State University, Ames, Iowa

INTRODUCTION

Climate change during the Pleistocene has long been attributed to changes in insolation caused by variations of the earth's orbit on time scales ranging from 10^4 to 10^5 years (Hays et al., 1976; Lorius et al, 1990; Imbrie et al., 1992, 1993). However, superimposed on these long-term fluctuations in climate are shorter-term changes that occur over periods ranging from 10^2 to 10^3 years (Dansgaard et al., 1982; Oeschger et al, 1984; Bond and Lotti, 1995; Grootes and Stuiver, 1997). These short-term events may be the result of sudden changes in the circulation of the North Atlantic Ocean due to massive inputs of fresh water. One source of freshwater was the melting of icebergs originating from the Laurentide Ice Sheet (Keigwin et al., 1991; Charles and Fairbanks, 1992; Lehman and Keigwin, 1992; Bond et al., 1992; Broecker, 1994; Oppo and Lehman, 1995), which underwent rapid, quasi-periodic surging through Hudson Straight (Andrews and Tedesco, 1992; Grousset et al., 1993). Similar-ice sheet instability has also been documented along the southern margin of the Laurentide ice sheet (Clayton et al., 1985, Mickelson et al., 1983).

Ice-sheet instability and fast glacier flow may be related to pervasive deformation of water-saturated, weak, subglacial sediment (Boulton and Jones, 1979; Alley et al., 1986, 1987a; Clark, 1992; Boulton, 1996). This idea gained widespread support when seismic data

revealed that rapidly moving Ice Stream B in West Antarctica was underlain by a thick (5-10 m) layer of porous till rather than bedrock (Blankenship et al., 1986). Owing primarily to its high porosity, the bed was inferred to be deforming pervasively and controlling the motion of the ice stream (Alley et al., 1986, 1987, 1989). Support for this idea came from data collected beneath Breidamerkurjökull, an Icelandic glacier, where measurements indicated about 90% of basal motion was by bed deformation (Boulton and Hindmarsh, 1987). Subsequently, others have suggested that the Laurentide ice sheet, which was underlain by essentially continuous till sheets along it southern margin, might have moved by this mechanism (Alley, 1991; Jenson et al., 1995, 1996; Clark et al., 1996; Clark, 1994, 1997; Licciardi et al., 1998).

A more thoroughly studied mechanism of fast glacier flow involves separation of ice from the bed when water pressure in the subglacial hydrologic system nears the ice overburden pressure (e.g., Kamb et al., 1985; Raymond and Harrison, 1988; Iken and Truffer, 1997). Such ice-bed separation accelerates regelation and creep of ice past roughness elements on the bed, the two classical mechanisms of glacier sliding (e.g., Weertman, 1964; Lliboutry, 1979). In addition, in the case of a till bed, plowing may be enhanced. Plowing is the process in which clasts protruding from the basal ice are dragged through the till bed (Brown et al., 1987, Iverson, 1999). Decoupling of ice from the bed due to ice/bed separation and plowing has been hypothesized to be an important mechanism of motion of portions of Pleistocene ice lobes (Brown et al., 1987; Piotrowski and Tulaczyk, 1999).

Distinguishing between bed deformation and plowing and sliding at the ice/bed interface is not only important in understanding glacier motion, it is an essential step toward

a full understanding of glacial sediment transport and landform development. For example, pervasive bed deformation has been invoked as an important process in the formation of various landforms including drumlins (Smalley and Unwin, 1968; Boulton, 1987), eskers (Clark and Walder, 1995), and moraines (Clark, 1997). This process may also account for high inferred sediment fluxes of some lobes of the Laurentide Ice Sheet (Alley, 1991; Jensen et al., 1995; 1996) and elsewhere (Hooke and Elverhøi, 1996; Dowdeswell and Siegert, 1999). Glacial geologic observations, however, frequently conflict with these hypotheses. For example, the preservation of thin lenses of sorted sediment within basal tills seems to indicate that deformation of the bed was minimal (e.g., Brown et al., 1987; Clayton et al, 1989; Piotrowski and Kraus, 1997).

Research on modern glaciers that rest on till indicates that the distribution of motion with depth is variable. Direct measurements of bed deformation using tiltmeters at Storglaciären, Sweden (Iverson, et al., 1995; Hooke et al., 1997) and of sliding at Trapridge Glacier, Canada (Blake et al, 1994, Fischer and Clarke, 1997) indicate that when basal water pressures are high, these glaciers accelerate, and motion is focused near the bed surface. A similar observation has been made at Ice Stream B (Engelhardt and Kamb, 1998), where basal water pressures are continuously high. Iverson (1999) thought that ice/bed separation and plowing were responsible for decoupling ice from the till. However, there is conflicting evidence. Displacement of markers placed in till beneath Breidamerkurjökull, Iceland, seem to indicate that most glacier motion occurs at depth in the bed, if averaged over a number of water-pressure fluctuations (Boulton and Hindmarsh, 1987). Additional support for till deformation beneath modern glaciers comes from a bent drill stem recovered from beneath

Columbia Glacier, Alaska (Humphrey, 1993) and a recent measurement of sliding beneath Ice Stream D in West Antarctica (Engelhardt, pers. comm. 9/99).

Geologic data along the southern margin of the Laurentide Ice Sheet provide an opportunity to evaluate mechanisms of glacier motion over large areas inaccessible beneath modern glaciers. In this chapter, the possible flow mechanisms of the Des Moines Lobe are evaluated. From geologic data, the lobe is reconstructed to determine its surface morphology and calculate its driving stress. Results from geotechnical tests on till samples allow the effective pressure on the bed during the glacial maximum to be estimated. A model of sliding and plowing (Iverson, 1999) provides a basis for estimating the shear strength of the ice/bed interface from the effective pressure. The model results, together with field observations of till fabric and mixing, indicate that most motion probably occurred by sliding and plowing at the bed surface.

REGIONAL SETTING

The Des Moines Lobe was the most conspicuous of several large ice lobes of the Laurentide ice sheet that extended into the mid-continent region of North America during the last glaciation. At its maximum extent, approximately 13.8 ka before present, the lobe was approximately 700-900 km long, 200 km wide, and covered a large portion of southern Minnesota and north-central Iowa (Fig. 1). An arm of the Des Moines Lobe, the Grantsburg Sublobe, flowed to the northeast into western Wisconsin. In Minnesota, the Des Moines Lobe followed the lowland now occupied by the Minnesota River. The lobe was bounded by the older glacial deposits of the Coteau Des Prairies to the southwest and by the St. Croix Moraine of the Superior Lobe to the northeast (Hobbs and Goebel et al., 1982). At the border

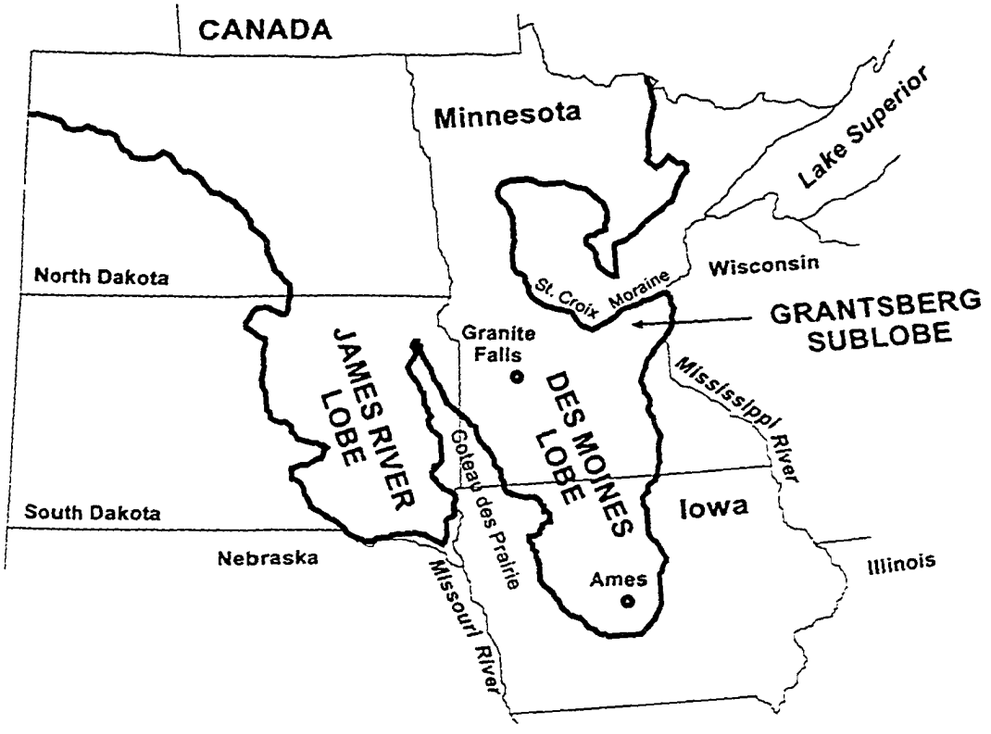

Figure 1. Maximum extent of the Des Moines Lobe and the Grantsberg Sublobe.

of Minnesota and Iowa, the lobe flowed into central Iowa along the ancestral Des Moines River valley (Wright, 1973).

Reconstructions of the surface morphology of the Des Moines Lobe indicate that it was probably thin and gently sloping (Mathews, 1974, Clark, 1992). Driving stresses calculated from the reconstruction of Clark (1992) range from 0.7-4.3 kPa, more than twenty times smaller than that considered typical for glaciers (Paterson, 1994, p. 240). Furthermore, rates of ice-margin advance for the lobe were on the order of 2000-3000 m a^{-1}, as determined from the radiocarbon chronology (Fig. 2) (Clayton and Moran, 1982). Advance rates provide a lower bound for the glacier flow rate. Based on these rapid flow rates and low driving stresses, the Des Moines Lobe has been compared to the poorly understood ice streams of the Siple coast in West Antarctica (Clark, 1992; Patterson, 1998).

The till deposited by the Des Moines Lobe, called the Dows Formation in Iowa, is on average 15-20 m thick and is divided into the Alden Member and the overlying Morgan Member (Hallberg and Kemmis, 1986). The Alden Member is a structureless diamicton, ranging in thickness from 10 to 20 m, and is interpreted to be a subglacial till. The Morgan Member, not present everywhere, is texturally heterogeneous, interbedded, and contains sorted sediment. It is interpreted as supraglacial till deposited in an ice-marginal setting (Bettis et al., 1996). In Minnesota, the till of the Des Moines Lobe is referred to as the New Ulm till. It is bit thinner than in Iowa, ranging from 5-10 m in thickness (Patterson, 1996). The till in both states typically overlies drift associated with earlier glaciations. The total thickness of these units varies locally between 20-60 m, although in areas adjacent to the Coteau Des Prairies, the lobe overrode unconsolidated sediment that is over 200 m thick (Patterson et al., 1995; Bettis et al., 1996).

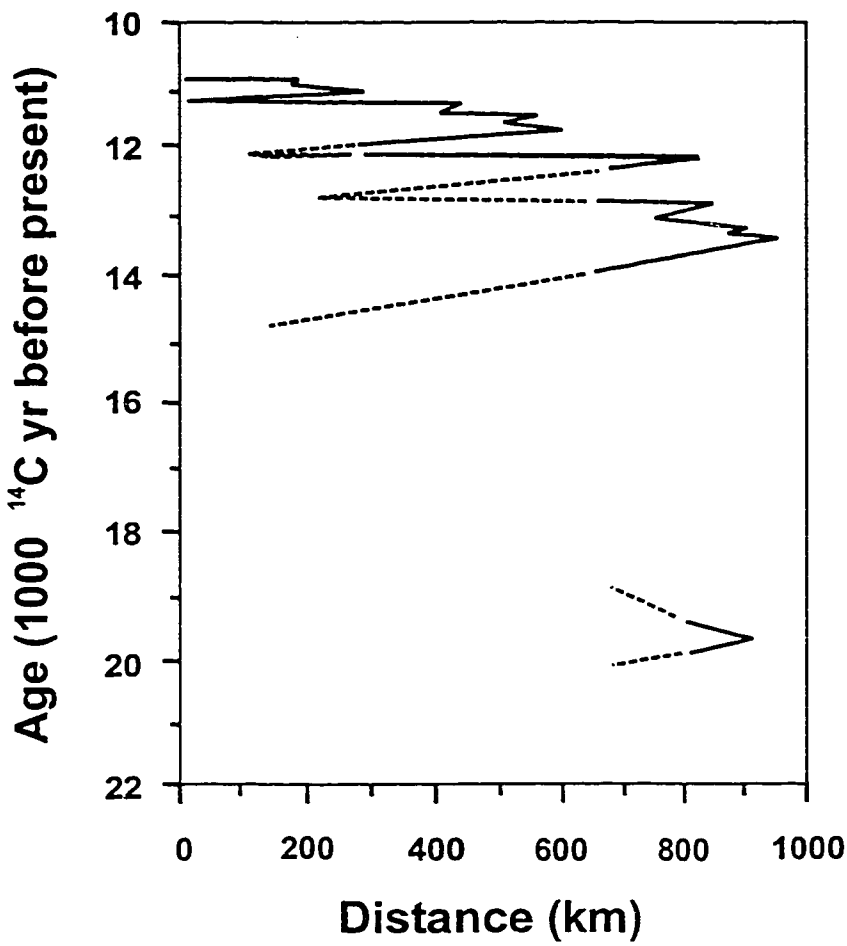

Figure 2. Time-distance diagram of the Des Moines Lobe showing oscillations of the margin between 22,000 and 10,000 ^{14}C years before present. The distance is referenced to the border between Minnesota and Canada (modified from Clayton and Moran, 1982).

The maximum extent of the Des Moines Lobe is well defined by a 5-15 km wide band of elevated hummocky topography known as the Bemis Moraine. The moraine is coeval with the Pine City Moraine of the Grantsburg Sublobe (Wright and Ruhe, 1965; Wright et al, 1973; Goebel and others, 1983), which is hereafter considered part of the Bemis Moraine. Numerous other moraines within the margin of Bemis Moraine represent subsequent stable positions of the lobe. These include the Altamont and Algona Moraines in Iowa (Bettis et al., 1996) and the Gary and Big Stone Moraines in Minnesota (Hobbs and Goebel, 1982). Some other dominant geomorphic features of the lobe include aligned hummocks (Gwynne, 1942, 1951; Stewart et al., 1988, Colgan, 1996), poorly defined tunnel valleys (Patterson, 1996), eskers (Hobbs and Goebel, 1982), and large areas of hummocky relief (Kemmis, 1991).

The presence of tunnel valleys and eskers suggests that there was a significant meltwater at the bed of the glacier. This is not surprising given that the lobe advanced into a relatively warm climate as indicated by silt and fine sand at the base of the Dows Formation that contains abundant insect faunas (Schwert and Torpen, 1996), plant macrofossils, (Baker, 1996) and trees (Bettis et al., 1996). This biological evidence suggests that the lobe advanced into a boreal forest dominated by ponds, fens, and other wetlands with spruce present on the drier uplands (Schwert and Torpen, 1996). Additional support for a warm climate is the lack of periglacial features adjacent to the ice margins, indicating that permafrost was not pervasive (Konen, pers. com., 10/1999).

RECONSTRUCTION

Method

A first step toward evaluating the principal flow mechanism of past ice sheets is reconstructing their surface morphology. Clark (1992) reconstructed the Des Moines Lobe using the elevation of its terminal moraine and flow lines inferred from aligned hummocks and shale isopleths. Here, I reconstruct the Des Moines Lobe using additional flow-line indicators and also examine the sensitivity of the reconstruction to the elevation of the Bemis Moraine, which may have been ice-cored and hence higher than its present elevation.

To reconstruct the Des Moines Lobe, first the position and elevation of the Bemis Moraine are determined from geologic maps (Hobbs and Goebel, 1982; Goebel et al., 1983; Hallberg et al., 1991) and from 1:24,000 U.S.G.S topographic maps, respectively. The highest moraine elevation is measured every 2-5 km. This elevation is assumed to be that of the glacier margin when the lobe was at its maximum extent. The premise for moraine deposition is that basal debris is transported to the glacier surface near the ice margin due to upward flow in the ablation area (Fig. 3A). If the glacier is in a steady state, debris will accumulate at the ice margin forming a moraine that is modified by fluvial and mass wasting processes (Eyles, 1979, Benn and Evans, 1998, p. 245). Upon ice lobe retreat, the moraine is similar in elevation and morphology to that observed today.

Modern moraine elevations, however, may not reflect the elevation of the moraine during the glacial maximum if the moraine was ice-cored, a common observation along retreating modern ice margins (e.g., Østrem and Arnold, 1970; Hooke, 1970, 1973; Østrem, 1971; Fitzsimons, 1997). If the Bemis Moraine was ice-cored, then its elevation during the maximum extent of the lobe would have been higher than its modern elevation implying that

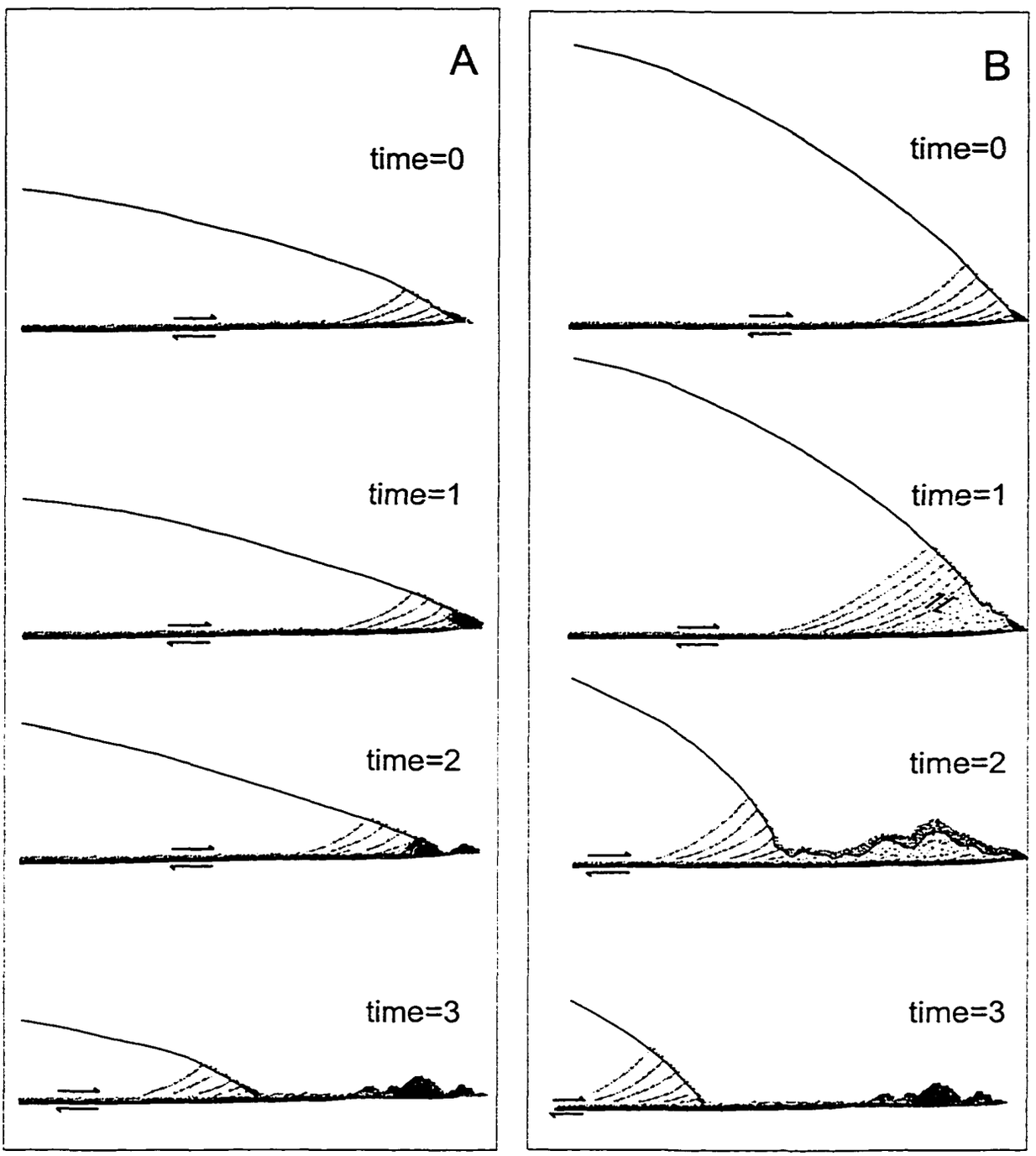

Figure 3. Two depositional models for the construction of the Bemis end moraine. (A) End moraine forms adjacent to a thin ice lobe where basal debris accumulates by melting at an active ice margin. (B) End moraine forms adjacent to a thick ice lobe where the active ice overrides stagnant ice, resulting in an ice-cored moraine. The ice core eventually melts and the debris is lowered onto the surface resulting in a moraine with an elevation less than that at the glacial maximum.

the lobe could have been significantly thicker (Fig. 3B). As the lobe retreated, subsequent melting of the stagnant, debris-rich margin would have reduced its elevation to its current level (Johnson, 1971; Eyles, 1979).

To estimate the decrease in moraine elevation that could have occurred since retreat of the lobe, it is assumed that the Morgan Member melted from stagnant marginal ice. The minimum thickness of this till, T_m, was estimated by measuring the relief on the Bemis Moraine using closed and semi-closed depressions (Fig. 4). The past thickness of the moraine assuming that it was ice-cored during the lobe's maximum extent is $T_m(1\text{-}p)/C_d$, where p is the porosity of the modern moraine sediment (~0.3) and C_d the volumetric debris fraction in the ice-cored moraine. A reasonable value of C_d is 0.15 (Kirkbride, 1995), which yields an ice-cored moraine elevation 25-100 m higher than the current moraine. Examination of an ice-cored moraine at the terminus of the Miles Glacier, Alaska, between 1910 (Tarr and Martin, 1914) and 1959 (1:24,000 U.S.G.S. topographic map) indicates that such a reduction in elevation is possible.

The paleo ice-flow direction is determined from aligned hummocks oriented transverse to ice flow (Gwynne, 1942; Ruhe, 1969; Palmquist and Connor, 1978; Stewart et al., 1988) and from tunnel valleys and eskers oriented parallel to flow (Fig. 5) (Hobbs and Goebel, 1982, Patterson, 1996). The concentration of sand-sized shale fragments in the basal till is also used as an ice-flow indicator (Matsch, 1972). A reduction in concentration of these particles is interpreted to be the result of comminution that increases as a function of transport distance from the shale source outcrop. Isopleths of shale content, therefore, are perpendicular to ice flow. Important uncertainties are whether aligned hummocks, the most ubiquitous flow indicators, actually form subglacially (e.g., Stewart et al., 1988) and hence

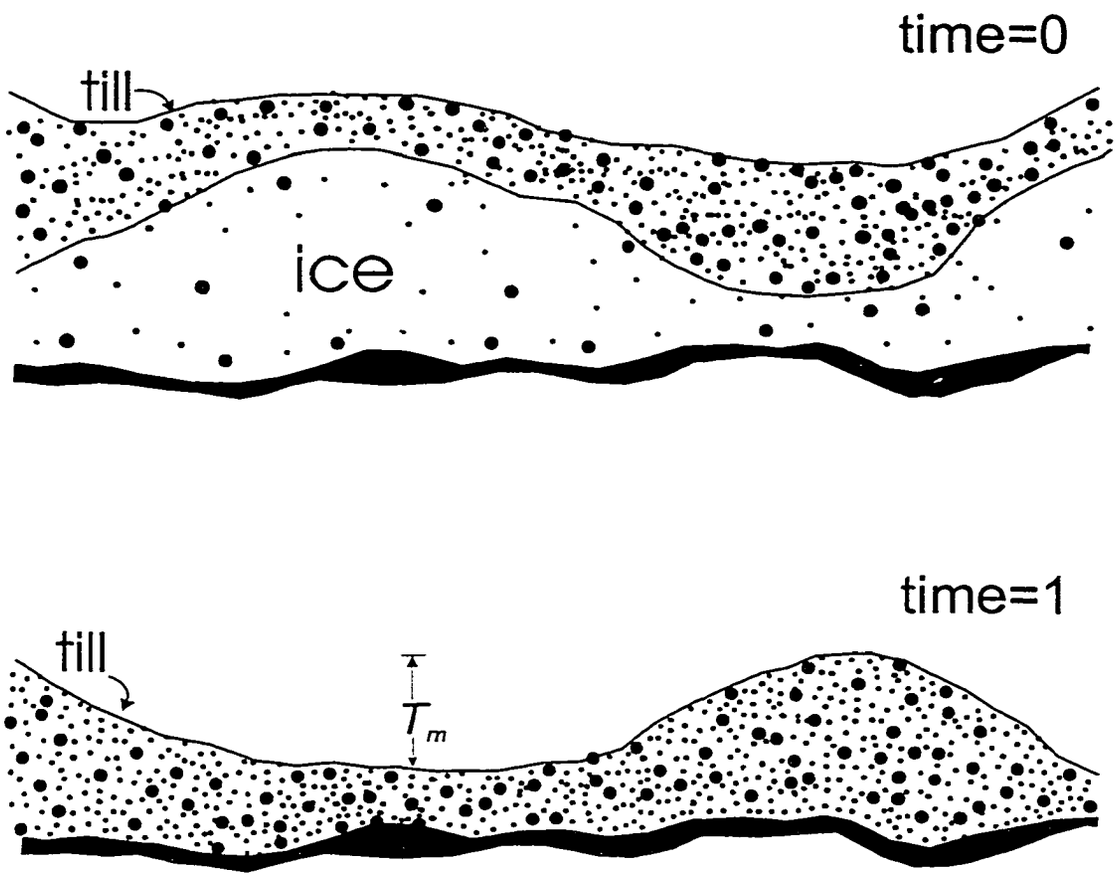

Figure 4. A Cross-section of an ice-cored moraine during melting and after melting is complete. The minimum thickness of supraglacial debris, T_m, was used to estimate the minimum ice-cored moraine elevation (modified from Eyles, 1979).

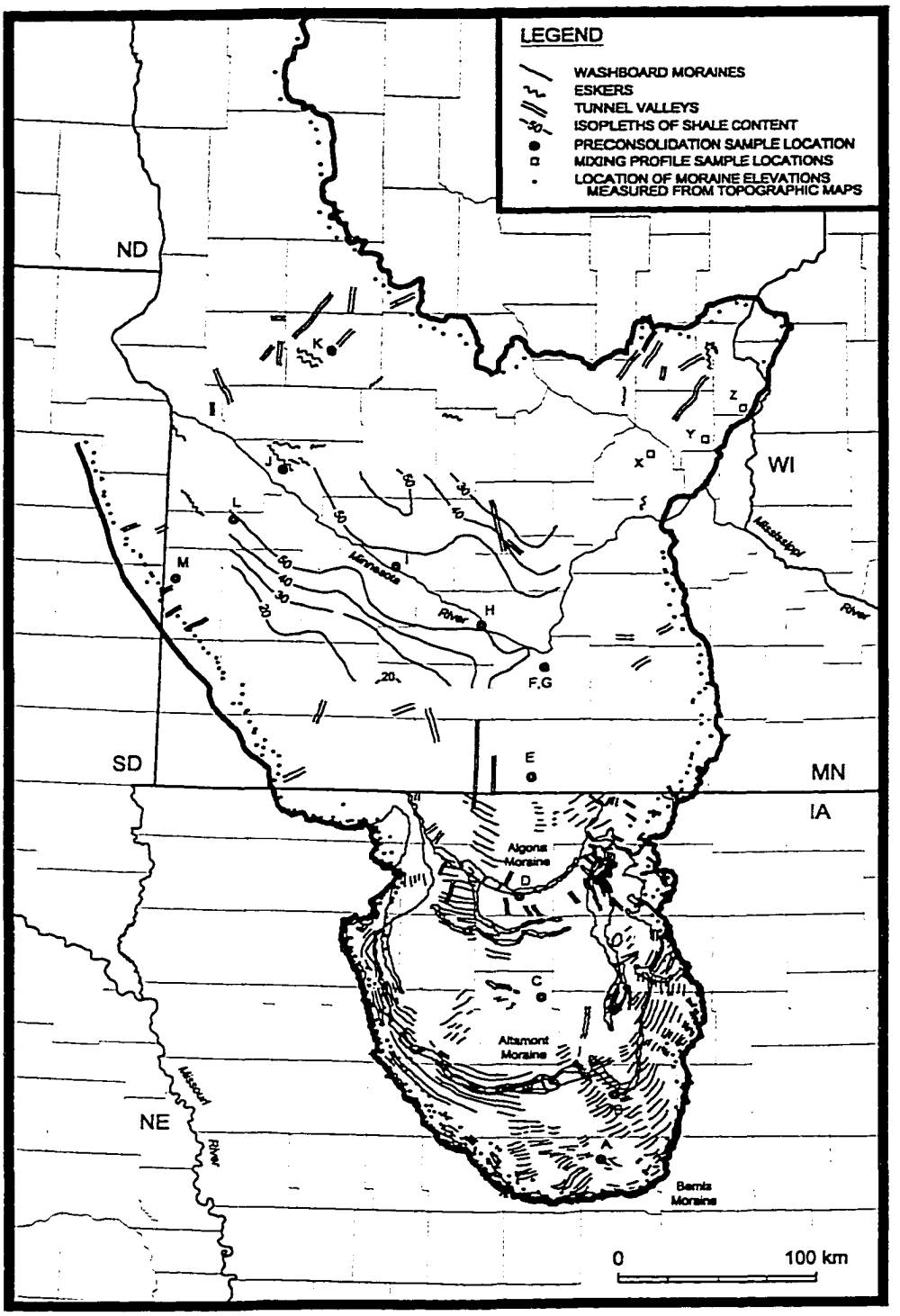

Figure 5. Geomorphic features and shale isopleths of the Des Moines Lobe. Letters indicate the locations of samples taken for consolidation tests and mixing profiles. The small dots near the glacier margin represent the location of the Bemis Moraine elevations measured from topographic maps.

lie normal to ice flow and whether all flow indicators developed during the glacial maximum. Following Clark (1992), these assumptions are considered to be generally valid, although the second assumption, in particular, is clearly imperfect.

Once elevations along the Bemis Moraine are known and flow-direction indicators are defined, elevations from the Bemis Moraine are projected across the lobe normal to the flow direction to produce contours of the ice surface.

Results

Reconstructions of the Des Moines Lobe using modern moraine elevations (Case 1) and the estimated ice-cored moraine elevations (Case 2) are presented in Figures 6 and 7, respectively. For Case 1, the lobe is thin; moraine elevations range from only about 300 m above sea level (m a.s.l.) at the southern margin to 600 m a.s.l. near the Minnesota/South Dakota border. A longitudinal profile along the axis of the lobe (A-A', Fig. 6) is similar to that determined by Clark (1992) (Fig. 8A). In contrast the lobe is almost twice as thick if Case 2 is considered (Fig. 7, 8A). These results indicate that modern moraine elevations may yield a significant underestimate of glacier thickness and surface slope.

From the reconstructed profiles, the basal shear stress is calculated. In the absence of side drag from valley walls or adjacent slow moving ice, a good assumption for the Des Moines Lobe, the driving stress for glacier motion can be equated with the basal shear stress τ_b, given by

$$\tau_b = \rho_i g H \sin\alpha , \qquad (1)$$

where ρ_i is the density of ice (916 kg m^{-3}), g is the acceleration due to gravity, H is the glacier thickness and α the surface slope. Values of τ_b were calculated over distances of $20H$

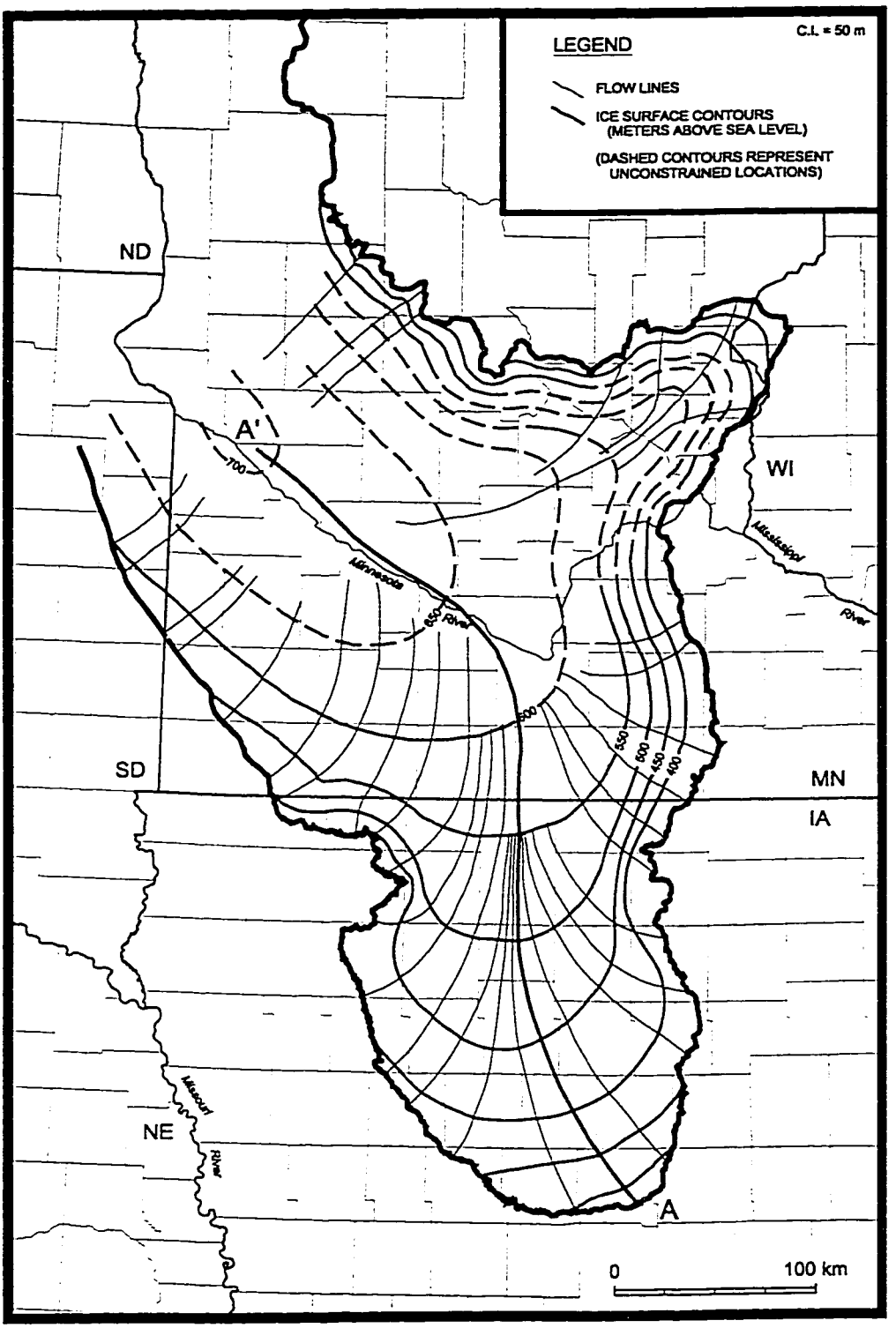

Figure 6. Reconstructed ice-surface morphology and flowlines for the 13.8 ka Des Moines Lobe based on existing moraine elevations. Flowline A-A' is the trace of the longitudinal ice-surface profile shown in Figure 8.

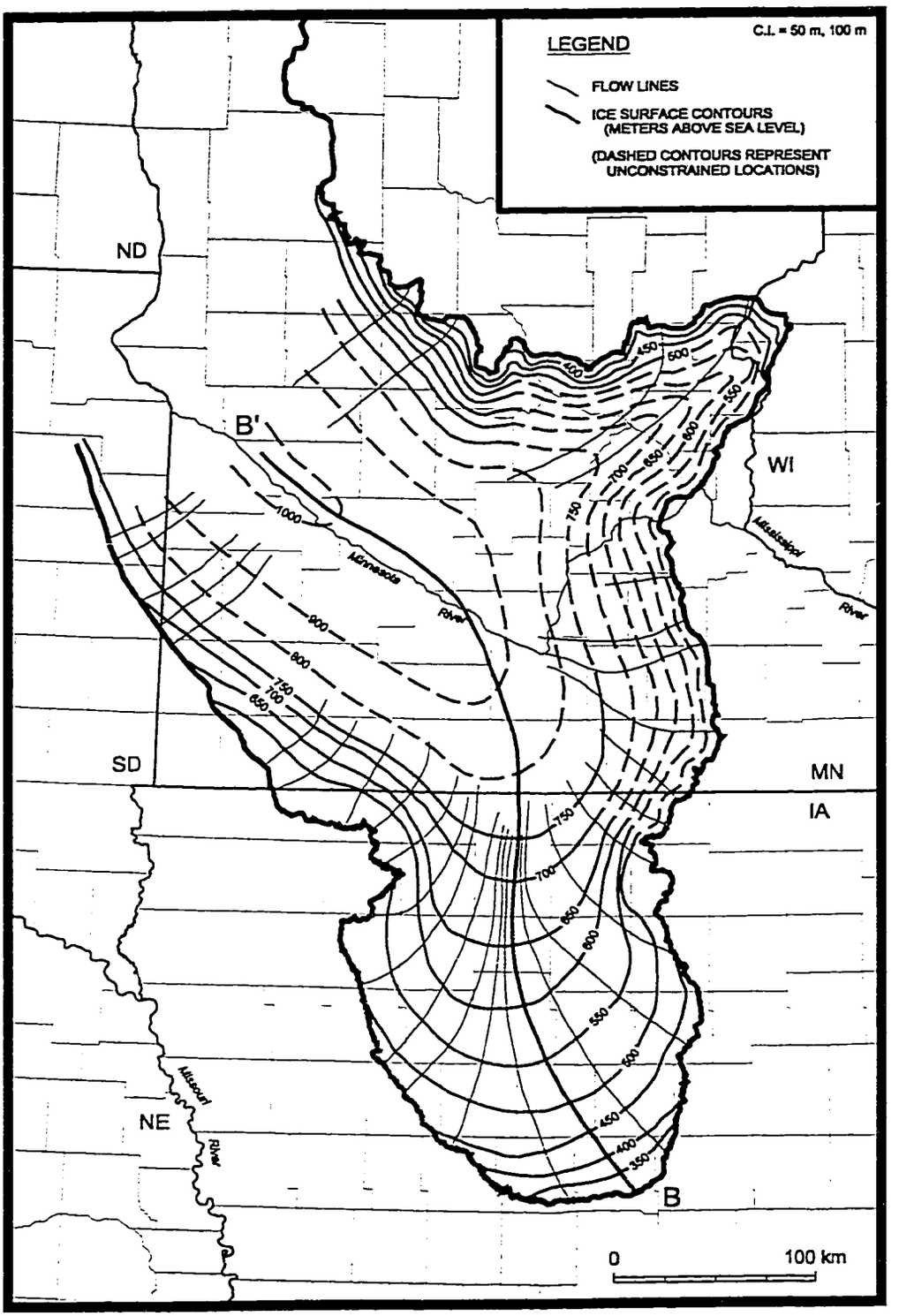

Figure 7. Reconstructed ice-surface morphology and flowlines for the 13.8 ka Des Moines Lobe based on the elevation of an ice-cored moraine. Flowline B-B' is the trace of the longitudinal ice-surface profile shown in Figure 8.

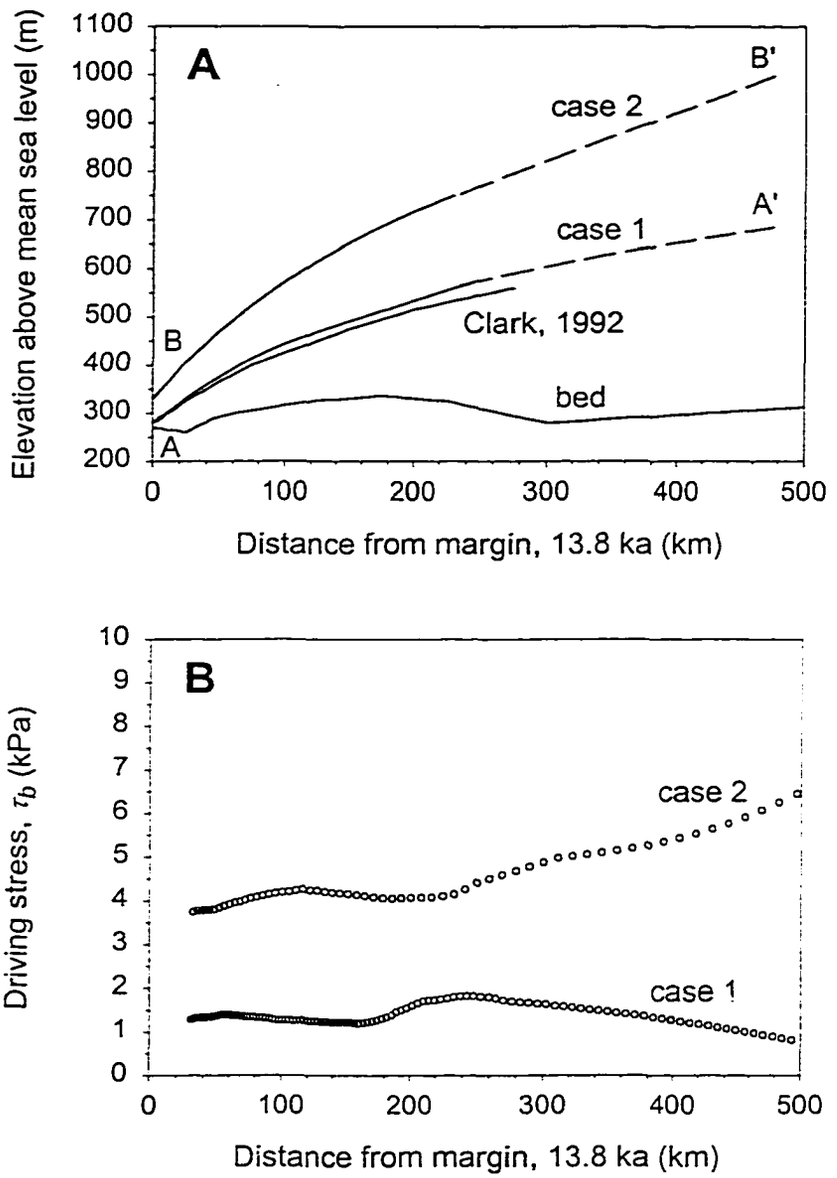

Figure 8. (A) Longitudinal ice-surface profiles for the 13.8 k.a. Des Moines Lobe compared with that of Clark (1992). (B) Basal shear stress calculated every $20H$ for the two cases shown in (A).

along the flow line. This distance is large enough to ensure that longitudinal stress gradients, which affect the basal shear stress, are negligible (Paterson, 1994, p. 264).

Case 2 yields shear stresses more than twice as great as those determined by Clark (1992) (Fig. 8b). Nevertheless, given that typical glaciers have driving stresses on the order of 100 kPa, even Case 2 yields shear stresses that are unusually small. This precludes the possibility that the ice was frozen to its bed, a conclusion consistent with the evidence for subglacial meltwater mentioned previously.

POTENTIOMETRIC SURFACE

High water pressure in the subglacial hydraulic system may be responsible for the low basal shear stresses. In this section, the water pressure in this system and the elevation of the potentiometric surface are determined from the results of consolidation tests on intact till specimens and from the reconstructed ice thickness. The technique relies on the concept of effective pressure, defined as the difference between the overburden pressure on the till and the pore-water pressure. Consolidation tests, described hereafter, yield an estimate of the largest effective pressure on the till since its deposition, P_e^{max}. For till sampled at depth, d_T, in the basal till unit, the overburden pressure, P_o, is given by

$$P_o = \rho_i g H + \rho_T g d_T , \tag{2}$$

where ρ_T is the saturated bulk density of the till (1600 to 2000 kg m^{-3}) determined from laboratory measurements. Subtracting P_e^{max} from P_o yields the minimum pore-water pressure, P_w^{min}, at depth in the till. Thus,

$$P_w^{min} = \rho_i g H + \rho_T g d_T - P_e^{max} \tag{3}$$

However, what is desired is the water pressure at the ice/bed interface where meltwater flowed either in discrete channels (Röthlisberger, 1972; Walder and Fowler, 1994) or in a more distributed system, such as linked cavities (e.g. Walder, 1986) or a layer of non-uniform thickness (Alley, 1989). If it is assumed that there was not significant downward groundwater flow through the till, then the minimum water pressure at the ice/bed interface, $P_{wi}^{\min}$, is less than $P_w^{\min}$ by an amount equal to the change in hydrostatic pressure over d_T. Thus,

$$P_{wi}^{\min} = P_w^{\min} - \rho_w g d_T = \rho_i g H + (\rho_T - \rho_w) g d_T - P_e^{\max}, \quad (4)$$

where ρ_w is the density of water. The difference in water pressure between that at the ice/till interface and that at depth in the till is usually not considered in determining $P_{wi}^{\min}$ (e.g., Harrison, 1957; Sauer et al., 1993; Piotrowski and Kraus, 1997). Note that in the case of downward groundwater flow, consolidation tests would yield a larger value of $P_e^{\max}$, which would result in a smaller value of $P_{wi}^{\min}$. Where the Des Moines Lobe basal till is underlain by less permeable sediment, such as fine-grained, overconsolidated, pre-Wisconsinan tills, downward groundwater flow may have been minimal. In general, however, such flow cannot be dismissed and is, thus, a source of uncertainty in reconstructing the minimum elevation of the potentiometric surface.

In a consolidation test, a confined, intact, soil specimen that is water-saturated is subjected to incremental increases in axial stress. After each increase in stress, excess pore-water pressure in is allowed to dissipate as the specimen consolidates. Initial stress increments are small, resulting in mostly elastic deformation of the soil skeleton. At a

sufficiently large stress, however, the specimen begins to consolidate permanently due to a reduction in porosity. The stress at which this occurs is called the preconsolidation pressure and is inferred to be the maximum effective pressure that the till experienced during ice-sheet loading (P_e^{max}) assuming negligible specimen disturbance during collection and minimal pedogenesis. It is determined for each sample by plotting void ratio as a function of the log of the axial stress (Fig. 9). A change in slope on this plot indicates the value of P_e^{max}. Unfortunately, this change in slope is almost never abrupt but occurs gradually over a range of axial stress (Lambe and Whitman, 1969, p. 297).

One technique used commonly to determine P_e^{max} from such plots is the empirical method of Casagrande (1936). A point is first established visually at the minimum radius of curvature (see "a" in Fig. 9). Two lines are drawn through this point, one tangent to the curve (bc) and the other horizontal (ae). The acute angle formed by these two lines is then bisected (ad). A straight line (fg) is extended from the lower portion of the consolidation curve until it intersects this bisector line (ad). The abscissa at this point of intersection is P_e^{max}. Casagrande found that this method reproduced preconsolidation pressures on soil specimens with known loading histories. Intact samples of the Des Moines Lobe basal till were collected at 13 locations in Iowa and Minnesota for consolidation tests (Fig. 5). Each sample was collected by exposing a 0.04 m^2 platform in unweathered basal till. A thin-walled brass cylinder, 16 mm high by 75 mm in diameter, was pushed downward into the till until it was flush with the platform. The till around and below the cylinder was then removed leaving an intact specimen. A wire saw was used to trim the top and bottom of the specimen. The specimens were transported to the laboratory, inserted in a fixed-ring oedometer, fully

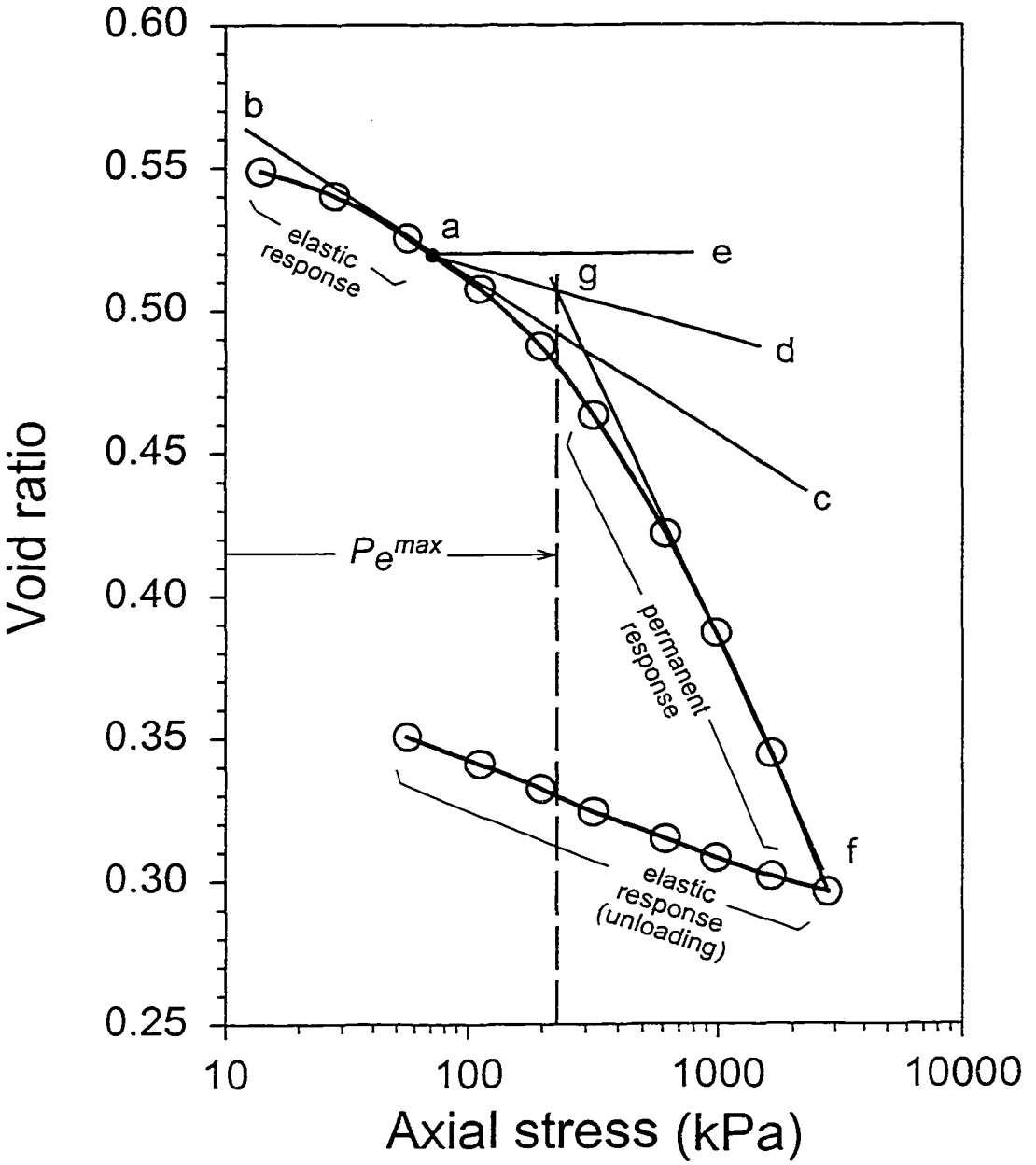

Figure 9. Typical consolidation curve for the Des Moines Lobe basal till. Labeled line segments refer to the graphical method of Casagrande (1936) for determining preconsolidation pressure.

saturated, and loaded incrementally following a standard procedure (Das, 1994, p. 250). Axial stress increments were applied every 24 hours, thereby allowing sufficient time for excess pore-water pressure to dissipate.

The results of these tests are presented in Figure 10. P_e^{max} values, determined using the Casagrande procedure, range from 125-300 kPa (Table 1). These values are relatively low for till that was loaded by an ice mass that ranged in thickness from 80 - 690 m over the sampling area. This implies that till consolidation was complete, which is reasonable given that the overlying ice was present for at least 1000 years. Similarly small values of P_e^{max} have been measured in other consolidation tests on basal till (e.g. Solheim et al., 1991; Sauer et al., 1993; Piotrowski and Kraus, 1997) and are comparable to effective pressures measured beneath Ice Stream B, which is about 1 km thick (Engelhardt et al., 1990).

From these values of P_e^{max} and the reconstruction of the lobe, minimum water pressures at the ice/till interface (P_{wi}^{min}) are calculated using Equation 4 (Table 1). The minimum height of the potentiometric surface above the bed is $h_w=P_{wi}^{min}/\rho_w g$. The reconstructed potentiometric surface is plotted on longitudinal and transverse profiles of the Des Moines Lobe in Figures 11 and 12, respectively. Average ratios of P_{wi}^{min} to P_i are 0.91 and 0.95 for Case 1 and Case 2, respectively. The Des Moines Lobe was, therefore, very near flotation. This probably rules out a drainage system consisting of tunnels cut into ice, like those analyzed by Röthlisberger (1972). Channels cut into the till (Walder and Fowler, 1994) fed by a distributed water system in intervening zones (e.g., Engelhardt and Kamb, 1997) would support higher water pressures more like those inferred here. The high basal water pressure probably strongly affected the basal motion of the Des Moines Lobe.

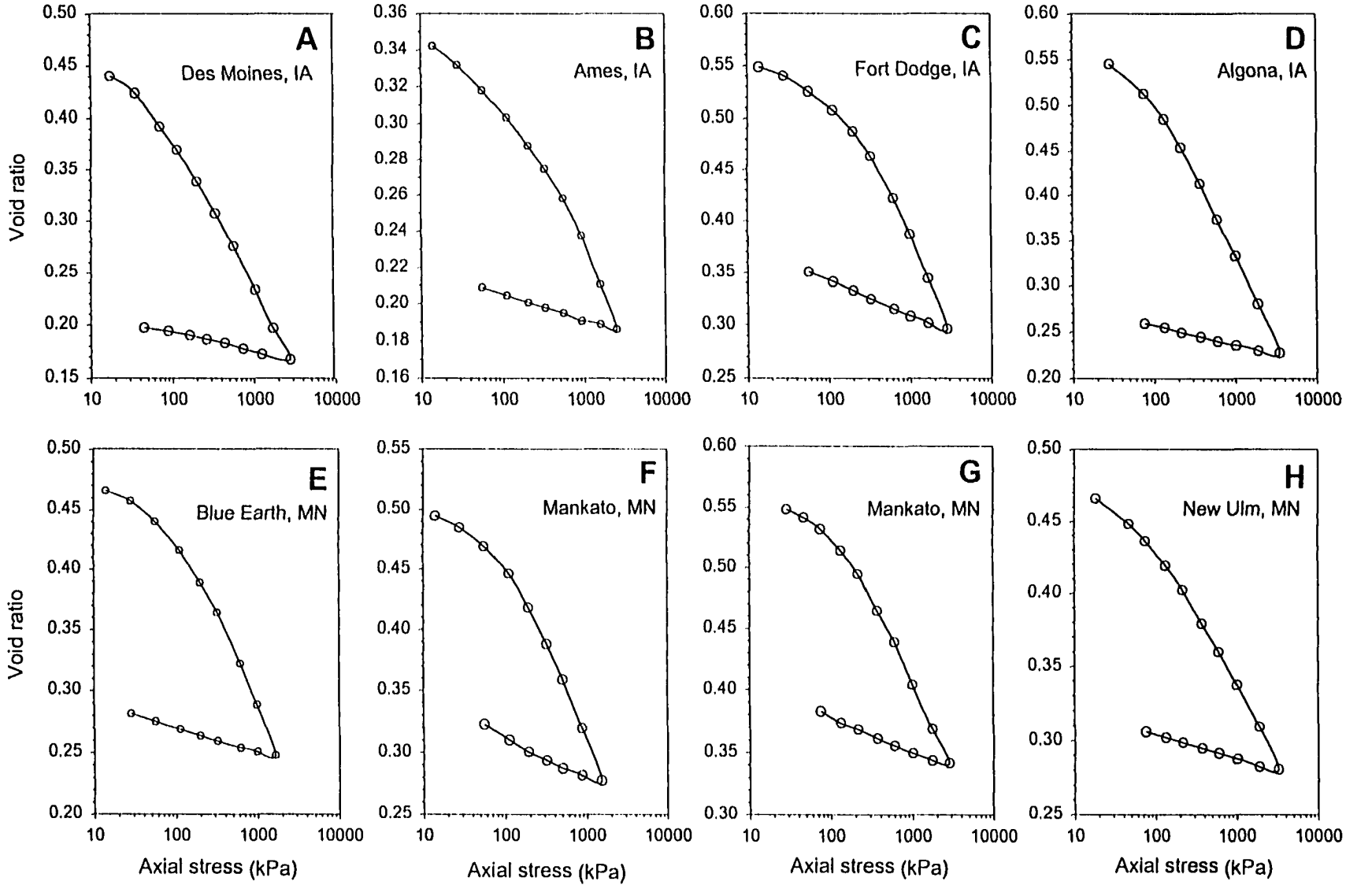

Figure 10. (A-H) Consolidation curves for Des Moines Lobe basal till samples. The location of each sample is shown on Figure 5.

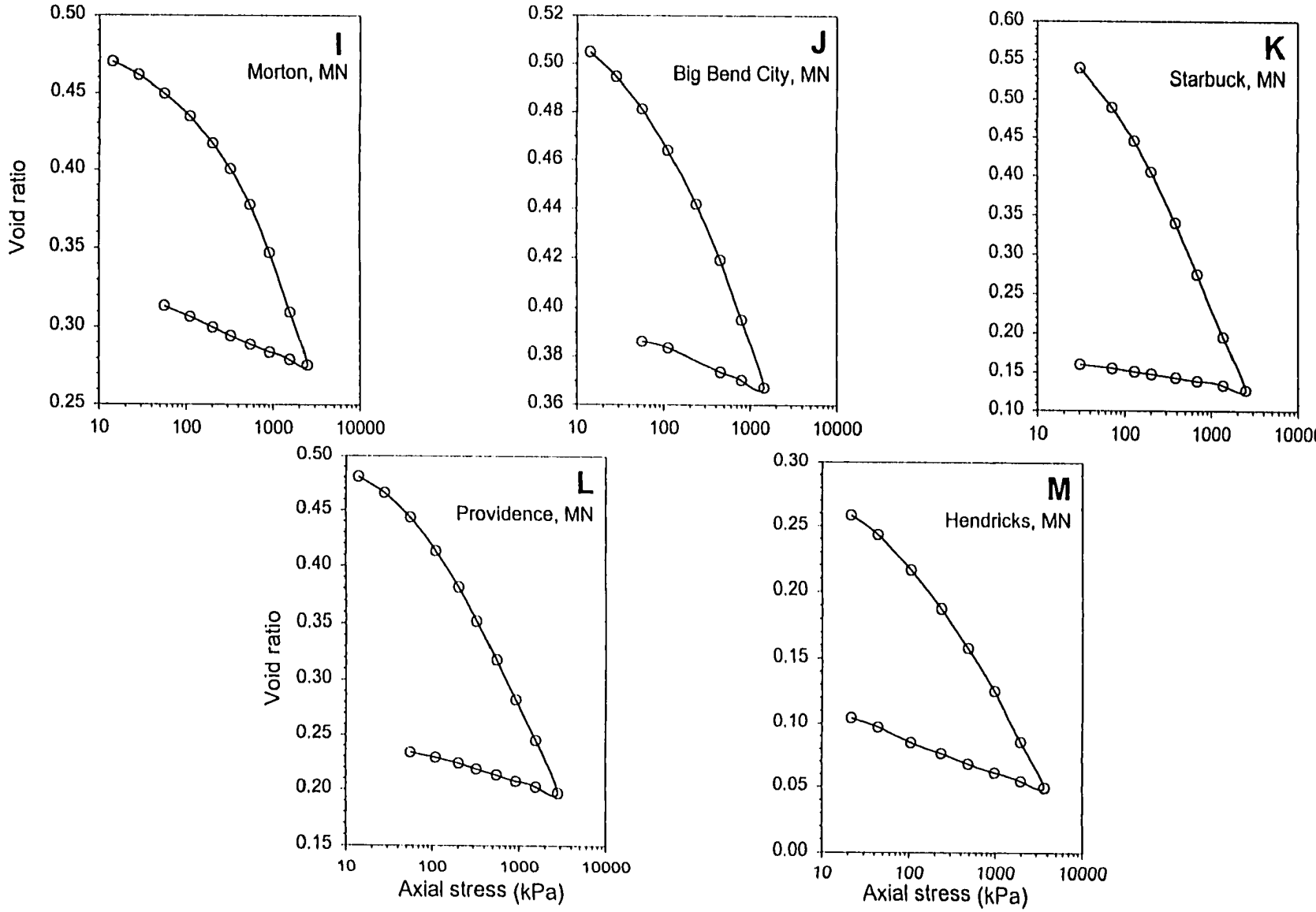

Figure 10 (continued).

Table 1. Results of consolidation experiments.

Nearest city to sample location	Distance from margin (km)	Till thickness d_T, (m)	Case 1 H, (m)	Case 2 H, (m)	P_e^{max} (kPa)	Case 1 P_i, (kPa)	Case 2 P_i, (kPa)	Case 1 P_{wi}^{min}, (kPa)	Case 2 P_{wi}^{min}, (kPa)	Case 1 h_w, (m a.s.l.) [b]	Case 2 h_w, (m a.s.l.) [b]	Case 1 P_{wi}^{min} / P_i	Case 2 P_{wi}^{min} / P_i
Des Moines, IA	40	5	79	175	170	710	1573	576	1438	333	427	0.81	0.92
Ames, IA	58	7	107	207	280	902	1860	752	1651	363	461	0.78	0.89
Fort Dodge, IA	115	2	135	275	200	1213	2471	1043	2301	438	575	0.86	0.93
Algona, IA	177	4	178	352	125	1600	3163	1486	3050	498	668	0.93	0.96
Blue Earth, MN	258	2	276	474	150	2480	4259	2350	4129	560	754	0.95	0.97
Mankato, MN	306	3	327	547	150	2938	4915	2826	4802	588	803	0.96	0.98
Mankato, MN	306	6	327	547	200	2938	4915	2776	4752	582	798	0.95	0.97
New Ulm, MN	348	2	341	582	120	3064	5230	2956	5122	610	846	0.97	0.98
Morton, MN	398	1	356	622	300	3194	5589	2948	5351	619	879	0.93	0.96
Big Bend City, MN	483/100[a]	2	365	688	200	3460	6182	3269	5992	671	968	0.95	0.97
Starbuck, MN	170[a]	2	174	374	125	1564	3361	1447	3244	584	779	0.93	0.97
Providence, MN	67[a]	3	367	663	175	3298	5958	3142	5802	647	937	0.95	0.97
Hendricks, MN	21[a]	3	228	390	225	2049	3505	1852	3308	592	750	0.90	0.94

a, distance from the south lateral margin (see Figure 12)
b, m a.s.l. = meters above sea level

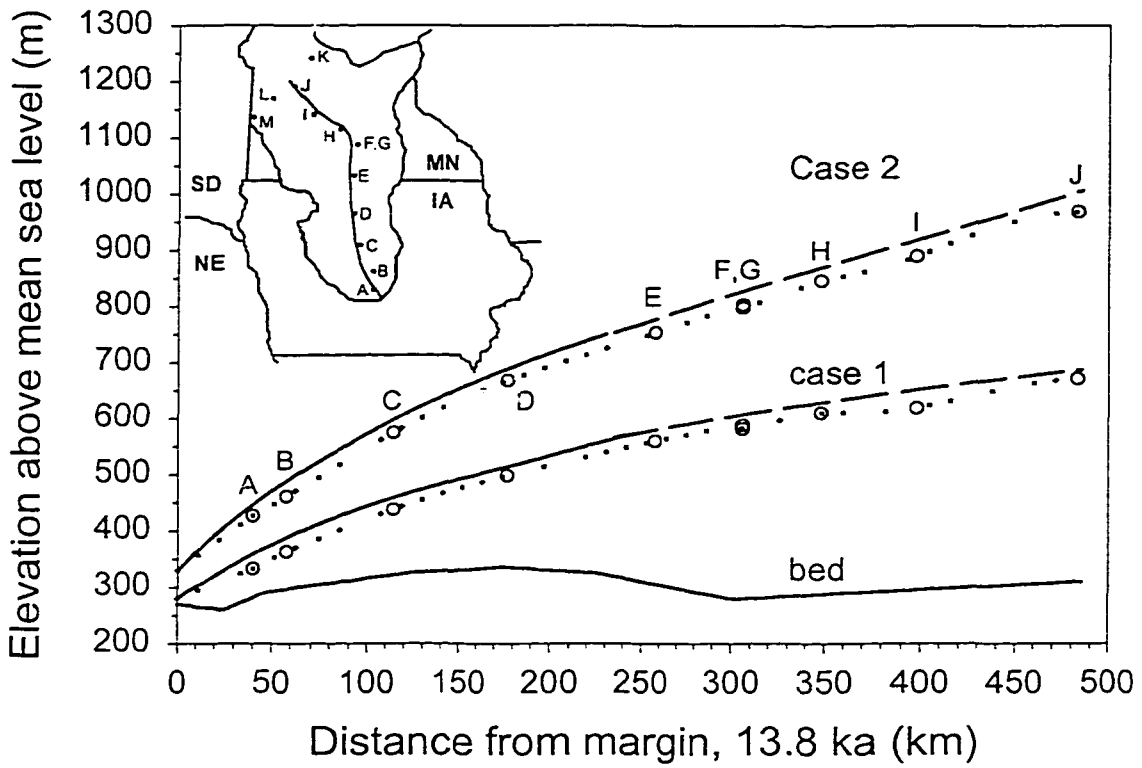

Figure 11. Longitudinal potentiometric surfaces. Letters A through I are sampling locations projected onto the longitudinal transects A-A" (Fig. 6) and B-B' (Fig. 7).

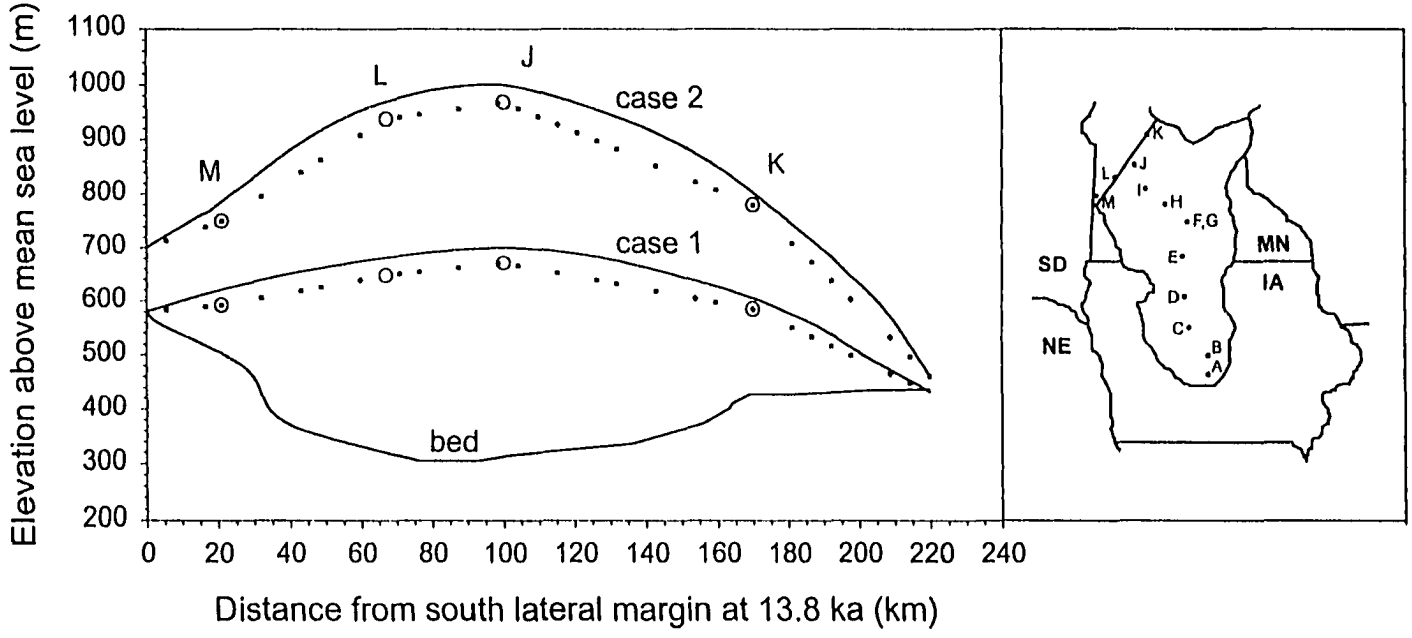

Figure 12. Transverse potentiometric surfaces. Letters M, L, J, and K are sampling locations projected onto the transect

FLOW MECHANISMS

The low shear stresses and low effective pressures at the bed of the Des Moines Lobe indicate that most motion of the lobe must have occurred with little flow by internal ice deformation. To demonstrate this, the average velocity associated with internal ice deformation, U_i, can be determined from

$$U_i = \frac{2AE\tau_b^n H}{n+2}, \tag{5}$$

where A is the temperature dependent ice-creep parameter, proportional to the inverse of the effective ice viscosity, E is an enhancement factor for soft Wisconsin-age ice, and n is the stress exponent in the flow relation for ice (Paterson, 1994, p. 243). Using maximum values of τ_b and H determined from the reconstruction to maximize U_i (Case 2), and reasonable values for A (6.8×10^{-15} kPa^{-3} s^{-1}), n (3), and E (2.5) (Paterson, 1994, p. 282), U_i is 0.18 m a^{-1}. This value is approximately four orders of magnitude less than advance rates of the Des Moines Lobe (Fig. 2). Thus, motion must have occurred by some combination of sliding, plowing or bed deformation.

An effort is now made to assess whether motion of the Des Moines Lobe was focused near the ice/till interface by ploughing and sliding or whether the bed deformed pervasively at depth. Distinguishing between these mechanisms is important if a relationship between driving stress and basal motion is to be determined for Pleistocene ice lobes. Without such a constitutive relation, it is difficult to model the response of these lobes to climatic forcing. Furthermore, as long as the importance of these mechanisms is unclear, the primary mechanism of subglacial sediment transport and deposition will remain ambiguous.

Two approaches are used to distinguish between these flow mechanisms. First, with a model of sliding and plowing (Iverson, 1999), the shear strength of the ice/bed interface is estimated for comparison with the bulk strength of the till. These calculations indicate that bed deformation, although possible, was unlikely. This hypothesis is then tested by analyzing the clast fabric of the Des Moines Lobe basal till and the mixing that has occurred along its basal contact.

Model calculations

Model description

The strength of the ice/till interface depends on its roughness, which is provided by clasts at the bed surface that protrude into the glacier sole (Brown et al., 1987; Alley, 1989). In the model of Iverson (1999), these clasts are treated as isolated spheres centered on the bed surface. The roughness, therefore, depends on the grain-size distribution, which in the case of basal till can be conveniently characterized with a single parameter, the fractal dimension (Hooke and Iverson, 1995; Iverson et al., 1996). This parameter indicates the number of particles in each size class and allows the area of the bed occupied by each size class to be easily calculated (Iverson, 1999, Equation 18).

Downglacier from particles of sufficient size, ice should separate from the bed, forming water-filled cavities. These cavities are likely linked, resulting in a water layer of non-uniform thickness that submerges the smallest particles at the bed surface (Alley, 1989; Iverson, 1999). In the model, particles smaller than the mean thickness of this water layer do not contribute to the bed roughness.

Some particles at the bed surface do not plow through the bed and are, hence, stationary. Motion of ice past these particles is by regelation and creep of ice. The relation between U_s, the sliding speed, and the shear stress on a particle, τ_s, is

$$U_s = A\tau_s^3 R + C\tau_s / R \,, \tag{6}$$

where R is the particle size, and C is a constant that depends on the thermal properties of the ice and particles (Lliboutry, 1979). Cavities form behind clasts within the range of particles sizes given by

$$R = \frac{U_s \pm (U_s^2 - 4ACP_e^4)^{\frac{1}{2}}}{2AP_e^3} \,, \tag{7}$$

where P_e, the effective pressure at the bed surface, is the difference between the water pressure in cavities and the ice-overburden pressure (Iverson, 1999). The shear stress on these particles, τ_c, can be approximated from

$$\tau_c = \frac{1}{2}(\tau_s + P_e). \tag{8}$$

Equations 6 and 8 are used to calculate the shear stress on stationary particles as a function of U_s and P_e.

If the force exerted on particles by ice exceeds the resistance provided by the surrounding till, particles will plow through the bed. In this case, the till strength will determine the shear stress. In order to calculate the shear stress due to plowing, an appropriate constitutive relation for till deformation is required. It is well established that till,

like other granular materials, behaves as a Coulomb-plastic material, such that its ultimate strength, τ_u, is independent of its rate of deformation and given by

$$\tau_u = c_i + P_e \tan\phi_u \ , \tag{9}$$

where c_i and ϕ_u are the cohesion intercept and the ultimate friction angle, respectively (Lambe and Whitman, 1969, p. 139; Kamb, 1991; Fischer and Clarke, 1994; Iverson et al., 1994; Tika et al., 1996; Hooke et al, 1997; Iverson et al., 1998; Tulaczyk, 1999). The significance of this relationship is that the till strength depends on P_e, and that yielding sediment in front of plowing particles will not strengthen (or weaken) with changes in particle speed. Under these assumptions, the shear stress supported by plowing particles at the bed, τ_p, is given by the following relationship developed by Iverson (1999)

$$\tau_p = \frac{1}{2 + N_F k}\left[N_F\left(P_e + \frac{c_i}{\tan\phi_u} \right) - \frac{c_i}{\tan\phi_u} \right], \tag{10}$$

where k is a pressure-shadow factor that takes into consideration the reduction in ice pressure in the lee of particles, and N_F is the bearing-capacity factor:

$$N_F = \tan^2\left(\frac{\pi}{4} + \frac{\phi_u}{2} \right) e^{(\pi - 2\beta)\tan\phi_u} \tag{11}$$

(Janbu and Senneset, 1974; Senneset and Janbu, 1985) where β is the angle between slip surfaces in the till and a normal to the bed (see Iverson, 1999, Fig. 1). Using Equation 10, the shear stress supported by plowing particles is calculated.

To calculate the shear strength of the ice/till interface due to both sliding and plowing, τ_{sp}, for each size class of particles either τ_s (Equation 6) or τ_c (Equation 8) is calculated

depending upon whether Equation 7 indicates that particles of that size should have leeward cavities. This value is then compared with the value of τ_p for that size class (Equation 10). If τ_s (or τ_c) exceeds τ_p, then the particle will plow and the shear stress that the size class supports, τ_i, is equal to τ_p. If the converse is true, the particle will be stationary and the shear stress is given by either τ_s or τ_c, depending upon whether leeward cavities are expected (Iverson, 1999). For each size clast i, the value of τ_i is calculated and multiplied by the fractional area of the bed occupied by that size class, A_{if}. Summing these products for all size classes yields the shear strength of the ice/till interface:

$$\tau_{sp} = \sum_{i=1}^{m} \tau_i A_{if}, \tag{12}$$

for specified values of U_s and P_e (Iverson, 1999).

Parameter selection

To apply this model to the Des Moines Lobe, the geometrical properties of the bed, the physical properties of the ice and sediment, the sliding speed, and the effective pressure must all be specified. Parameter values are listed in Table 2.

The friction angle of the Des Moines Lobe basal till was determined in drained ring-shear test following the procedure outlined by Iverson et al. (1997, 1998). The results are presented in Figure 13 and indicate an ultimate friction angle of 18.5°, similar to other clay-rich tills (Iverson et al, 1998, Tika et al., 1996). The cohesion intercept, c_i, for the till is 4.3 kPa; however, during critical (steady) state deformation it should be zero (Lambe and Whitman, 1969, p. 312). If tests could have been performed at lower normal stresses, it is

Table 2. Model parameters.

Parameter	Symbol	Value
sliding speed	U_s	440 m a^{-1}
ice creep parameter	A	1.2 x 10^{-25} Pa^{-3} s^{-1}
regelation parameter	C	2.8 x 10^{-15} m^2 Pa^{-1} s^{-1}
ultimate friction angle	ϕ_u	18.5°
cohesion intercept	c_i	0.0 kPa
angle between slip surfaces in till and a normal to the bed	β	15 °
pressure-shadow factor	k	0.1
effective pressure	P_e	varies (0-300 kPa)
water-layer thickness	-	varies (0.001-10 mm)
fractal dimension	-	2.96
particle-size distribution	R	see Chapter 3, Figure 3

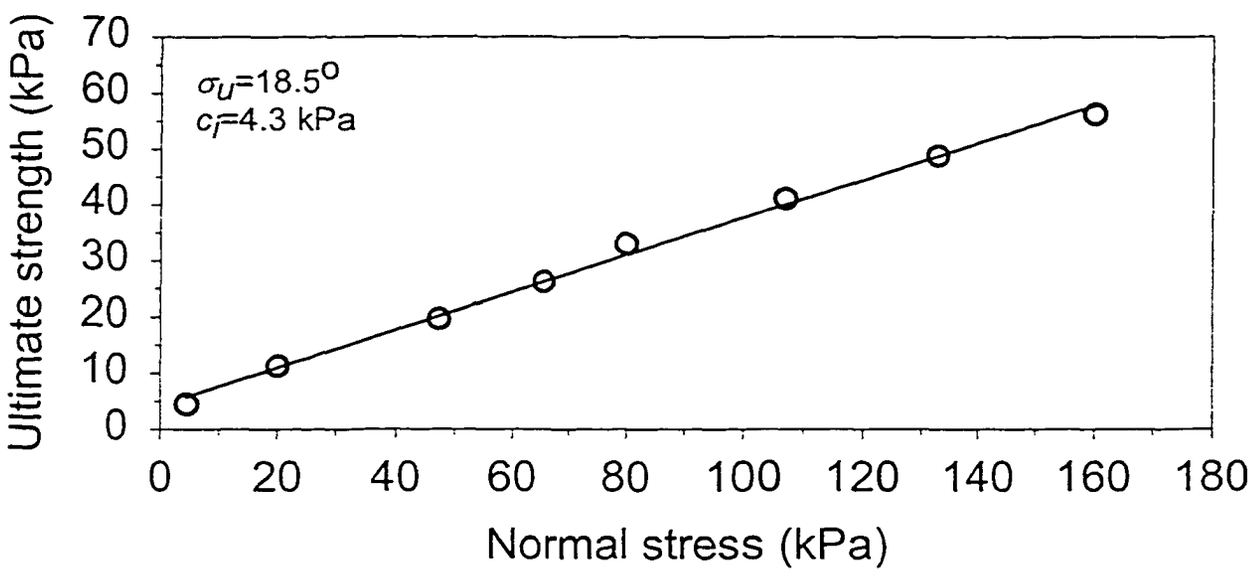

Figure 13. Ultimate strength of the Des Moines Lobe till as a function of normal stress. The parameter ϕ_u and c_i are the ultimate friction angle and the cohesion intercept, respectively.

assumed that the failure envelope would have curved downward through the origin (Lambe and Whitman, 1969, p. 308). Therefore, true cohesion is assumed to equal zero. The orientation of slip surfaces, β, is taken to be 15 ° following cone-penetration experiments performed in fine-grained sediment (Janbu and Senneset, 1974; Senneset and Janbu, 1985).

The grain-size distribution for the Des Moines Lobe was determined by mechanically sieving the coarse fraction (>50 μm) and using hydrometer analyses for the fine fraction (1-50 μm) (Fig. 3, Chapter 3). The calculated fractal dimension is 2.96. This is similar to values calculated for other tills including Ice Stream B (2.99) (Iverson, 1999) and Storglaciären, a valley glacier in northern Sweden (2.92) (Hooke and Iverson, 1995). It is assumed that this value can be extrapolated to grain sizes larger than those measured. The largest particle size that contributes to the till roughness, the so-called upper fractal limit, is taken to be the radius of the largest boulder observed in the Des Moines Lobe basal till. Examination of approximately 25 outcrops indicates a reasonable value is 0.5 m, although several other values are also considered to assess the sensitivity of the results to this parameter.

Parameters for the ice include the regelation parameter, C, and the ice creep parameter, A. These are taken to be 2.81×10^{-15} $m^2 Pa^{-1} s^{-1}$ and 1.16×10^{-25} $Pa^{-3} s^{-1}$, respectively (Lliboutry, 1979), appropriate values for clean ice. The pressure shadow, k, is assumed to be 0.1, the value appropriate for regelation-dominated flow, based on the analysis of Brown et al. (1987). This value is reasonable because as will be shown subsequently, regelation rather than ice creep is the primary mechanism of ice flow past particles.

The sliding speed of the Des Moines Lobe is unknown, although its advance rates were on the order of 2000-3000 m a^{-1} (Fig. 2). I choose a smaller value, 440 m a^{-1}, equal to that of

Ice Stream B (Engelhardt and Kamb, 1997) but consider several values to test the sensitivity of the results to this parameter.

A range of values for the effective pressure in the basal water system is considered based on the results of the consolidation tests discussed previously. The effective pressures calculated from these tests are maximum values, and hence pore-water pressure in the till could have been higher. Therefore, effective pressures between 0 and 300 kPa are considered.

To calculate the shear strength of the ice/till interface, it is assumed that the sliding speed does not vary as a function of effective pressure. Although there is good evidence that these parameters are correlated for some valley glaciers (e.g., Iverson et al., 1995; Iken and Bindschadler, 1986), data from Ice Stream B in West Antarctica reveal that U_s, at least locally, does not vary significantly with changes in P_e (Engelhardt and Kamb, 1997).

The thickness of the water layer at the ice/till contact is unknown. Therefore, five different layer thicknesses are considered ranging from 0.001 to 10.0 mm. This range was selected based on theory (Alley, 1989) and various empirical studies (Engelhardt and Kamb, 1997; Hooke et al., 1997, Iverson, 1999, Piotrowski and Tulaczyk, 1999). As noted earlier, the thickness of the water layer in Iverson's model is a parameterization for the extent of microcavity development in the lee of particles. Such cavities may grow unstably as basal effective pressure approaches zero (Walder and Fowler, 1994; Kamb, 1987) and thus, following Iverson (1999), an exponential increase in the thickness of the water layer with decreasing effective pressure is also considered.

Results and discussion

In Figure 14A the shear strength of the ice/bed interface is plotted as a function of effective pressure for several water-layer thicknesses, assuming that the sliding speed was similar to that of Ice Stream B (440 m a^{-1}). The results indicate a linear relationship between shear strength and effective pressure and that as the water layer thickens the shear strength of the bed decreases. For example, an increase in the water- layer thickness from 0.1 mm to 10.0 mm will reduce the shear strength by about 50%. This is not surprising, given that a thicker water layer will submerge a larger fraction of the bed. The results for various water-layer thicknesses are compared to the ultimate strength of the till determined in ring-shear tests. The results show that the water-layer thickness must be greater than about 0.1 mm for $\tau_{sp}<\tau_u$ and hence for motion to be focused near the ice/till interface over the range of effective pressure considered. Based on borehole studies, a thickness of about 0.1 mm has been suggested for Ice Stream B (Engelhardt and Kamb, 1997) and for Storglaciären (Hooke et al., 1997). However, theoretical analyses of glaciers resting on soft beds suggest a minimum water-layer thickness an order of magnitude larger (Alley et al., 1987). Furthermore, some modeling results fit to data collected from Storglaciären indicate a water-layer thickness that may be on the order of several centimeters (Iverson, 1999). A relatively thick water layer of 5-35 mm has also been calculated based on the thickness of sand stringers in a Pleistocene basal till in northwest Germany (Piotrowski and Tulaczyk, 1999).

The plowing of particles through the bed, rather than regelation or ice creep, limits the shear strength of the ice/bed interface (Fig. 14B). At effective pressures less than 200 kPa, all particles in contact with ice plow. These particles cover about 19% of the bed; smaller particles are submerged in the water layer. At effective pressures greater than 200 kPa, some

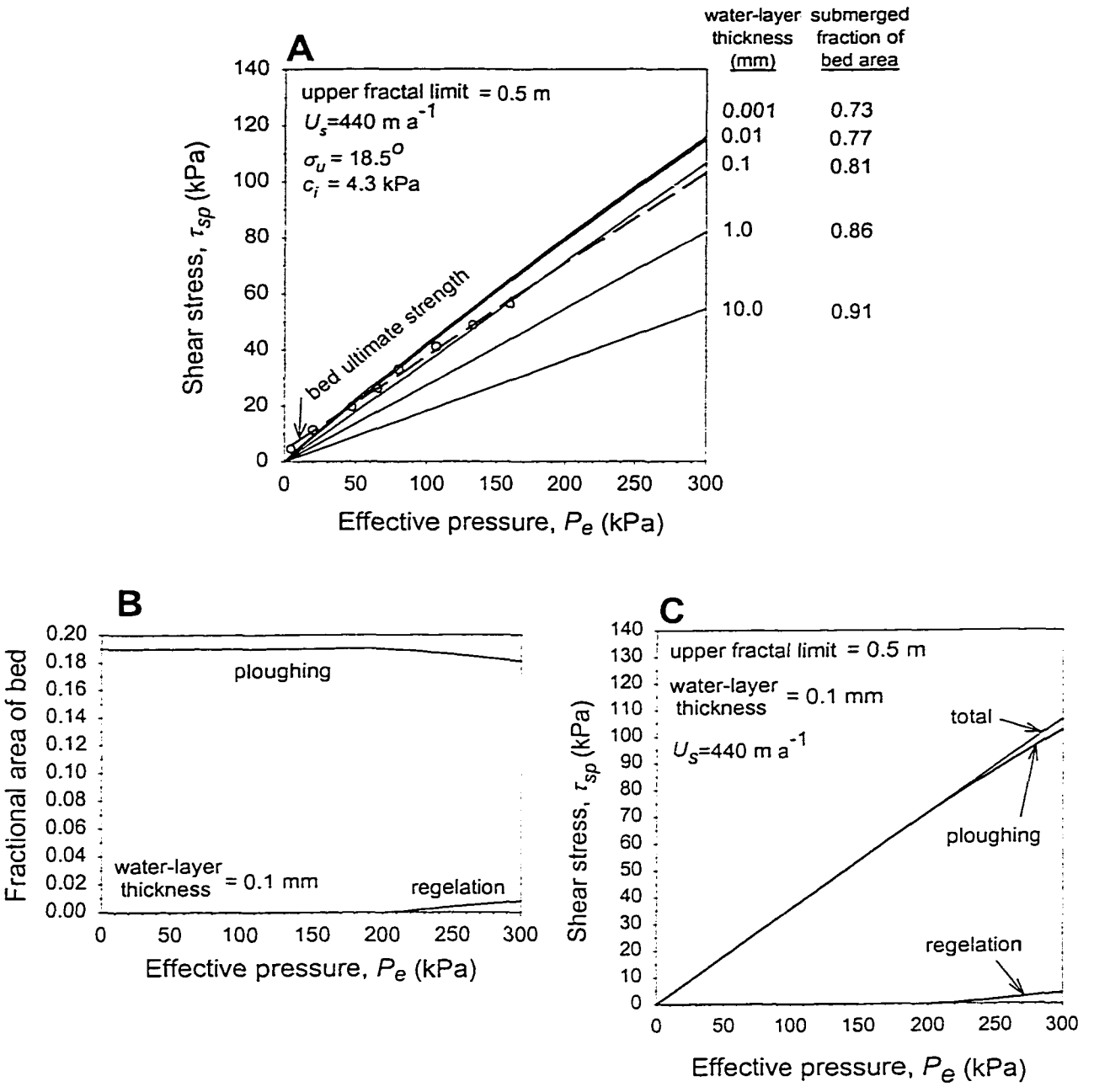

Figure 14. (A) Calculated values of τ_{sp} as a function of effective pressure for various water-layer thicknesses. (B) Fractional area of the bed occupied by plowing particles and by stationary particles accommodated by regelation for a water-layer thickness of 0.1 mm. (C) Calculated values of τ_{sp} as a function of effective pressure. The total shear stress has been divided into its two components: the shear stress supported by plowing particles and the shear stress supported by stationary particles accommodated by regelation.

particles that plow at lower effective pressures will remain stationary because the till is stronger. Basal ice, therefore, will regelate around these particles. Ice creep does not occur because particles large enough to be accommodated by this mechanism plow through the bed for the range of effective pressure considered. The contributions of plowing and regelation to the shear strength of the ice/till interface, assuming a water-layer thickness of 0.1 mm, are shown in Figure 14C.

The sensitivity of these calculations to the upper fractal limit of the grain-size distribution and to the sliding speed, two poorly known parameters, is now explored. Thus far, model calculations have assumed an upper fractal limit of 0.5 m. Upper fractal limits (radii of the largest boulders considered) ranging from 0.05-2.5 m are considered in Figure 15. The results indicate slight strengthening of the ice/till interface as the maximum boulder size increases. If the sliding velocity is increased by more than a factor of 4 to 2000 m a^{-1}, a rate similar to the advance rate of the Des Moines Lobe based on the radiocarbon chronology (Clayton and Moran, 1982), the change in strength of the interface is negligible (Fig. 16). This is because plowing is the dominant mechanism of motion at both the lower and higher velocities, and the shear stress supported by plowing particles is independent of sliding velocity. In contrast, at a sliding velocity of 50 m a^{-1} the strength at the ice/till interface is reduced because more particles are accommodated by regelation, which exerts shear stresses on particles that are linearly proportional to the sliding speed.

The water-layer thickness has, thus far, been assumed to be independent of effective pressure. As noted earlier, however, a reduction in effective pressure may result in an increase in cavity size, and hence, in the mean thickness of the water layer. An exponential increase in this thickness to a value of 0.01 m as effective pressure decreases to zero is now

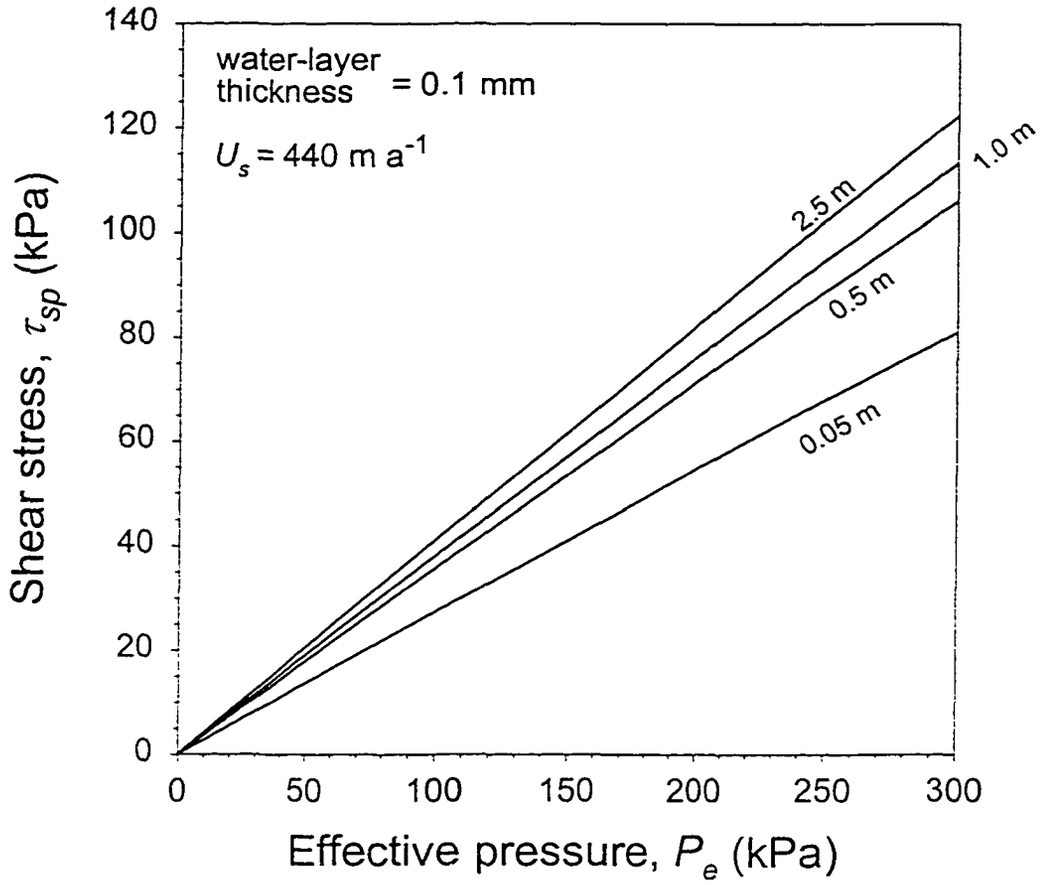

Figure 15. Calculated values of τ_{sp} as a function of effective pressure for various values of the upper fractal limit of the grain-size distribution, assuming a water-layer thickness of 0.1 mm.

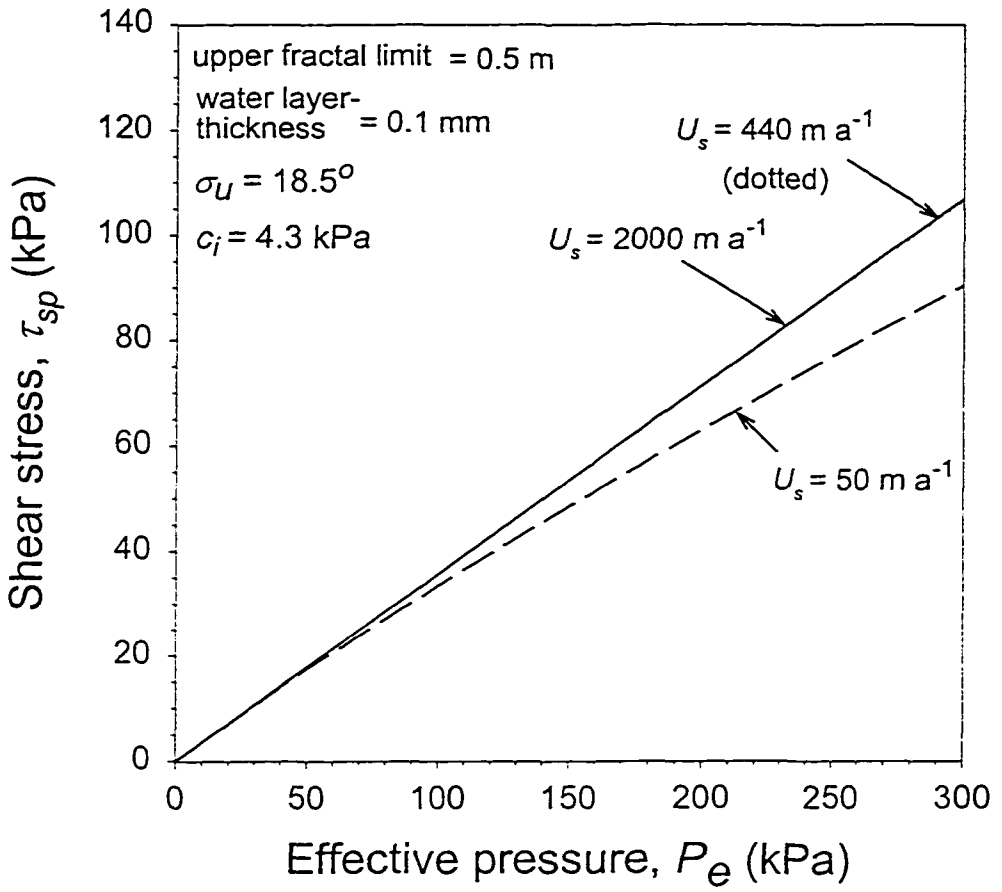

Figure 16. Calculated values of τ_{sp} as a function of effective pressure for various values of sliding speed, assuming a water-layer thickness of 0.1 mm.

considered (Fig. 17). This relationship is based on a good fit of the model described herein to field data collected at Storglaciären (see Iverson, 1999, Fig. 8). As expected, incorporating this effect causes more particles at the bed surface to be submerged at lower effective pressures (Fig. 18). This results in a slight reduction in interface strength compared to the case of a constant water-layer thickness. The converse is true at higher effective pressures (>100 kPa).

Although some of the parameters in the model are poorly known, the model results are not extremely sensitive to these parameters. In general, these results indicate that for water-layer thicknesses thought to exist beneath modern glaciers, the ultimate strength of the bed should generally exceed the shear strength of the ice/till interface, resulting in motion focused at the glacier sole with little bed deformation. This hypothesis is now tested using field techniques calibrated with the ring-shear tests described in previous chapters.

Field observations

Fabric

Weak clast fabrics in basal till have been interpreted to be the result of subglacial deformation (e.g., Hart, 1994; Dowdeswell and Sharp, 1986; Clark, 1997). This interpretation is based on the theory of Jeffery (1922), who demonstrated that elongate clasts in a shearing fluid rotate periodically through the plane of shearing resulting in a weak but discernable fabric in the direction of shearing. Furthermore, Jeffery postulated that at extremely high strains, clasts should eventually align their long axes transverse to the shearing direction. To test Jeffery's theory, clast rotation in shearing viscous putty and in till was studied using a ring-shear device (Hooyer and Iverson, in press). The results from the

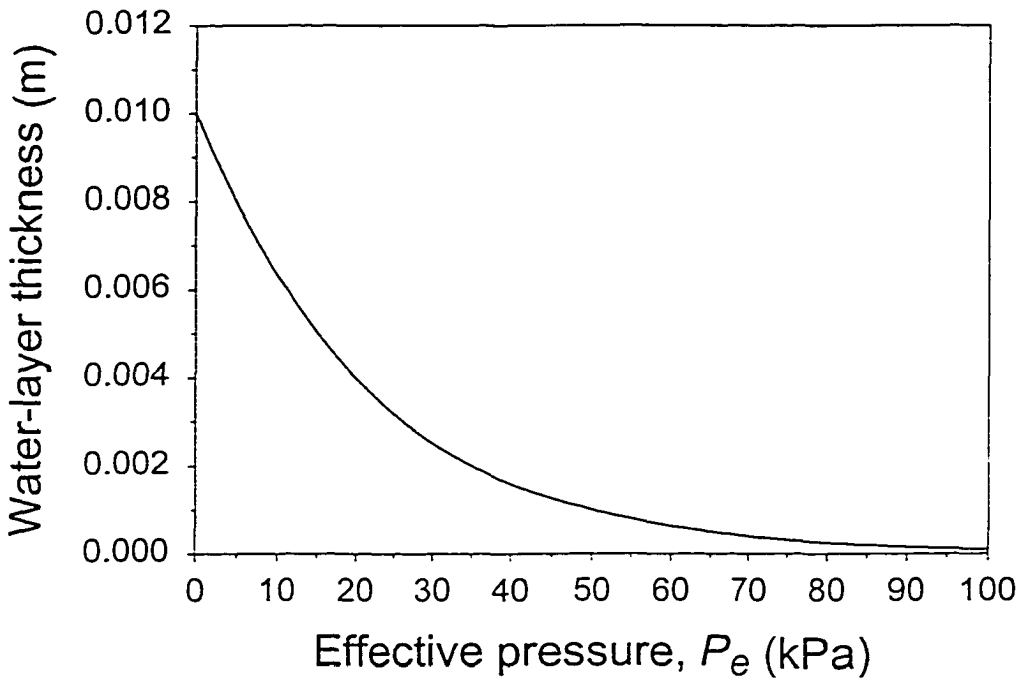

Figure 17. Assumed relation between the thickness of the water-layer and effective pressure, following Iverson (1999).

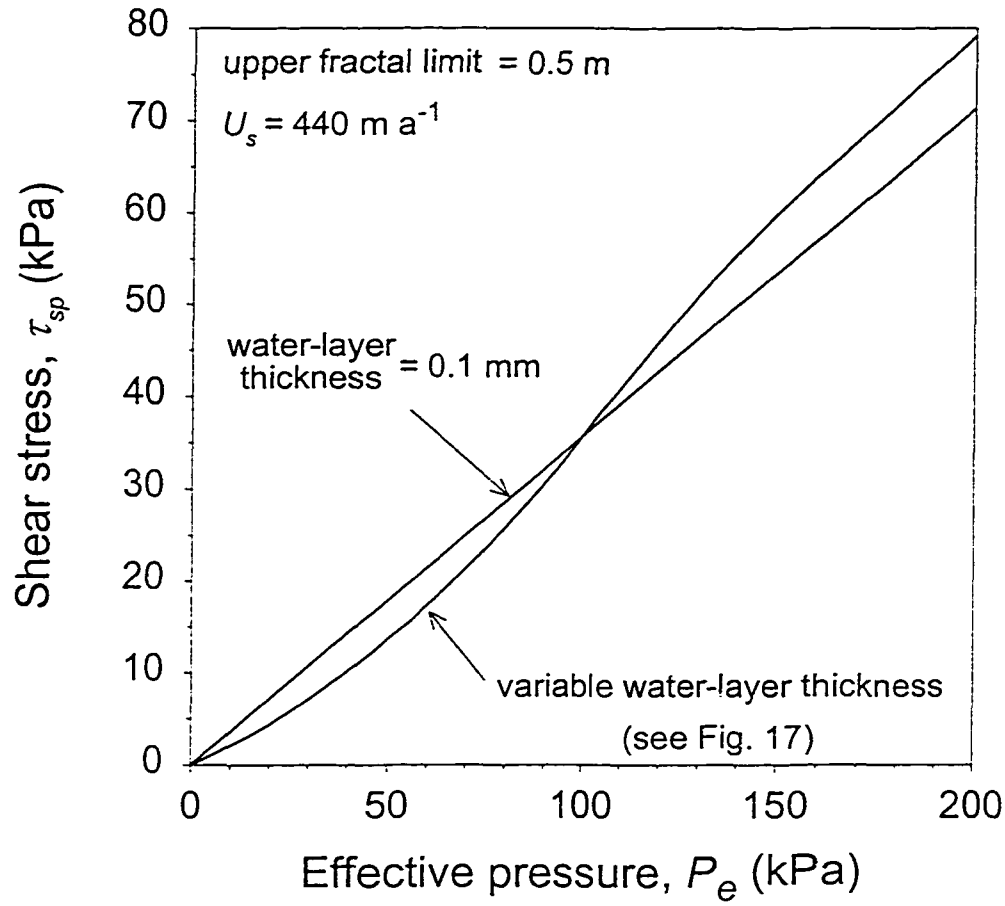

Figure 18. Calculated values of τ_{sp} for a constant water-layer thickness of 0.1 mm and the variable water-layer thickness illustrated in Figure 17.

putty experiments match Jeffery's theory. The results from the till experiments, however, are considerably different: clasts rotate into the shear plane and remain there to high strains resulting in a strong fabric parallel to the direction of shearing. The difference in clast behavior in the two materials is likely the result of slip that occurs between the till matrix and the surface of the clast, a factor not considered by Jeffery. From these results, it was concluded that basal tills with weak fabrics probably have not undergone the extremely high strains required of the deforming-bed mechanism. In contrast, basal tills with a strong fabric parallel to the shearing direction may have been deformed pervasively.

Clast fabrics from Des Moines Lobe basal till were measured at eight locations across Minnesota and Iowa (Fig. 19). Fabric was measured by exposing a fresh cut along an outcrop surface and measuring the trend and plunge of 25 to 100 gravel-sized clasts using a compass. Only prolate clasts were measured that had long to short axis ratios greater than 1.5. The fabric was evaluated using the method of Mark (1973) to calculate eigenvectors and corresponding eigenvalues. The eigenvalues S_1, S_2 and S_3 represent the strength of the fabric, or the degree of clustering around each of the axes defined by the eigenvectors, V_1, V_2 and V_3, respectively. S_1 values near 1.0 represent strongly aligned clasts, whereas S_1 values near 0.33 indicate randomly oriented clasts (Mark, 1973).

Results are presented in Figure 19. Fabrics are weak with a mean S_1 value of 0.54 (Table 3). Plotting S_3 as a function of S_1 for each location measured in this study shows that these fabrics are far weaker than those produced by till deformation in experiments in which clasts were initially oriented either randomly or normal to the shearing direction (Fig. 20). The results from this study indicate that the Des Moines Lobe till probably did not undergo

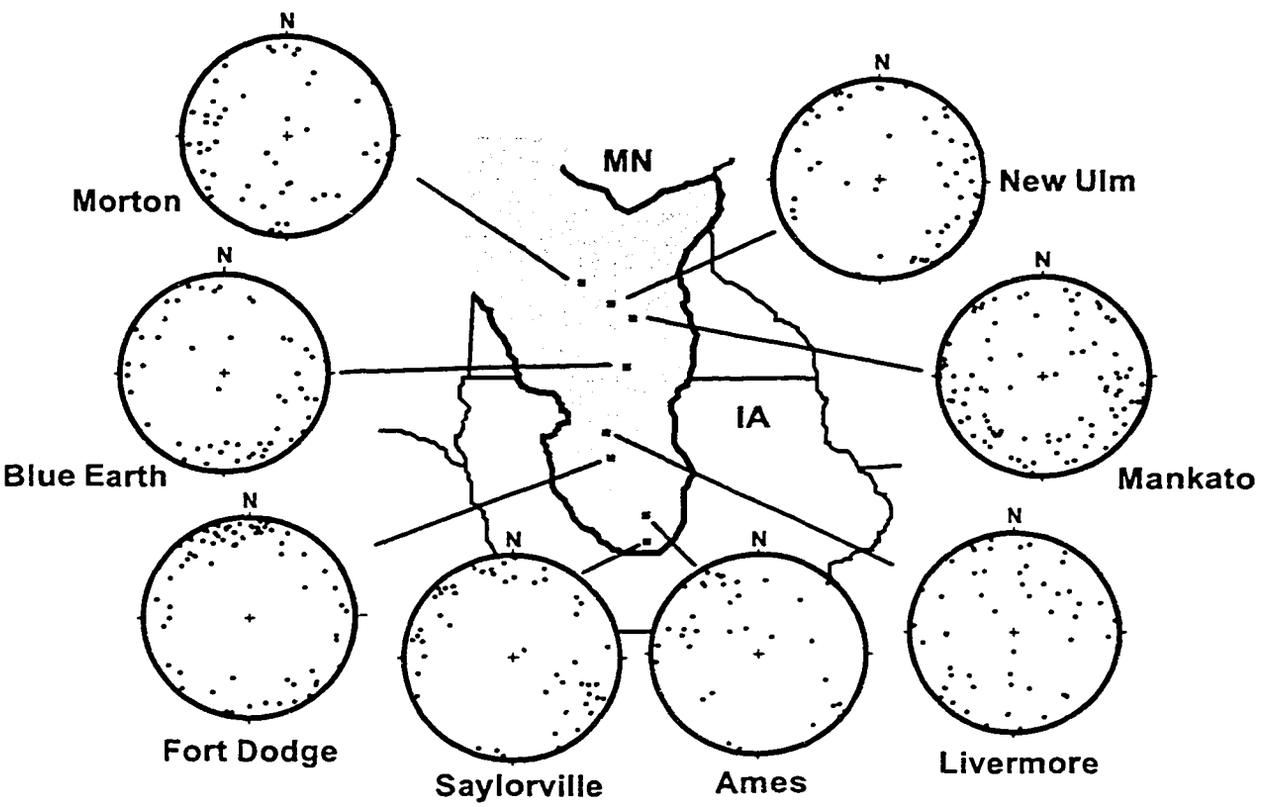

Figure 19. Clast fabric stereograms for the Des Moines Lobe basal till. The label next to each stereogram is the major geographic feature that is closest to the sample location.

Table 3. Fabric results for the Des Moines Lobe till.

Location	No. of clasts	Eigenvalues S_1	Eigenvalues S_3	V_1 Trend (degrees)	V_1 Plunge (degrees)
Morton, MN	50	0.44	0.18	263.2	19.8
New Ulm, MN	50	0.54	0.12	124.2	5.0
Mankato, MN	95	0.46	0.17	79.4	1.1
Blue Earth, MN	50	0.54	0.14	142.6	6.8
Livermore, IA	52	0.46	0.23	22.0	8.5
Fort Dodge, IA	73	0.67	0.06	344.4	6.1
Ames, IA	36	0.60	0.16	317.5	19.0
Saylorville, IA	50	0.58	0.11	134.5	1.6

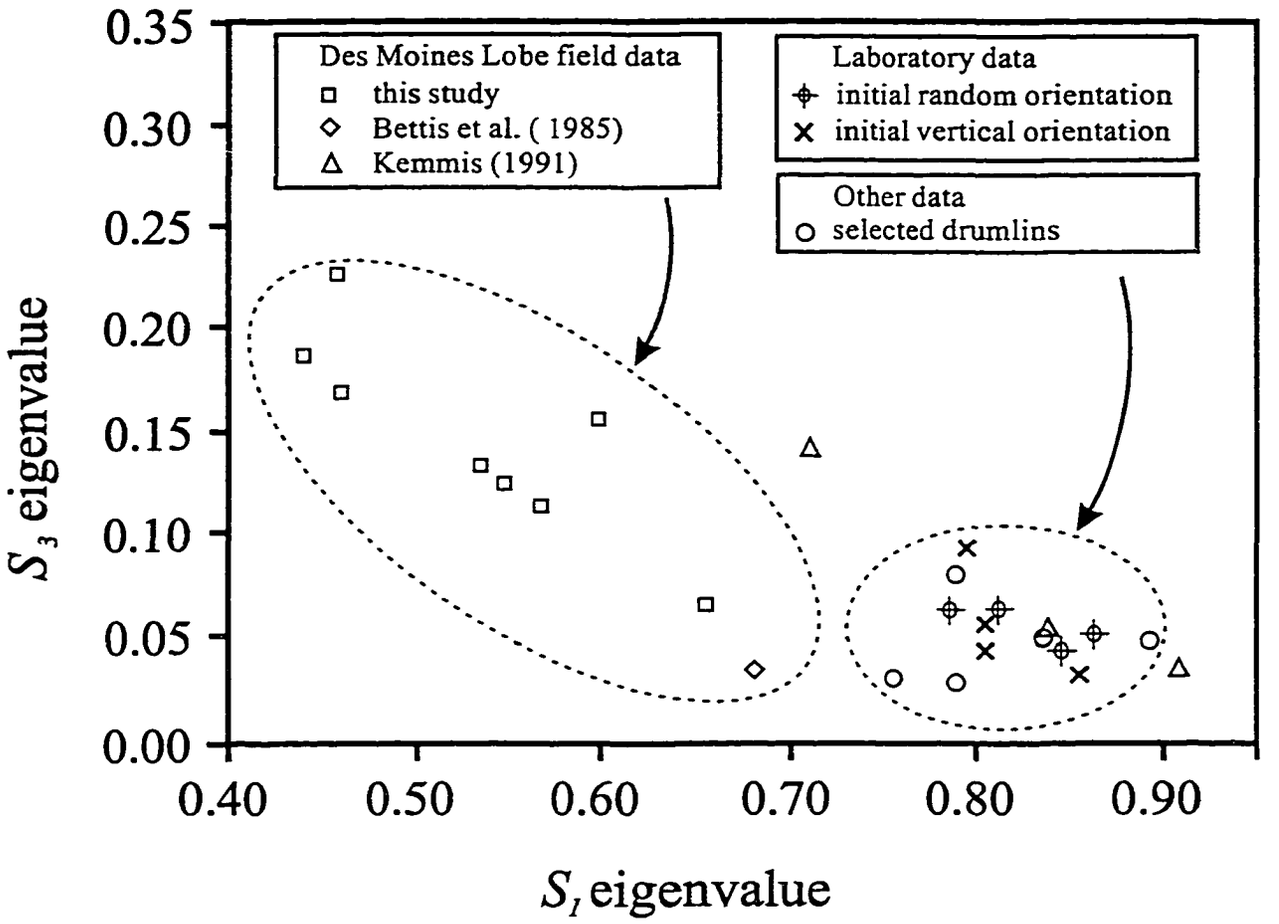

Figure 20. S_1 verses S_3 eigenvalues for the Des Moines Lobe basal till, ring-shear tests, and selected drumlins (Evenson, 1971; Krüger and Thomsen, 1984; Stanford and Mickelson, 1985). The drumlin data are included because an independent case has sometimes been made for their formation by a mobile bed (Smalley and Unwin, 1968; Boulton, 1987; Menzies, 1989).

the extremely high strains required of the deforming-bed mechanism of glacier motion, unless the till was somehow disturbed after deposition. This is unlikely given that most fabrics were measured in unoxidized till below any visible soil horizons.

Mixing

Visually sharp contacts between lithologically distinct Pleistocene tills have been used as evidence both for and against bed deformation (Kemmis, 1981; Clayton et al., 1989; Alley, 1991). If two till layers are sheared beneath an ice mass then diffusive mixing between them should be proportional to the cumulative shear strain. To test this hypothesis, laboratory experiments were conducted using the ring-shear device to shear two tills to various strains. The gray Des Moines Lobe till and the red Superior Lobe till were selected for the experiments because they have different lithologies and are in stratigraphic contact in the area overridden by the Grantsburg Sublobe (Chernicoff, 1983). Mixing was determined to be linearly diffusive, and thus, can be characterized by a single mixing coefficient, D. This parameter is similar to a diffusivity but with different units (m^2). This coefficient determined from the laboratory tests, together with concentration profiles measured across the contact between these till units in the field, yield an estimate of the maximum shear strain as noted in Chapter 3. This method allows an upper limit to be placed on the strain experienced across the contact of the Des Moines Lobe and Superior Lobe tills.

At four locations (Fig. 5) the concentration of 1-2 mm shale grains was measured across the contact between the two tills to determine vertical mixing profiles. Shale is the most appropriate index lithology due to its abundance in the Des Moines Lobe till (3-15%) and its absence in the overlying Superior Lobe till. Samples were collected over a 2-m thick

section centered at the visual contact between the two tills. Samples were collected by scraping 1-2 mm thick layers of till from a 0.3 x 0.3 m platform that was progressively excavated downward through the thickness of the section. A point gauge, accurate to 1.0 mm, was used to measure the vertical location of each sample. The samples were then returned to the laboratory where the 0.4-1.0 mm grain-size fraction was isolated using wet-sieving techniques. This fraction was oven-dried and spilt numerous times to obtain approximately 300-500 grains for identification. Shale grains were then identified under a binocular microscope. These grains, as well as the total number of grains, were counted to determine the concentration of shale in each sample and then plotted as a function of depth.

The four mixing profiles are presented in Figure 21 in which the percentage of shale grains is plotted as a function of the vertical distance from the visual contact, z_c. The data indicate that mixing occurred over a thickness of 5-40 mm and is symmetrical about the visual contact between the tills. This zone of mixing is thin relative to the overall thickness of the till units, which ranges from 2 to 5 m. According to the diffusion model, the dimensionless concentration of shale with depth, C (number of shale grains per total number of grains), is

$$C = C_1 C_2 + \frac{C_1}{2} erfc\left(\frac{z_c}{2\sqrt{D\gamma}}\right), \qquad (13)$$

where C_1 and C_2 are the initial dimensionless concentrations of shale particles in the two tills. Using a D value of 0.004 mm^2, the smallest value determined in the ring-shear experiments Chapter 3), the best fit of Equation 13 to the data yields values of γ that range from 867 to 8015 with a mean of 2910.

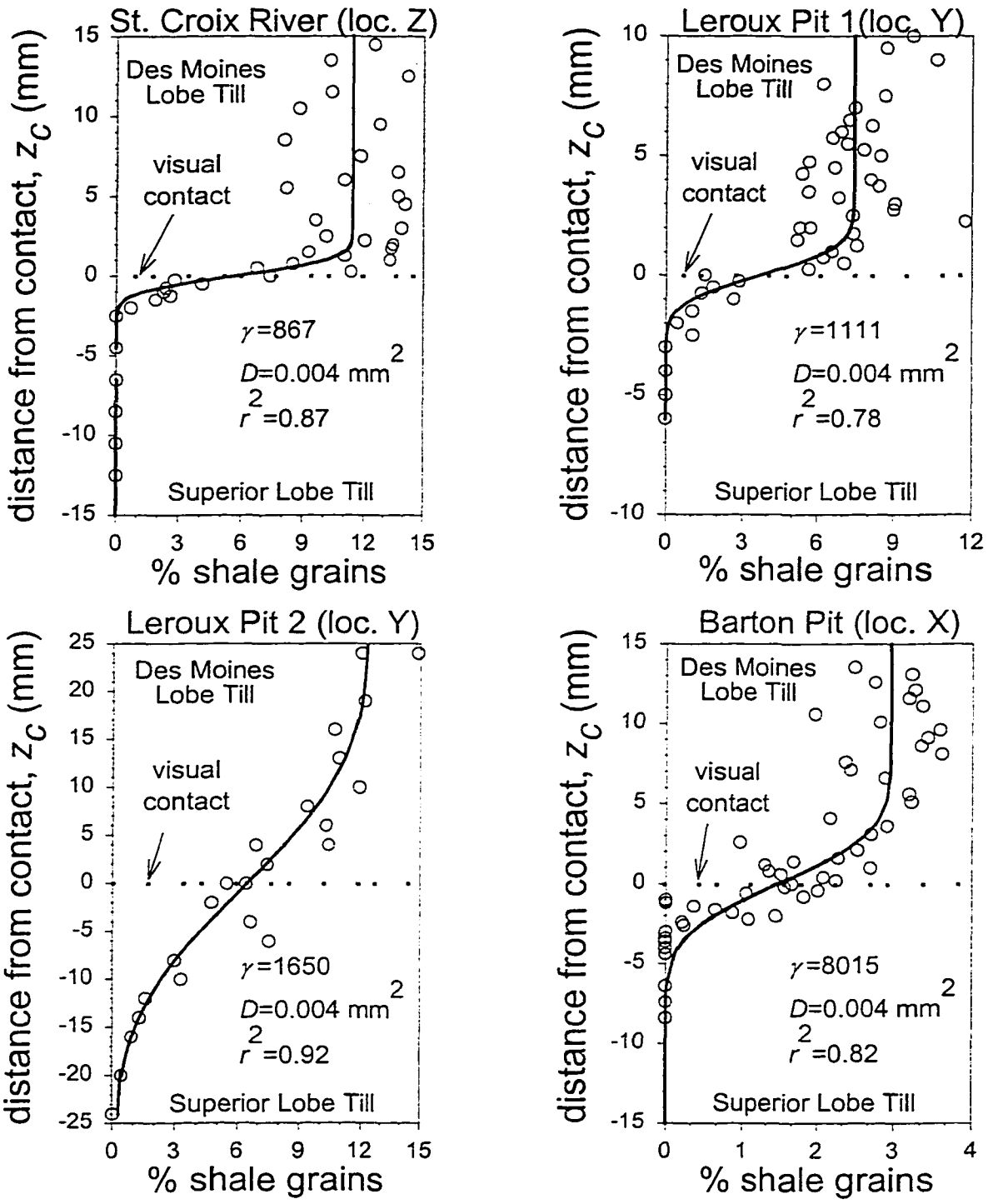

Figure 21. Mixing profiles measured across contacts of the Des Moines Lobe and Superior Lobe tills at four locations shown on Figure 5. The curved line represents the fit of the diffusion model to the data using $D = 0.004$ mm^2, the minimum value determined in ring-shear tests, to calculate the shear strain (γ).

Because a minimum value for D was chosen, the shear strains calculated are maximum values. In addition, it was implicitly assumed that the initial contact between the tills was smooth. If the contact between the two tills was initially irregular, as expected, then the mixing observed is the result of smaller cumulative strains.

Maximum shear strains ranging from 867-8015 likely indicate that only a small portion of the Grantsburg Sublobe's displacement was due to shearing of subglacial sediment. A conservative estimate of the shear strain expected if motion was entirely by bed deformation can be made by first assuming a reasonable basal ice velocity of 400 m a^{-1}, comparable to the velocity of Ice Stream B. Varves in the glacial Lake Grantsburg, dammed by the Grantsburg Sublobe, indicate that the lobe covered the area for a minimum of 2000 years (Wright, 1973). The minimum displacement at the ice/bed interface would have thus been 800 km. Assuming that the bed deformed to a depth of 5 meters, similar to the thickness of the till layer thought by some to be deforming beneath Ice Stream B (Alley et al., 1986; Blankenship et al., 1986), the resulting shear strain would be 160,000. This is 20 to 185 times larger than the maximum values inferred from mixing profiles and shows that less than 5% of the lobe's displacement can be accounted by bed deformation. Assuming a thinner deforming layer would reduce this percentage.

Key assumptions in the above calculation are that bed deformation was responsible for mixing, that the lobe did not move at its base slower than 400 m a^{-1}, and that deformation occurred at a depth sufficient to influence the contact between the two till units. The first assumption may not be correct, but does not bear on the overall objective of placing an upper limit on deformation of the bed. Basal-ice velocities may have been lower, although that seems unlikely given that advance rates were on the order of 2000-3000 m a^{-1} (Clayton and

Moran, 1982). Such high velocities, rather than the smaller value used here, would reduce the fraction of motion accounted for by bed deformation. Finally, there is no way to infer from the mixing profiles that deformation was not focused above the contact between the tills. This seems unlikely, however, in light of the fabric data.

DISCUSSION

Reconstruction of the Des Moines Lobe from ice flow indicators and modern moraine elevations corroborates previous studies (Matthews, 1974; Clark, 1992) that the lobe was relatively thin. However, reconstruction of the lobe assuming that its terminal moraine was ice-cored results in a lobe almost twice as thick as previously estimated. If moraines of other lobes along the southern margin of the Laurentide Ice Sheet and elsewhere were ice-cored, then these ice margins were also thicker than reconstructions indicate. This might have significant implications for models of atmospheric circulation (Manabe and Broccoli, 1985; Lautenschlager and Herterich, 1990) and estimates of global ice volume related to changes in sea level (Shackleton, 1987) during the last glaciation.

Basal shear stresses based on these reconstructions are small (<10 kPa). Such low shear stresses indicate that the lobe was not frozen to its bed and that motion was focused at the base of the lobe with little internal ice deformation.

The well-lubricated base of the Des Moines Lobe was most likely the result of high water pressure in the subglacial hydraulic system. Based on the reconstructions and consolidation tests on basal till, water pressures at the ice/bed interface were 78-98% of the ice-overburden pressure, assuming no downward flow of groundwater through the till. Water pressures may have been higher because consolidation tests yield maximum values of

effective stress, although the water pressure would be overestimated if downward groundwater flow was significant. High basal water pressures are consistent with the hydrological model of Walder and Fowler (1994), which predicts flow in channels cut into the till bed, roughly similar perhaps to the poorly defined tunnel channels beneath the Des Moines Lobe noted by Patterson (1996). These channels may have been fed by a water layer, like that which apparently feeds Walder-Fowler channels beneath Ice Stream B (Engelhardt and Kamb, 1997).

The model of Iverson (1999) indicates that for water-layer thicknesses thought to be appropriate for modern ice masses, the shear strength of the ice/till interface was likely less than the ultimate strength of the till, with ice motion focused at the glacier sole. The dominant mechanism of motion should have been plowing, with a few of the smallest particles on the bed stationary and accommodated by regelation. Pervasive deformation of the bed at depth should have been minimal, unless the water layer at the bed surface was less than 0.1 mm. This seems unlikely, however, given the warm environment of the Des Moines Lobe and the expected meltwater input to the bed. For example, artificially induced pulses of meltwater through boreholes to the bed of Ice Stream B locally thickened the water layer from ~0.1 mm to 2-4 mm (Engelhardt and Kamb, 1997).

An important process that should enhance plowing and that is not considered in the model used here is the build up of pore-water pressure in excess of hydrostatic pressure in front of plowing clasts. Whether this should have occurred can be determined by calculating the particle radius, δ, at which the time scale for till compaction exceeds that for pore-pressure diffusion and consequent excess pore-pressures develop (Iverson, 1999). The value of δ is given by

$$\delta = k_p / U_p \alpha \mu r \quad (14)$$

where k_p is the intrinsic permeability of the till, U_p is the plowing velocity, roughly equal to the sliding speed, α is the compressibility of the till (Freeze and Cherry, 1979, p. 54), and μ is the dynamic viscosity of water at 0° C (1.8×10^{-3} Pa s). The parameter r is dimensionless and was determined from cone-penetration data of Campanella et al. (1983) following Iverson et al. (1994). These data indicate that r=5. U_p is assumed equal to the surface speed of Ice Stream B (440 m a^{-1}). For unoxidized basal till of the Des Moines Lobe $k_p = 1.1 \times 10^{-15}$ m^2, as determined from slug tests (Seo, 1996). The consolidation tests described previously yielded $\alpha = 3.1 \times 10^{-7}$ Pa^{-1} for effective pressures ranging from 0-350 kPa. These parameter values in Equation 14 indicate that δ = 0.08 m. Thus, excess pore pressures should have occurred in front of plowing clasts of this size and larger, thereby reducing the shear stresses that these clasts supported and reducing the likelihood of pervasive bed deformation.

Despite two strong fabrics measured by Kemmis (1981) at one location, field data from this study and that of Bettis et al. (1985) support the uncertain model prediction that motion of the Des Moines Lobe was focused near the ice/bed interface and not at depth within its basal till (Fig. 20). A similar, albeit more equivocal, result was obtained by measuring the mixing across the basal contact of the till. These results suggest that bed deformation accounted for less than 5% of the basal motion of the Grantsburg Sublobe, although shearing above the Des Moines Lobe/Superior Lobe till contact cannot be ruled out.

The results of this study indicate that motion of the Des Moines Lobe occurred at the bed surface predominantly by plowing. This implies that the transport of sediment must have

occurred primarily in the basal ice rather than in a pervasively deforming till layer. Similar conclusions have been reached for other Pleistocene ice lobes, including the Puget Lobe of the Cordilleran ice sheet (Brown et al., 1987) and a portion of the Scandinavian ice sheet in northwest Germany (Piotrowski and Kraus, 1997; Piotrowski and Tulaczyk, 1999) based on modeling, ice-lobe reconstructions, and field evidence. In contrast, it is assumed in many models of Pleistocene ice sheets that basal motion occurs by bed deformation (Clark et al., 1996; Jenson, et al., 1996; Licciardi et al., 1998; Boulton, 1996; Dowdeswell and Siegert, 1999). In addition, still other studies have called exclusively upon bed deformation to explain large basal sediment fluxes (Alley, 1991; Jenson, et al., 1995; Hooke and Elverhøi, 1996; Shipp and others, 1999). These are unsupported assumptions for the Des Moines Lobe.

CONCLUSIONS

Plowing, and to a lesser degree, regelation are thought to be the primary mechanisms of motion for the Des Moines Lobe. Motion, therefore, was probably focused at the ice/till interface with little deformation of the bed at depth. This is consistent with low basal shear stresses calculated from the reconstruction of the lobe and high basal water pressures determined from consolidation tests, which indicate that the lobe was near flotation. Motion by internal ice deformation was negligible.

Given the uncertainties in the plowing and sliding model, the most convincing support for motion at the bed surface is the lack of sedimentological features indicative of pervasive bed deformation. Weak clast fabrics and the lack of mixing between lithologicallly distinct till units indicate that bed deformation accounted for, at most, 5% of the Des Moines Lobe's basal motion. Therefore, the instability of the Des Moines Lobe, as indicated by its rapid

advance and retreat rates, is attributed to decoupling at the ice/bed interface rather than bed deformation.

REFERENCES

Alley, R.B., Blankenship, D.D., Bentley, C.R. and Rooney, S.T., 1986, Deformation of till beneath Ice Stream B, West Antarctica: Nature, 322, p. 57-59.

Alley, R.B., Blankenship, D.D., Bentley, C.R., and Rooney, S.T., 1987, Till beneath Ice Stream B. 3. Till deformation: evidence and implications: Journal of Geophysical Research, v. 92, p. 8921-8929.

Alley, R.B., 1989, Water-pressure coupling of sliding and bed deformation: II. Velocity-depth profiles: Journal of Glaciology, v. 35, p. 119-129.

Alley, R.B., 1991, Deforming-bed origin for southern Laurentide till sheets?: Journal of Glaciology: v. 37, p. 67-76.

Alley, R.B., and MacAyeal, D.R., 1994, Ice-rafted debris associated with binge/purge oscillations of the Laurentide Ice Sheet: Paleoceanography, v. 9, p. 503-511.

Andrews, J.T., and Tedesco, K., 1992, Detrital carbonate-rich sediments, northwestern Labrador Sea: implications for ice-sheet dynamics and iceberg rafting (Heinrich) events in the North Atlantic: Geology, v. 20, p. 1087-1090.

Baker, R.G., 1996, Pollen and plant macrofossils, in: Bettis, E.A., Quade, D.J., and Kemmis (eds.), Hogs, Bogs, and Logs: Quaternary deposits and environmental geology of the Des Moines Lobe, Iowa Department of Natural Resources, Guidebook Series, n. 18, p.105-109.

Benn, D.I. and Evans, D.J.A., 1998, Glaciers & Glaciation, London, Arnold Publishers, 734 p.

Bettis III, E.A., Kemmis, T.J. Witzke, B.J., 1985, After the great flood: Exposures in the Emergency Spillway, Saylorville Dam: Geological Society of Iowa, Guidebook 43.

Bettis, E.A., Quade, D.J., and Kemmis, T.J., 1996, Overview, In: Bettis, E.A., Quade, D.J., and Kemmis (eds.), Hogs, Bogs, and Logs: Quaternary deposits and environmental geology of the Des Moines Lobe, Iowa Department of Natural Resources, Guidebook Series, n. 18, p. 1-79.

Blake, E.W., Fischer, U.H., and Clarke, G.K.C., 1994, Direct measurement of sliding at the glacier bed: Journal of Glaciology, v. 40, p. 595-599.

Blankenship, D.D., Bentley, C.R., Rooney, S.T. and Alley, R.B., 1986, Seismic measurements reveal a saturated porous layer beneath an active Antarctic ice stream: Nature, v. 322, p 54-57.

Bond, G., Heinrich, H., Broecker, W., Labeyrie, L., and McManus J., and others, 1992, Evidence for massive discharges of icebergs into the North Atlantic ocean during the last glacial period: Nature, v. 360, p. 245-249.

Bond, G.C., and Lotti, R., 1995, Iceberg discharges into the North Atlantic on millennial time scales during the last deglaciation: Science, v. 267, p. 1005-1010.

Boulton, G.S., and Jones, A.S., 1979, Stability of temperate ice caps and ice sheets resting on beds of deformable sediment: Journal of Glaciology: v. 24, p. 29-43.

Boulton, G.S., 1987, A theory of drumlin formation by subglacial sediment deformation: In *Drumlin Symposium*, eds. Menzies, J., and Rose, J., A.A. Balkema, Rotterdam, p. 25-80.

Boulton G.S., and Hindmarsh, R.C.A., 1987, Sediment deformation beneath glaciers: rheology and geological consequences. Journal of Geophysical Research, v. 92, p. 9059-9082.

Boulton, G.S., 1996, The theory of glacial erosion, transport and deposition as consequence of subglacial sediment deformation: Journal of Glaciology, v. 42, p. 43-62.

Broecker, W.S., 1994, Massive iceberg discharges as triggers for global climate change: Nature, v. 372, p. 421-424.

Brown, N.E., Hallet, B., and booth, D.B., 1987, Rapid soft bed sliding of the Puget glacial lobe: Journal of Geophysical Research, v. 92, p. 8985-8997.

Campanella, R.G., Robertson P.K., and Gillespie, D., 1983, Cone penetration testing in deltaic soils: Canadian Geotechnical Journal, v. 20, p. 23-35.

Casagrande, A., 1936, The determination of the preconsolidation load and its practical significance: Proceedings: First International Conference on Soils Mechanics and Foundation Engineering, 3, p. 60-64, Cambridge, MA

Charles, C.D., and Fairbanks, R.G., 1992, Evidence from Southern ocean sediments for the effect of north Atlantic deep-water flux on climate: Nature, v. 355, p. 416-418.

Chernicoff, S.E., 1983, Glacial characteristics of a Pleistocene ice lobe in east-central Minnesota: Geological Society of America Bulletin, v. 94, p. 1401-1414.

Clark, P.U., 1992, Surface form of the southern Laurentide Ice Sheet and its implications to ice-sheet dynamics: Geological Society of America Bulletin, v. 104, p. 595-605.

Clark, P.U., 1994, Unstable behavior of the Laurentide Ice Sheet over deforming sediment and its implications for climate change: Quaternary Research, v. 41, p. 19-25.

Clark, P.U., and Walder, J.S., 1995, Subglacial drainage, eskers, and deforming beds beneath the Laurentide and Eurasian ice sheets: Geological Society of America Bulletin, v. 106, p. 304-314.

Clark, P.U., Licciardi, J.M., MacAyeal, D.R., and Jenson, J.W., 1996, Numerical reconstruction of a soft-bedded Laurentide Ice sheet during the last glacial maximum: Geology, v. 24, p. 679-682.

Clark, P.U., 1997, Sediment deformation beneath the Laurentide Ice Sheet, *in* Martini, I.P., ed., *Late glacial and postglacial environmental changes, Quaternary, Carboniferous-Permian and Proterozoic*: Oxford University Press, New York, p. 81-97.

Clayton, L., and Moran, S.R., 1982, Chronology of late Wisconsinan Glaciation in middle North America: Quaternary Science Reviews, v.1, p. 55-82.

Clayton, L., Teller, J.T., and Attig, J.W., 1985 Surging of the southwestern part of the Laurentide Ice Sheet: Boreas, v. 14, p. 235-242.

Clayton, L., Teller, J.T., Attig, J.W., and Mickelson, D.M., 1989, Evidence against pervasively deformed bed material beneath rapidly moving lobes of the southern Laurentide ice sheet: Sedimentary Geology, v. 62, p. 203-208.

Colgan, P.M., 1996, The Green Bay and Des Moines Lobes of the Laurentide ice sheet: evidence for stable and unstable glacier dynamics: unpublished thesis, University of Wisconsin, Madison, WI, 293 p.

Das, B.M., 1994, *Principles of Geotechnical Engineering*, PWS Publishing Company, Boston, MA, 672 p.

Dansgaard, W., Clausen, H.B., Gundestrup, N., Hammer, C.U., Johnsen, S.J., Kristinsdottir, P., and Reeh, N., 1982, A new Greenland deep ice core: Science, v. 218, p. 1273-1277.

Dowdeswell, J.A., and Sharp, M.J. 1986, Characterization of pebble fabrics in modern terrestrial glacigenic sediments: Sedimentology, v. 33, p. 699-710.

Dowdeswell, J.A., and Siegert, M.J., 1999, Ice-sheet numerical modeling and marine geophysical measurements of glacier-derived sedimentation on the Eurasian Arctic continental margins: Geological Society of America Bulletin, v. 111, p. 1080-1097.

Engelhardt, H., Humphrey, N., Kamb, B., and Fahnestock, M., 1990 Physical conditions at the base of a fast moving Antarctic ice stream: Science, v. 248, p. 57-59.

Engelhardt, H. and Kamb, B. 1997, basal hydraulic system of a West Antarctic ice stream: constraints from borehole observations: Journal of Glaciology, v. 43, p. 207-230.

Engelhardt, H. and Kamb, B. 1998, Basal sliding of Ice Stream B, West Antarctica: Journal of Glaciology, v. 44, p. 233-230.

Eyles, N., 1979, Facies of supraglacial sedimentation on Icelandic and alpine temperate glaciers: Canadian Journal of Earth Science, v. 16, p. 1341-1362.

Evenson, E.B., 1971, The relationship of macro- and microfabric of till and the genesis of glacial landforms in Jefferson County, Wisconsin, in Goldthwait, R.P., ed., *Till: a symposium*: Columbus, OH, Ohio State University Press, p. 345-64.

Fischer, U.H., Clarke, G.K.C., 1994, Ploughing of subglacial sediment: Journal of Glaciology, v. 40, p. 97-106.

Fischer, U.H., Clarke, G.K.C., 1997, Stick-slip sliding behaviour at the base of a glacier: v. 40, p. 97-106.

Fitzsimons, S.J., 1997, Depositional models for moraine formation in East Antarctic coastal oases: Journal of Glaciology, v. 43, p. 256-264.

Freeze, R.A., and Cherry, J.A., 1979, *Groundwater*: Engelwood Cliffs, NJ, Prentice-Hall,

Goebel, J.E., Mickelson, D.M., Farrand, W.R., Clayton, L., Knox, J.C., Cahow, A., Hobbs, H.C., and Walton, M.S., Jr., 1983, Quaternary geologic map of the Minneapolis 4° x 6° quadrangle, United States: U.S. Geological Survey Miscellaneous Investigations Series Map I-1420 (NL-15).

Grootes, P.M., Stuiver, M. 1997, Oxygen 18/16 variability in Greenland snow and ice with 10^{-3} to 10^{-5}-year time resolution: Journal of Geophysical Research, v. 102, p. 26455-26470.

Grousset, F.E., Labeyrie, L., Sinko, J.A., Cremer, M., Bond, G., et al. 1993, Patterns of ice-rafted detritus in the glacial North Atlantic (40-55° N): Paleoceanography, v. 8, p. 175-192.

Gwynne, C.S., 1942, Swell and swale pattern of the Mankato lobe of the Wisconsin drift plain in Iowa: Journal of Geology, v. 50, p. 200-208.

Gwynne, C.S., 1951, Minor moraines in South Dakota and Minnesota: Geological society of America Bulletin, v. 62, p. 233-250.

Hallberg, G.R., and Kemmis, J.J., 1986, Stratigraphy and correlation of the glacial deposits of the Des Moines and James lobes and adjacent areas in North Dakota, Minnesota, and Iowa: Quaternary Science Reviews, v. 5, p. 65-68.

Hallberg, G.R., and 13 others, 1991, Quaternary Geologic map of the Des Moines 4° x 6° quadrangle, United States, Miscellaneous Investigations Series, 1:1,000,000, United States Geological Survey.

Harrison, W., 1958, Marginal zones of vanished glaciers reconstructed from the pre-consolidation-pressure values of overridden silts, Journal of Geology, v. 66, p. 72-95.

Hart, J.K., 1994, Till fabric associated with deformable beds: Earth Surface Processes and Landforms, v. 19, p. 15-32.

Hays, H.D., Imbrie, J., and Shackleton, N.J., 1976, Variations in the earth's orbit: pacemaker of the ice ages: Science, v. 194, p. 1121-1134.

Hobbs, H.C., and Goebel, J.E., 1982, Geologic Map of Minnesota: Quaternary Geology: Minnesota Geological Survey State Map Series S-1: 1:500,000.

Hooke, R. LeB., 1970, Morphology of the ice-sheet margin near Thule, Greenland: Journal of Glaciology, v. 9, p. 303-324.

Hooke, R. LeB., 1973, Flow near the margin of the Barnes Ice Cap, and the development of ice-cored moraines: Geological Society of America Bulletin, v. 84, p. 3929-3848

Hooke, R. LeB., and Iverson, N.R., 1995, grain-size distribution in deforming subglacial tills: role of grain fracture: Geology, v. 23, no. 1, p. 57-60.

Hooke, R. LeB., and Elverhøi, A., 1996, Sediment flux from a fjord during glacial periods, Isfjorden, Spitsbergen: Global and Planetary Change, v. 12, p. 237-249.

Hooke, R. LeB., Hanson, B., Iverson, N.R., Jansson, P. and Fischer, U.H., 1997, rheology of till beneath Storglaciären, Sweden: Journal of Glaciology: v. 43, p. 172-179.

Hooyer, T.H., and Iverson, N.R., in press, Clast-fabric development in a shearing granular material: Implications for subglacial till and fault gouge: Geological Society of America Bulletin.

Humphrey, N., 1993, Characteristics of the bed of the lower Columbia Glacier, Alaska: Journal of Geophysical research, v. 98, p. 837-846.

Iken, A. and Bindschadler, R., 1986, Combined measurements of subglacial water pressure and surface velocity of Findelengletscher, Switzerland: conclusions about drainage system and sliding mechanism: Journal of Glaciology, v. 32, p. 101-119.

Iken, A., and Truffer, M., 1997, The relationship between subglacial water pressure and velocity of Findelengletscher, Switzerland, during its advance and retreat: Journal of Glaciology, v. 43, p. 328-338.

Imbrie, J., Boyle, E.A., Clemens, S.C., Duffy, A., Howard, W.R., et al. 1992, On the structure and origin of major glaciation cycles 1. Linear responses to Milankovitch forcing; Paleoceanography, v. 7, p. 701-738.

Imbrie, J., Berger, a., Boyle, E.A., Clemens, S.C., Duffy, A., et al. 1993, On the structure and origin of major glaciation cycles: 2. The 100,000-year cycle, Paleoceanography, v. 8, p. 699-735.

Iverson, N.R., Jansson, P., and Hooke, R. LeB., 1994, In-situ measurement of the strength of deforming subglacial till: Journal of Glaciology, v. 40, p. 477-503.

Iverson, N.R., Hanson, B., Hooke, R. LeB., and Jansson, P., 1995, Flow mechanism of glaciers on soft beds: Science, v. 267, p. 80-81.

Iverson, N.R., Hooyer, T. and Hooke, R. LeB., 1996, A laboratory study of sediment deformation: Stress heterogeneity and grain-size evolution: Annals of Glaciology, 22, p. 167-175.

Iverson, N.R., Baker, R., and Hooyer, T., 1997, A ring-shear device for the study of till deformation: tests on a clay-rich and a clay-poor till: Quaternary Science Reviews, v. 16, p. 1057-1066.

Iverson, N.R., Hooyer, T.S., and Baker, R., 1998, Ring-shear studies of till deformation: Coulomb-plastic behavior and distributed strain in glacier beds: Journal of Glaciology, v. 44, p. 634-642.

Iverson, N.R., 1999, Coupling between a glacier and a soft bed: II. Model results: Journal of Glaciology, v. 45, p. 41-53.

Janbu, N. and Senneset, 1974, Effective stress interpretation of in-situ static penetration tests. In Broms, B.B., ed. Proceedings of the European symposium on Penetration Testing, Stockholm, Sweden, June 5-7, v. 2 (2), Stockholm, National Swedish Building Research, p. 181-194.

Jeffery, G.B., 1922, The motion of ellipsoidal particles immersed in a viscous fluid: Proceedings of the Royal Society of London, Ser. A, v. 102, p. 169-179.

Jenson, J.W., Clark, P.U., MacAyeal, D.R., Ho, C., and Vela, J.C., 1995, Numerical modeling of advective transport of saturated deforming sediment beneath the Lake Michigan Lobe, Laurentide Ice Sheet: Geomorphology, v. 14, p. 157-166.

Jenson, J.W., MacAyeal, D.R., Clark, P.U., Ho, C.L. and Vela, J.C., 1996, Numerical modeling of subglacial sediment deformation: implications for the behavior of the Lake Michigan Lobe, Laurentide Ice Sheet: Journal of Geophysical Research, v. 101, p. 8717-8728.

Johnson, P.G., 1971, ice-cored moraine formation and degradation, Donjek Glacier. Yukon Territory, Canada: Geografiska Annaler, v. 53A, p. 198-203.

Kamb, B., Raymond, C.R., Harrison, W.D., Engelhardt, H., Echelmeyer, K.A., Humphrey, N., Brugman, M.M., and Pfeffer, T., 1985, Glacier surge mechanism: 1982-1983 surge of Variegated Glacier, Alaska: Science, v. 227, p. 469-479.

Kamb, B., 1991, Rheological nonlinearity and flow instability in the deforming bed mechanism of ice stream motion. Journal of Geophysical Research, v. 96, no. B10, p. 16,585-16,595.

Kemmis, T.J., 1981, Importance of the regelation process to certain properties of basal tills deposited by the Laurentide Ice Sheet in Iowa and Illinois, U.S.A.: Annals of Glaciology, v. 2, p. 147-152.

Kemmis, T.J., 1991, Glacial landforms, sedimentology, and depositional environments of the Des Moines Lobe, northern Iowa: unpublished thesis, University of Iowa, p. 390.

Keigwin, L.D., Jones, G.A., Lehman, S.J., and Boyle, E., 1991, Deglacial meltwater discharge, North Atlantic deep circulation, and abrupt climate change: Journal of Geophysical Research, v. 96, p. 16811-16826.

Kirkbride, M.P., 1995, Processes of Transportation, in Menies, J., ed., *Modern Glacial Environments: processes, dynamics and sediments*, v. 1, Menzies, J., ed. Butterworth-Heinemann, p. 261-291.

Krüger, J., and Thomsen, H.H., 1984, Morphology, stratigraphy, and genesis of small drumlins in front of the glacier Myrdalsjokull, south Iceland: Journal of Glaciology, v. 30, p. 94-105.

Lambe, T.W., and Whitman, R.V., 1969, *Soil Mechanics*: John Wiley and Sons, New York, 553 p.

Larsen, E., Sandven, R., Heyerdahl, H., and Hernes, S., 1995, Glacial geological implications of preconsolidation values in sub-till sediments at Skorgens, western Norway: Boreas, v. 24, p. 37-46.

Lautenschlager, M., and Herterich, K., 1990, Atmospheric response to ice age conditions: Climatology near the earth's surface: Journal of Geophysical Research, v. 95, p. 22547-22557.

Lehman, S.J., and Keigwin, L.D., 1992, Sudden changes in the North Atlantic circulation during the last deglaciation: Nature, v. 356, p. 757-62.

Licciardi, J.M., Clark, P.U., Jenson, J.W., and MacAyeal, D.R., 1998, Deglaciation of a soft-bedded Laurentide Ice Sheet: Quaternary Science Reviews, v. 17, p. 427-448.

Lliboutry, L., 1979, Local friction laws for glaciers: a critical review and new openings: Journal of Glaciology, v. 23, no. 89, p. 67-95.

Lorius, C., Jouzel J., Raynaud, D., Hansen J., Le Treut, H., 1990, The ice-core record: climate sensitivity and future greenhouse warming: Nature, v. 347, p. 139-145.

Manabe, S., and Broccoli, A.J., 1985, The contributions of continental ice, atmospheric CO^2, and land albedo to the climate of the last glacial maximum: Climate Dynamics, v. 1, p. 87-99.

Mark, D.M., 1973, Analysis of axial orientation data, including till fabrics: Geological Society of America Bulletin, v. 84, p. 1369-1374.

Mathews, W.H., 1974, Surface profiles of the Laurentide Ice Sheet in its marginal areas: Journal of Glaciology, v. 13, p. 37-43.

Matsch, C.L., 1972 Quaternary geology of southwestern Minnesota, in Sims, P.K., and Morey, G.B., eds., Geology of Minnesota: A centennial volume: Minneapolis, Minnesota, Minnesota Geological Survey, p. 548-560.

Menzies, J., 1989, Drumlins – products of controlled or uncontrolled glaciodynamic response?: Quaternary Science Reviews, v. 8, p. 151-158.

Mickelson, D.M., Clayton, L., Fullerton, D.S., and Borns, H.W., Jr., 1983, The late Wisconsin glacial record of the Laurentide Ice sheet in the United States, in Porter, S.C., ed., Late-Quaternary Environments of the United states: Minneapolis, Minnesota, University of Minnesota Press, p. 3-37.

Oeschger, H., Beer, U., Siegenthaler, U., Stauffer, B., Dansgaard, W., and Langway, C.C., Jr., 1984, Late-Glacial climate history from ice cores, A.G.U., Geophys. Monograph 29, Climate processes and Climate Sensitivity, M. Ewing Ser., p. 299-306

Oppo, D.W., and Lehman, S.J., 1995, Suborbital time-scale variability of North Atlantic Deep Water formation during the last 200,000 years: Paleoceanography, v. 12, p. 191-205.

Østrem, G., and Arnold, K., 1970, Ice-cored moraines in southern British Columbia and Alberta, Canada, Geografiska Annaler, v. 52A, p. 120-128.

Østrem, G, 1971, Rock glaciers and ice-cored moraines, a reply to D. Barsch: Geografiska Annaler, v. 53A, p. 207-213.

Palmquist, R., and Connor, K., 1978 Glacial landforms: Des Moines drift sheet, Iowa: Association of American Geographers Annals, v. 68, p. 166-179.

Paterson, W.S.B, 1994, *The Physics of Glaciers*: New York, Pergamon Press, 380 p.

Patterson, C.J., 1995, Surficial geologic map, plate 1 of Setterholm, D.R., project manager, Regional hydrogeologic assessment: Quaternary geology-southwestern Minnesota: Minnesota Geological Survey Regional Hydrogeologic Assessment Series RHA-2, Part A, scale 1:200,000.

Patterson, C.J., 1996, The glacial geology of southwestern Minnesota with emphasis on the deposits and dynamics of the Des Moines Lobe: unpublished thesis, University of Minnesota, 1996, 143 p.

Patterson, C.J., 1998, Laurentide glacial landscapes: the role of ice streams: Geology, v. 26, p. 643-646.

Piotrowski, J.A., and Kraus, A.M., 1997, Response of sediment to ice-sheet loading in northwestern Germany: effective stresses and glacier-bed stability: Journal of Glaciology, v. 43, p. 495-502.

Piotrowski, J.A., and Tulaczyk, S., 1999, Subglacial conditions under the last ice sheet in northwest Germany: ice-bed separation and enhanced basal sliding: Quaternary Science Reviews, v. 18, p. 737-751.

Raymond, C.F., and Harrison, W.D., 1988, Evolutions of Variegated Glacier, Alaska, U.S.A., prior to its surge: Journal of Glaciology, v. 34, p. 1-16.

Röthlisberger, H., 1972, Water pressure in intra- and subglacial channels, Journal of Glaciology, v. 11, p. 177-203.

Ruhe, R.V., 1969, *Quaternary landscapes in Iowa*: Ames, Iowa, Iowa State University Press, 255 p.

Sauer, E.K., England, A.K., and Christiansen, E.A., 1993, Preconsolidation of tills and intertill clays by glacial loading in southern Saskatchewan, Canada: Canadian Journal of Earth Sciences, v. 30, p. 420-433.

Schwert, D.P., and Torpen, H.J., 1996, Insect remains: a faceted eye's perspective on the advance of the Des Moines Lobe into north-central Iowa, in: Bettis, E.A., Quade, D.J., and Kemmis (eds), Hogs, Bogs, and Logs: Quaternary deposits and environmental geology of the Des Moines Lobe, Iowa Department of Natural Resources, Guidebook Series, n.18, p. 99-104.

Senneset, K and Janbu, 1985, Shear strength parameters obtained from static cone penetration tests, In Chaney, R.C. and Demars, K.R., eds., *Strength testing of marine sediments: laboratory and in-situ measurements.* Philadelphia, PA, American Society for Testing and Materials, Special Technical Publication 883, p. 41-54.

Seo, H.H, 1996, Hydraulic properties of Quaternary stratigrapahic units in the Walnut Creek watershed, unpublished thesis, Iowa State University, Ames, IA., 85 p.

Shackleton, N.J., 1987, Oxygen isotopes, ice volume and sea level: Quaternary Science Reviews, v. 6, p. 183-190.

Shipp, S., Anderson, J., and Domack, E., 1999, Late Pleistocene-Holocene retreat of the West Antarctic Ice Sheet system in the Ross Sea: Part 1-Geophysical results: Geological Society of America Bulletin, v. 111, p. 1486-1516.

Smalley, I.J., and Unwin, D.J., 1968, The formation and shape of drumlins and their distribution and orientation in the drumlin fields: Journal of Glaciology, v. 7, p. 377-390.

Solheim , A., Forsberg, C.F., and Pittenger, A., 1991, Stepwise consolidation of glacigenic sediments related to the glacial history of Prydz Bay, East Antarctica: In Barron, J., larsen, B., eds., *Proceeding of the Ocean Drilling Program, Scientific Results*, v. 19, p. 169-181.

Stanford, S.D., and Mickelson, D.M., 1985, Till fabric and deformational structures in drumlins near Waukesha, Wisconsin, U.S.A.: Journal of Glaciology, v. 31, p. 220-228.

Stewart, R.A., Bryant, D., and Sweat, M.J., 1988, Nature and origin of corrugated ground moraine of the Des Moines Lobe, Story County, Iowa: Geomorphology, v. 1, p. 111-130.

Tarr, R.S. and Martin, L., 1914, *Alaskan Glacier Studies of the national Geographical Society in the Yakutat Bay, Prince William Sound and Lower Copper river regions*, National Geographical Society, Washington D.C., 498 p.

Tika, T.E., Vaughan, P.R., and Lemos, L.J., 1996, Fast shearing of pre-existing shear zones in soil: Geotechnique, v. 46, p. 197-233.

Tulaczyk, S., 1999, Basal mechanics and geologic record of ice streaming, West Antarctica: unpublished thesis, California Institute of Technology, Pasadena CA., 308 p.

Walder, J.S., 1986, Hydraulics of subglacial cavities: Journal of Glaciology, v. 32, p. 439-445.

Walder, J.S., and Fowler, A., 1994, Channelized subglacial drainage over a deformable bed, Journal of Glaciology, v. 40, p. 3-15.

Weertman, J., 1964, The theory of glacier sliding: Journal of Glaciology, v. 5, p. 287-303.

Wright, H.E., Jr., and Ruhe, R.V., 1965, Glaciation of Minnesota and Iowa, in Wright, H.E., Jr., and Frey, D.G., eds., *The Quaternary of the United States*: Princeton, New Jersey, Princeton University Press, p. 29-42.

Wright, H.E., Jr., Matsch, C.L., and Cushing, E.J., 1973 Superior and Des Moines lobes, in Black, R.F., Golthwait, R.P., and Willman, H.B., eds., *The Wisconsinan Stage*: Geological Society of America Memoir 136, p. 153-185.

CHAPTER 5. SUMMARY OF CONCLUSIONS

A major goal of this study was to develop criteria for identifying highly deformed basal tills. Toward that end, a ring-shear device was used to study both clast fabric development and mixing between lithologically distinct till layers as a function of shear strain. A second goal was to use these criteria, together with other data and a theoretical model of plowing and sliding, to determine the primary flow mechanism of the Des Moines Lobe.

Prolate clasts in slowly shearing till, regardless of their specific geometries and initial orientations, rotate into the plane of shearing and remain there with continued deformation. This behavior is likely to be the result of slip between the till matrix and clasts, which inhibits the periodic orbits expected of inclusions in a shearing fluid. As a consequence of this slip, strong clast fabrics (S_1~0.80) developed at low strains (25) and remained strong to strains as high as 475. These results dispel the widespread belief that weak clast fabrics result from subglacial shearing and, in fact, indicate the converse: that tills with weak fabrics have not been sheared pervasively to strains sufficient to account for significant glacier motion.

The degree of mixing between subglacial till layers provides a means of estimating bed shear strain. Ring-shear experiments indicate that an initially sharp contact between tills does not persist with deformation. The mixing across the contact can be modeled as a linearly diffusive process, and thus, can be characterized with a single coefficient. A comparable value for this coefficient was calculated independently using kinetic gas theory. The determination of this coefficient in ring-shear experiments allows maximum estimates of

bed shear strain from the distribution of index lithologies measured across the contact between two tills in the field.

These criteria for evaluating bed shear strain were used to help determine the primary flow mechanism of the Des Moines Lobe, an outlet glacier of the southern Laurentide ice sheet that rested on unlithified sediment. Reconstructions of the lobe indicate that its basal shear stress was small relative to that of most modern ice masses, although if its terminal moraine was ice-cored the thickness of the lobe may have been twice that estimated by Clark (1992). The small basal shear stress indicates that the lobe was not frozen to its bed during the glacial maximum and that motion must have been focused at the base of the lobe. Consolidation tests on intact basal till samples indicate that the basal effective pressure was low. This implies that water pressure in the subglacial hydraulic system was high and that the lobe was nearly floating on its till bed. A theoretical model of sliding and plowing (Iverson, 1999) indicates that for basal water layers of thicknesses comparable to those beneath modern glaciers, the strength of the bed surface should have been less than the ultimate strength of the lobe's basal till determined in ring-shear tests. This suggests that motion was probably focused near the ice/bed interface and not at depth within the bed. This result is supported by measurements of weak clast fabrics at eight locations along the axis of the lobe where its basal till was sampled. It is also consistent with the minimal mixing observed between the Des Moines Lobe till and the underlying Superior Lobe till in the area of the Grantsburg Sublobe.

This study demonstrates the utility of controlled laboratory experiments in glacial geomorphology, a field that relies almost exclusively on indirect inferences from the geologic record. Such inferences, although frequently provocative, are sometimes

sufficiently uncertain that criteria for interpretation that are essentially groundless are applied extensively. An example of this is the common belief that weak till fabrics result from till deformation (Hart, 1994, Clark, 1997), which has been shown to be false with this study.

This study also indicates that caution should be exercised in linking ice-sheet instability to the pervasive deformation of unlithified glacier beds. The presence of unlithified sediment beneath past ice masses does not imply that deformation of that sediment contributed significantly to glacier motion, as has been assumed in numerous models (e.g., MacAyeal, 1989; Jenson et al., 1995, 1996; Clark et al, 1996; Licciardi et al, 1998) and sedimentological interpretations (e.g., Clark, 1994; Boulton, 1996; Hooke and Elverhøi, 1996; Dowdeswell and Siegert, 1999). Such studies, therefore, should be viewed with skepticism.

References

Boulton, G.S., 1996, The theory of glacial erosion, transport and deposition as consequence of subglacial sediment deformation: Journal of Glaciology, v. 42, p. 43-62.

Clark, P.U., 1992, Surface form of the southern Laurentide Ice Sheet and its implications to ice-sheet dynamics: Geological Society of America Bulletin, v. 104, p. 595-605.

Clark, P.U., 1994, Unstable behavior of the Laurentide Ice Sheet over deforming sediment and its implications for climate change: Quaternary Research, v. 41, p. 19-25.

Clark, P.U., 1997, Sediment deformation beneath the Laurentide Ice Sheet, *in* Martini, I.P., ed., Late glacial and postglacial environmental changes, Quaternary, Carboniferous-Permian and Proterozoic: Oxford University Press, New York, p. 81-97.

Clark, P.U., Licciardi, J.M., MacAyeal, D.R., and Jenson, J.W., 1996, Numerical reconstruction of a soft-bedded Laurentide ice sheet during the last glacial maximum: Geology, v. 24, n. 8, p. 679-682.

Dowdeswell, J.A., and Siegert, M.J., 1999, Ice-sheet numerical modeling and marine geophysical measurements of glacier-derived sedimentation on the Eurasian Arctic continental margins: Geological Society of America Bulletin, v. 111, p. 1080-1097.

Hart, J.K., 1994, Till fabric associated with deformable beds: Earth Surface Processes and Landforms, v. 19, p. 15-32.

Hooke, R. LeB., and Elverhøi, A., 1996, Sediment flux from a fjord during glacial periods, Isfjorden, Spitsbergen: Global and Planetary Change, v. 12, p. 237-249.

Iverson, N.R., 1999, Coupling between a glacier and a soft bed: II. Model results: Journal of Glaciology, v. 45, no. 149, p. 41-53.

Jenson, J.W., Clark, P.U., MacAyeal, D.R., Ho, C., and Vela, J.C., 1995, Numerical modeling of advective transport of saturated deforming sediment beneath the Lake Michigan Lobe, Laurentide Ice Sheet: Geomorphology, v. 14, p. 157-166.

Jenson, J.W., MacAyeal, D.R., Clark, P.U., Ho, C.L. and Vela, J.C., 1996, Numerical modeling of subglacial sediment deformation: implications for the behavior of the Lake Michigan Lobe, Laurentide Ice Sheet: Journal of Geophysical Research, v. 101, B4, p. 8717-8728.

Licciardi, J.M., Clark, P.U., Jenson, J.W., and MacAyeal, D.R., 1998, Deglaciation of a soft-bedded Laurentide Ice Sheet: Quaternary Science Reviews, v. 17, p. 427-448.

MacAyeal, D.R., 1989, Large-scale ice flow over a viscous basal sediment: theory and application to Ice Stream B, Antarctica: Journal of Geophysical Research, v. 94, n. B4, p. 4071-4087.